Role of Usp9X in the Regulation of Axon Specification and Growth

Author

Tan, Men Chee

Published

2015

Thesis Type

Thesis (PhD Doctorate)

School

School of Biomolecular and Physical Sciences

DOI

10.25904/1912/379

Role of Usp9X in the Regulation of Axon Specification and Growth

Men Chee Tan

B.BioMedSc. (Hons)

School of Biomolecular and Physical Sciences

Griffith Sciences Group

Griffith University

Submitted in fulfilment of the requirements of the degree of

Doctor of Philosophy

August 2014

Abstract

Neurons are the core functional cells of the central nervous system (CNS). They are highly polarized with an axon and multiple dendrites, which are critical for the directional transfer of information in the CNS. The axon is the specialised region of the neuron which propagates the signal and forms neural circuits. Improper axon formation and migration can lead to various neurocognitive diseases such as epilepsy and X-linked intellectual disability. Axon formation occurs over three main phases: axon specification, growth and maturation. Axon specification and elongation have been linked to a range of neuronal signalling pathways, kinases and polarity proteins, which are the main regulators of microtubule and actin dynamics.

Several studies have shown that the substrate-specific de-ubiquitylating enzyme, Ubiquitin-specific protease located on the X chromosome (Usp9X) plays important roles in the formation and growth of neurons. Three pathological variants of Usp9X, which associate with X-linked intellectual disability, disrupt axonal growth and migration. To examine the role of Usp9X in axon formation and identify the molecular mechanism involved, cultured hippocampal neurons isolated from a brain-specific Usp9X conditional knockout mouse were used. The hippocampi were dissected out at embryonic day 18.5 and neurons were cultured up to 5 days to address the aims of the present studies.

To study the role, if any, of Usp9X in axonal specification, wild-type and Usp9X-null hippocampal neurons were compared during the first 48 hours *in vitro* and categorised into three stages. Stage 1 neurons are characterised by the extension of a prominent lamella around the cell body. Stage 2 neurons possess short symmetrical neurites. During the transition from stage 2 to 3, neurite symmetry is broken and one neurite is specified to become an axon, and rapidly grows. *In vitro*, Usp9X-null neurons significantly ($p=0.002$) lagged behind wild-type in progression from stage 1 to 2. However, despite an initial lag of about 10 hours the overall kinetics of progression from stage 1 to 2 was similar. A more dramatic effect of Usp9X loss was observed during stage 2 to 3 progression where Usp9X-null neurons required over 36 hours longer before axon specification ($p=0.001$). After this lag Usp9X-null neurons progressed to stage 3 at a similar rate to wild-type. Therefore Usp9X is required for

axon specification. In addition, Usp9X-null neurons have shorter axons, consistent with previous studies, confirming the importance of Usp9X for axonal growth.

Loss of Usp9X has been suggested to disrupt cytoskeletal proteins and transforming growth factor beta (TGFβ) pathway in the dissociated hippocampal neurons. The status of a number of candidate Usp9X substrates / binding proteins was examined by immunofluorescence and immunoblot analyses in cultured hippocampal neurons. Four putative Usp9X substrates (Kif5B, MARK4, stathmin-1 and PJA1) and their regulation by Usp9X during axon growth, warrant further investigation. Kif5B, MARK4 and stathmin-1 are involved in regulating microtubule dynamics, while the role of PJA1, an ubiquitin ligase of the TGFβ pathway, in axon formation remains unclear. The shorter axonal length observed in Usp9X null hippocampal neurons is consistent with the observed reduction in Kif5B and increased MARK4 expression level in the absence of Usp9X. Identifying critical neuronal substrates of Usp9X may have implications for neurodegenerative and neurocognitive diseases, such as X-linked intellectual disability and Parkinson's disease, which have been associated with Usp9X function.

Statement of Originality

This work has not previously been submitted for a degree or diploma in any university. To the best of my knowledge and belief, the thesis contains no material previously published or written by another person except where due reference is made in the thesis itself.

Men Chee Tan

Acknowledgements

I would like to thank, in the first place, my supervisor, Associate Professor Stephen Wood, for taking me into his research group, for his intellectual input and great enthusiasm throughout the years I spent in his lab, for his availability and being always open for discussion, for allowing me to participate in national and international meetings.

I would like to thank past and present FAMily group members: In particular, Dr Mariyam Murtaza for performing co-immunoprecipitation as described in Section 5.4; Lyn Tolley and Susitha Premaranthne for setting up mice mating and performing genotyping for my entire PhD; Caity Bridges and Devathri Nanayakara for helpful discussions and technical support.

I would like to acknowledge Dr Lachlan Jolly, University of Adelaide, 'pioneer' for the project, providing 2D proteomic data, for showing me how to isolate hippocampal neurons from the mouse embryos and invaluable discussions during meeting in Adelaide.

I would like to acknowledge Dr Victor Anggono for his great advice on growing hippocampal neurons and transfection. I acknowledge Professor Don Arnold, University of Southern California, Los Angeles, USA for provision of plasmids; Dr Jacques Camonis, Institute Curie, Paris, France for his yeast-2-hybrid data.

I would like to thank Dr Andreas Papadopulos and Rachel Gomal, QBI, University of Queensland for taking SIM images and helping in analyses for the images as described in Section 5.3.

I also appreciate the help from both Dr Jessica Clark and Dr Sunita Biswas for teaching me molecular cloning methods with patience.

I am grateful to Dr Ratneswary Sutharsan for her support and helpful advice during my candidature.

I would like to express gratitude to Julianne Spark, technical assistant of the animal house facilities for taking care of the mice.

A huge “thank you” goes to Dr Jeremy Newman for helping me with statistical analyses; Dr Kelly Hitchen for proof-reading parts of this thesis and for doing in such a short notice.

I would also like to thank all the people in Eskitis Institute who had made my long stay in this institute special particularly, Gautam Wali and Johana Tello Velasquez, for the good time in and out of the lab, great accompany and moral support during my PhD. A huge “thank you” goes to Pietro Panni for having faith in me and encouraging me to involve in animal works at the beginning of my project.

Last, but not least, it is hard to imagine myself at this point without the support of my family, who has always been there for me along these years.

Scholarships:

Griffith University Postgraduate Research Scholarship (GUPRS)

Science, Environment & Engineering Technology Group Postgraduate Research Scholarship (SEETPRS)

Eskitis Top-Up Scholarship - Griffith University

Conference presentations

International conference presentation:

An abstract and poster were presented at the **International Society for Developmental Neuroscience** (ISDN), Hilton Montreal Bonaventure, Montreal, Canada, July 2014.

National conference presentation:

An abstract and oral presentation was given at the 34th Annual Meeting of the Australian Neuroscience Society (ANS), Adelaide Convention Centre, Adelaide, Australia, January 2014.

An abstract and poster were presented at the Brisbane Cell and Developmental Biology Meeting 2013, Institute for Molecular Bioscience, University of Queensland, St Lucia, Brisbane, Australia, October 2013.

An abstract and poster were presented at Australian Society for Medical Research Queensland Postgraduate Medical Research Student Conference, Translational Research Institute, Princess Alexandra Hospital, Brisbane, Australia, May 2013.

Publication

Paemka, L., Mahajan, V. B., Ehaideb, S. N., Skeie, J. M., **Tan, M. C**., Wu, S., Cox, A. J., Sowers, L. P., Gecz, J., Jolly, L., Ferguson, P. J., Darbro, B., Schneider, A., Scheffer, I. E., Carvill, G. L., Mefford, H. C., El-Shanti, H., Wood, S. A., Manak, J. R. & Bassuk, A. G. 2015. Seizures Are Regulated by Ubiquitin-specific Peptidase 9 X-linked (USP9X), a De-Ubiquitinase. *PLoS Genet,* 11**,** e1005022

Table of Contents

List of Figures

Chapter 1

Chapter 3

Chapter 4

Appendix - Supplementary figures

List of Tables

Abbreviations

+TIPs	Microtubule plus-end tracking proteins
AF-6	acute lymphoblastic leukemia-1 (ALL-1) fusion partner from chromosome 6
AGS3	Activator of heterotrimeric G-protein Signaling 3
AJs	adherens junctions
ALL-1	acute lymphoblastic leukemia-1
APC	Adenomatous polyposis coli
aPKC	atypical protein kinase C
Arpc2	Actin-related protein 2/3 complex subunit 2
AZ	active zone
BDNF	brain-derived neurotrophic factor
BMP	Bone morphogenetic protein
BSA	Bovine serum albumin
Cdc42	cell division control 42
CH	calponin homology
cKO	conditional knockout
CNS	central nervous system
co-IP	Co-immunoprecipitation
CRIB	Cdc42/Rac interactive binding
CRMP-2	collapsin response mediator protein-2
DCX	Doublecortin
DIV	*days in vitro*

DOCK7	dedicator of cytokinesis 7
DUBs	deubiquitylating enzymes
E	embryonic day
E. coli	*Escherichia coli*
E1	ubiquitin activating enzyme ubiquitin
E2	conjugating enzyme/ubiquitin-carrier enzyme
E3	ubiquitin ligase
EB	end binding proteins
Ecto	Ectodermin
EFA6	exchange factor for ARF6
ELF	embryonic liver fodrin
GAP	GTPase-activating protein
GDP	guanosine diphosphate
GEF	nucleotide exchange factor
GNAO	guanine nucleotide-binding protein G (o) subunit alpha
GPRASP1	G protein-coupled receptor associated sorting protein 1
GSK-3β	glycogen synthase kinase-3β
GTP	guanosine triphosphate
GTP	guanosine triphosphate
HECT	Homology E6 C-terminus domain family
JAMM	Jab1/MPN/Mov34 metalloenzyme
JIP3	c-Jun N-terminal kinases-interacting protein-1
JNK	c-Jun N-terminal kinases

KIFs	kinesin superfamily proteins
KIFs	kinesin superfamily proteins
LKB1	liver kinase B1
MAP	microtubule-associated proteins
MARK	microtubule affinity regulated kinases
MDCK	Madin-Darby canine kidney
MJDs	Machado-Joseph disease protein domain proteases
mTOR	mammalian target of rapamycin
NMJ	neuromuscular junction
NPs	neural progenitors
OTUs	Ovarian tumor proteases
PAR	partitioning defective
PDK1	phosphoinositide dependent protein kinase-1
PDZ	postsynaptic density protein PSD-95/Drosophila disc large tumor suppressor protein Dlg, and zonula occludens-1 protein ZO-1
PFA	Paraformaldehyde
PI3K	Phosphatidylinositide 3-kinases
PIP3	phosphatidylinositol (3,4,5)-trisphosphate
PJA1	E3 ubiquitin ligase Praja 1
RAN	GTP-binding nuclear protein
RB3	stathmin-like gene
RHOK	rhodopsin kinase
RING	Really Interesting New Gene

SCG10	superior cervical ganglia neural-specific 10 protein
SCLIP	SCG10-like protein
SDS	sodium dodecyl sulphate
shRNA	short hairpin RNA
siRNA	short interfering RNA
Smurf 1	SMAD-specific E3 ubiquitin protein ligase 1
STRAD	STE20-related protein
TGFβ	Transforming growth factor beta
TIAM	T-cell lymphoma invasion and metastasis
TJs	tight junctions
TSC2	tuberous sclerosis complex 2
TβR2	type II TGF-β receptor
UBA	ubiquitin-associated domain
UCHs	ubiquitin C-terminal hydrolase
UPS	ubiquitin-proteasome system
USP	ubiquitin-specific protease
USP9X	ubiquitin-specific proteases number 9 X-linked
WT	wild-type

1. Introduction

1.1 Neuronal development and maturation

Neurons are the core functional cells of the central nervous system (CNS). They are highly polarized cells possessing multiple dendrites, which receive synaptic input from other neurons. When the synaptic input reaches a threshold, an action potential is generated and propagated away from the cell body along the axon where it synapses with another one or more neurons. Therefore the formation of axon-dendritic polarity is central to neuronal function (Andersen and Bi, 2000). Due to the highly complex nature of the developing CNS *in vivo* with multiple overlapping cell populations, cultures of embryonic hippocampal neurons have been widely used to study cellular and molecular aspects of neuronal development *in vitro* (Dotti et al., 1988, Witte et al., 2008). Commonly, hippocampal neurons are isolated from late-stage embryonic brains (embryonic day 18.5 (E18.5) in mice) and upon attachment to the tissue culture plates initiate a process of axon-dendritic polarization. The morphological maturation of neurons in culture is well established and widely studied (Shao et al., 2013, Devaux et al., 2012, Stagi et al., 2006). Upon plating, the immature post-mitotic neurons form lamellipodia and filipodia surrounding the nucleus (Stage 1, **Figure 1.1**). The outgrowth of minor processes results in the formation of multiple immature neurites, designated Stage 2. Stage 3 is the most critical step, where one of the neurites grows rapidly to become an axon. The remaining neurites which grow more slowly become dendrites at Stage 4. Finally at Stage 5, neurons are mature and ready for synapse formation as shown in **Figure 1.1** (Dotti et al., 1988, Craig and Banker, 1994, Barnes and Polleux, 2009).

Axon development can be divided into three main phases: (i) specification, which occurs during neuronal polarization, (ii) growth or extension and (iii) differentiation, in which the branches develop further for presynaptic synapse with the dendrites of another neuron (Lewis et al., 2013, Barnes and Polleux, 2009). Multiple factors regulate these phases, including those involved in the establishment of neuronal polarity, as well as those controlling actin/microtubule dynamics, which drives neuronal extension. Some of the components involved in these processes are

members of core neuronal signalling pathways such as TGFβ (Yi et al., 2010), Notch (O'Keefe et al., 2011) and mammalian target of rapamycin (mTOR) (Morita and Sobue, 2009, Li et al., 2008). The aim of this project was to examine the role of the deubiquitylase Usp9X in axon specification and growth and elucidate the possible molecular mechanisms involved in these processes using dissociated hippocampal neurons.

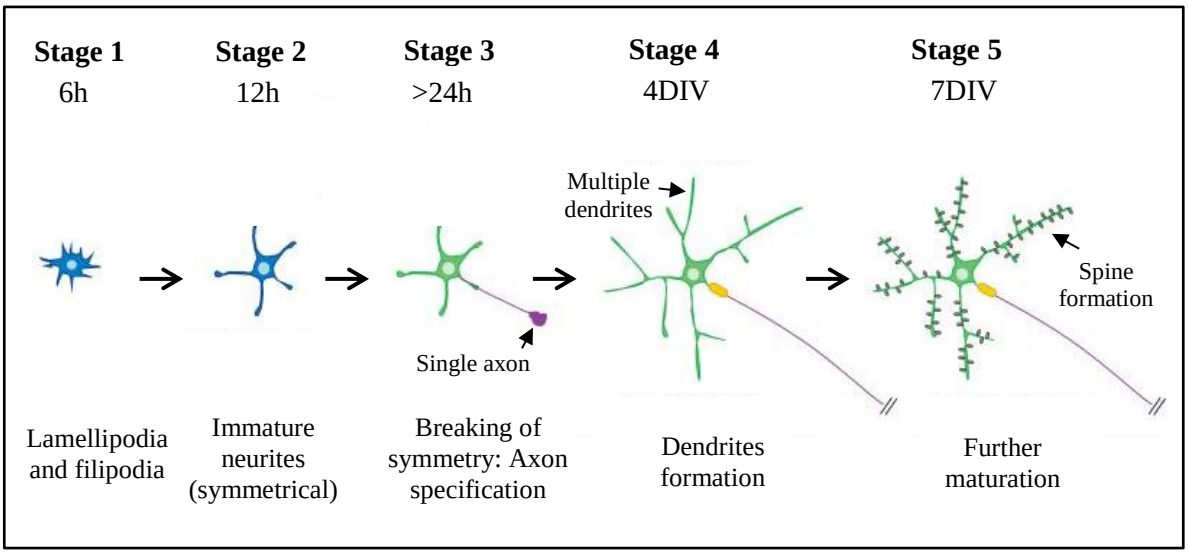

Figure 1.1 Establishment of polarity and stages of development in hippocampal neurons

Dissociated hippocampal neurons form lamellipodia or filopodia structures surrounding the nucleus a few hours after plating (Stage 1), and shortly after multiple neurites begin to sprout (Stage 2). These neurites extend and retract without net elongation. The following day, one of the neurites, with an enlarged growth cone at its tip, elongates rapidly without retraction to form the axon (Stage 3; see darkened arrow). Several days later, the remaining neurites continue to grow and branch to form the dendrites (Stage 4). In a final step of maturation, the axon and dendrites develop further and dendritic protrusions, or spines, appear (Stage 5). Reproduced with permission, from Barnes AP and Polleux F. (2009) Establishment of axon-dendrite polarity in developing neurons. *Annual Review of Neuroscience*, **32** 347-381.

1.1.1 Neuronal cytoskeleton: Microtubules and actin

Neuronal microtubules

Microtubules are the major structural proteins of the cytoskeleton and determine the polarized axon-dendrite compartment of the neuron. The microtubule is a long polarized filament which forms from the polymerization of α- and β-tubulin subunits which occurs only at the growing end ('plus end'), while at the negative end de-polymerization occurs (Conde and Caceres, 2009). At the plus end, microtubules also undergo cycles of growing and shrinking, and axon extension occurs when the microtubule is assembled. During polymerization, the αβ-tubulin dimer binds to GTP and becomes stable, forming a cap of GTP-bound tubulin, promoting assembly of microtubule. However, GTP hydrolysis over time converts GTP-tubulin in the lattice to GDP-tubulin. During microtubule de-polymerization, GDP-tubulin protofilaments curl and peel off the microtubule plus ends. The transition from growth to shrinkage is called a 'catastrophe' whereas the switch from shrinkage to growth called a 'rescue' (**Figure 1.2**).

There are two major differences in the organization of microtubules in axons and dendrites. First, in terms of orientation, axonal microtubules have uniform orientation, with their plus end directed away from the cell body. Dendritic microtubules, on the other hand, have mixed orientation, with equal amounts directing their plus end away or toward the cell body. Second, microtubules are bound by different microtubule-associated proteins (MAP). For example, Tau is found associated with microtubules mainly in the axon whereas MAP2 is found mostly in the dendrites (Hirokawa et al., 1996, Overly et al., 1996, Conde and Caceres, 2009). Deletion of MAP2 in mice and cultured hippocampal neurons has been shown to decrease the density of dendritic microtubules and their reduced dendritic length suggests that MAP2 is required for dendrite elongation (Harada et al., 2002, Dinsmore and Solomon, 1991). Tau on the other hand regulates microtubule stability and axonal transport. When Tau is hyper-phosphorylated, it detaches from the microtubule affecting microtubule dynamics. The amount of Tau on the microtubule surface also affects axonal transport (Matenia and Mandelkow, 2009, Timm et al., 2006).

In symmetrical (Stage 2) neurons, it is the local stability of microtubules in a single neurite that specifies axonal identity (Witte et al., 2008). In the axon, there is higher

expression of tyrosinated α-tubulin (dynamic microtubule) at the axonal tips and acetylated α-tubulin (stable microtubule) in the rest of the axon, suggesting that dynamic microtubules are located at the distal end of the axon and stable microtubules at the proximal region (Witte et al., 2008). Microtubules act as a railway for polarized transport and distribution of different protein cargos or organelles, which is essential for the maintenance of axon-dendritic compartments in neurons.

Actin

The polymerization of actin monomers (G-actin) into a double helical structure of actin filaments (F-actin) is also important for the formation of axon-dendritic structure in neurons (Lewis et al., 2013). Actin dynamics are important for both axon specification and growth. Local instability of actin in a single neurite, induced by cytochalasin-D, results in actin breakdown, which in turn specifies the neurite to become an axon (Bradke and Dotti, 1999).

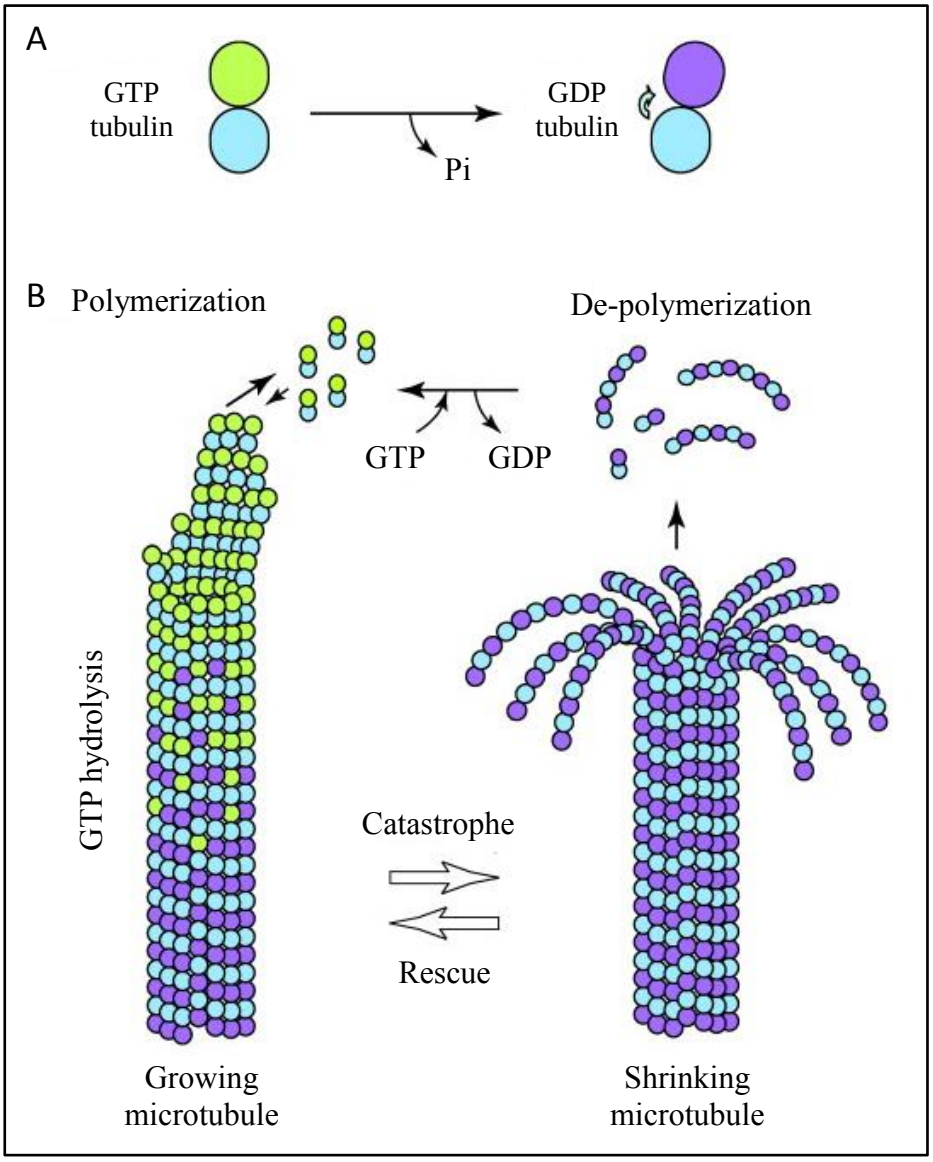

Figure 1.2 Polymerization and de-polymerization of dynamic microtubules

(A) Conformational change of αβ-tubulin accompanying GTP hydrolysis: a 'straight' tubulin dimer is formed when αβ-tubulin dimer (β-tubulin in green) binds to GTP. While a 'bent' tubulin dimer (arrow) is formed when the αβ-tubulin dimer binds to GDP. (B) Structural changes at microtubule plus ends: during microtubule polymerization, microtubule plus ends form a sheet-like group of straight protofilaments. GTP-tubulin dimers (green) assemble on the ends, forming a cap of GTP-tubulin. GTP hydrolysis over time converts GTP-tubulin in the lattice to GDP-tubulin. During microtubule de-polymerization, GDP-tubulin protofilaments curl and peel off the microtubule plus ends. The transition from growth to shrinkage is termed 'catastrophe' whereas the switch from shrinkage to growth is termed 'rescue'.

Reproduced with permission from (Al-Bassam and Chang, 2011) (License number 3557961045322).

1.1.2 Axonal growth cone

The axon consists predominantly of microtubules: however the axonal growth cone mainly consists of actin filaments because actin-dependent filopodia and lamellipodia structures form there (**Figure 1.3**). Both of these structures are largely composed of filamentous actin specifically, filopodia contain F-actin bundles and the lamellipodium form a dense F-actin meshwork (Korobova and Svitkina, 2008, Ichetovkin et al., 2002). In the growth cone, actin filaments are enriched in the peripheral domain and are organised into either F-actin bundles, or a F-actin meshwork or an actin arc. While microtubules are located predominantly in the central domain of the growth cone, they protrude into the actin-rich peripheral domain and interact with actin filaments **(Figure 1.3)** (Conde and Caceres, 2009, Lewis et al., 2013). The regulation of microtubule-actin interaction at the axonal growth cone is very important for both axon specification and growth. The factors regulating microtubule/actin dynamics, as well as the microtubule-actin interaction for both axon specification and growth are discussed in **Section 1.2 and 1.3**.

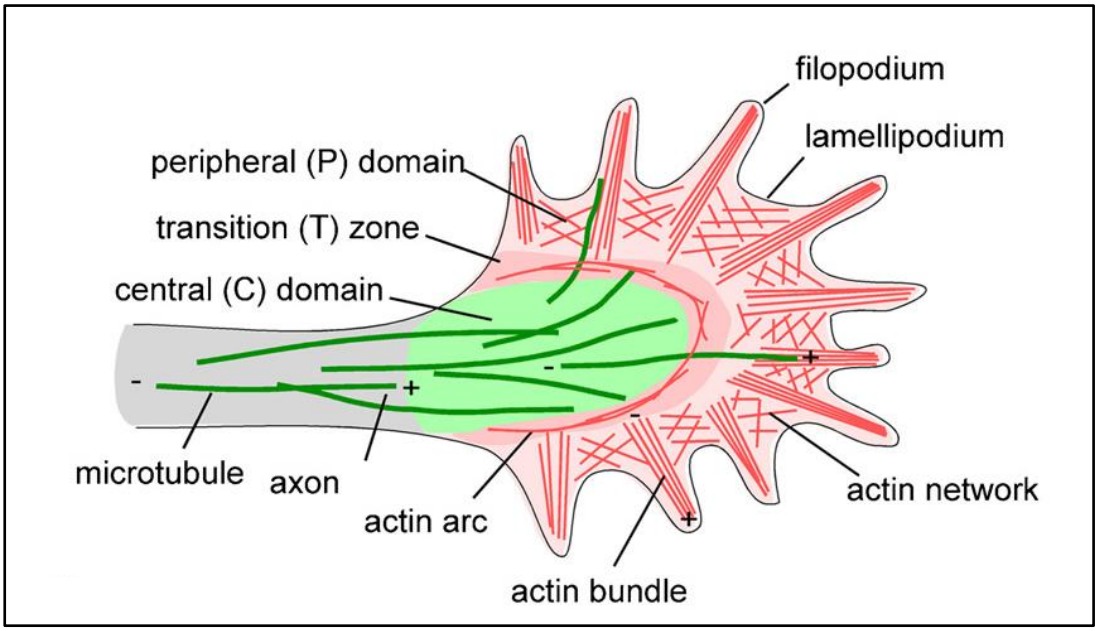

Figure 1.3 Schematic diagrams for the axonal growth cone

Plus (+) and minus (-) ends of microtubules and actin filaments are indicated. Reproduced with permission from (Suter and Miller, 2011) (License number 3557970226501).

1.2 Axon specification and neuronal polarity

1.2.1 Par complex and neuronal polarity

Neuronal polarization is the process of breaking cellular symmetry during the formation of axonal and dendritic compartments, analogous to apical-basal polarity in polarized epithelial cells (Dotti et al., 1988). One of the important factors regulating cell polarity is the partitioning defective (PAR) complex, which consists of Par3, Par6 and atypical protein kinase C (aPKC) (Fukuhara et al., 2002). The PAR polarity complex is highly conserved among species including flies, worms and mammals. Both Par3 and Par6 contain postsynaptic density protein PSD-95/Drosophila disc large tumor suppressor protein Dlg, and zonula occludens-1 protein ZO-1 (PDZ) domains which may interact with other PDZ domains or with specific sequence motifs. For instance, Par6 contains a PDZ domain, a cell division control 42, Cdc42 / Rac interactive binding (CRIB) domain which interacts with active forms of Cdc42 and Rac1, and the N-terminal domain which interacts with aPKC (Joberty et al., 2000, Johansson et al., 2000). Par3 contains three PDZ domains, one of which binds to the PDZ domain of Par6. The C-terminal region of Par3 interacts with the kinase domain of aPKC (Lin et al., 2000, Joberty et al., 2000). Therefore, Par3 can act as a scaffold to nucleate a multi-protein complex including Par6, activated Cdc42/Rac1 and aPKC (Lin et al., 2000, Joberty et al., 2000). Moreover, this complex has been shown to be involved in the establishment and maintenance of tight junctions and apical-basal polarity in epithelial cells. Over-expression of Par6 in Madin-Darby canine kidney (MDCK) cells has been shown to delay the assembly of functional tight junctions (Gao et al., 2002).

The PAR complex also plays a role during neuronal polarization. In symmetrical neurons both Par3 and Par6 are expressed uniformly in the soma and neurites. However, upon neuronal polarization, although they remain expressed in the soma they become enriched at the tip of the extending axon (Shi et al., 2003). The axonal localization of the Par3 / Par6 is likely to occur via the interaction of Par3 with the

microtubule plus-end directed motor protein kinesin KIF3A, as interference with KIF3A function leads to the delocalization of Par3 and aPKC from the axon tip (Nishimura et al., 2004). Ectopic expression of both Par3 and Par6 in dissociated hippocampal neurons has been shown to disrupt neuronal polarization and prevent axon specification, resulting in neurons that contain no axon but multiple projections of similar length (Shi et al., 2003). In addition, hippocampal neurons lost axon-dendritic polarization after treatment with bisindolylmaleimide, an inhibitor of aPKC (Shi et al., 2003). All these data indicate the importance of the PAR complex for proper neuronal polarization.

1.2.2 Kinases and axon specification

PI3K/Akt/GSK-3β pathway

The Phosphatidylinositide 3-kinases (PI3K) pathway is involved in axon specification as the pharmacological inhibition of PI3K activity, using LY294002 or Wortmannin, prevents axon formation (Kim et al., 2006, Shi et al., 2003, Polleux and Snider, 2010). Activated PI3K produces phosphatidylinositol (3,4,5)-trisphosphate (PIP3) and phosphoinositide dependent protein kinase-1 (PDK1) to phosphorylate Akt, which is also known as protein kinase B. Activated Akt in turn phosphorylates glycogen synthase kinase-3β (GSK-3β) inactivating its kinase activity. GSK-3β is able to phosphorylate multiple proteins including collapsin response mediator protein-2 (CRMP-2) **(Figure 1.4)**. CRMP-2 and tubulin are structural proteins related to microtubule dynamics, which is important for axonal growth (as discussed in **Section 1.3.1)**. Constitutive activation of GSK-3β disrupts neuronal polarization however, this can be rescued by the non-phosphorylated form of CRMP-2 (inactive), suggesting that GSK-3β regulates neuronal polarization via phosphorylation of CRMP-2 (Yoshimura et al., 2005). GSK-3β also regulates axon growth. Activated GSK-3β phosphorylates CRMP-2 at Thr-514 and abolishes the interaction between CRMP-2 and tubulin heterodimers, which are important for axon growth (Yoshimura et al., 2005). These data are consistent with studies showing that the depletion of GSK-3β, using either short interfering RNA (siRNA) or inhibition of GSK-3β activity with specific inhibitors, enhances axon growth and branching in cultured hippocampal neurons (Yoshimura et al., 2005, Kim et al., 2006).

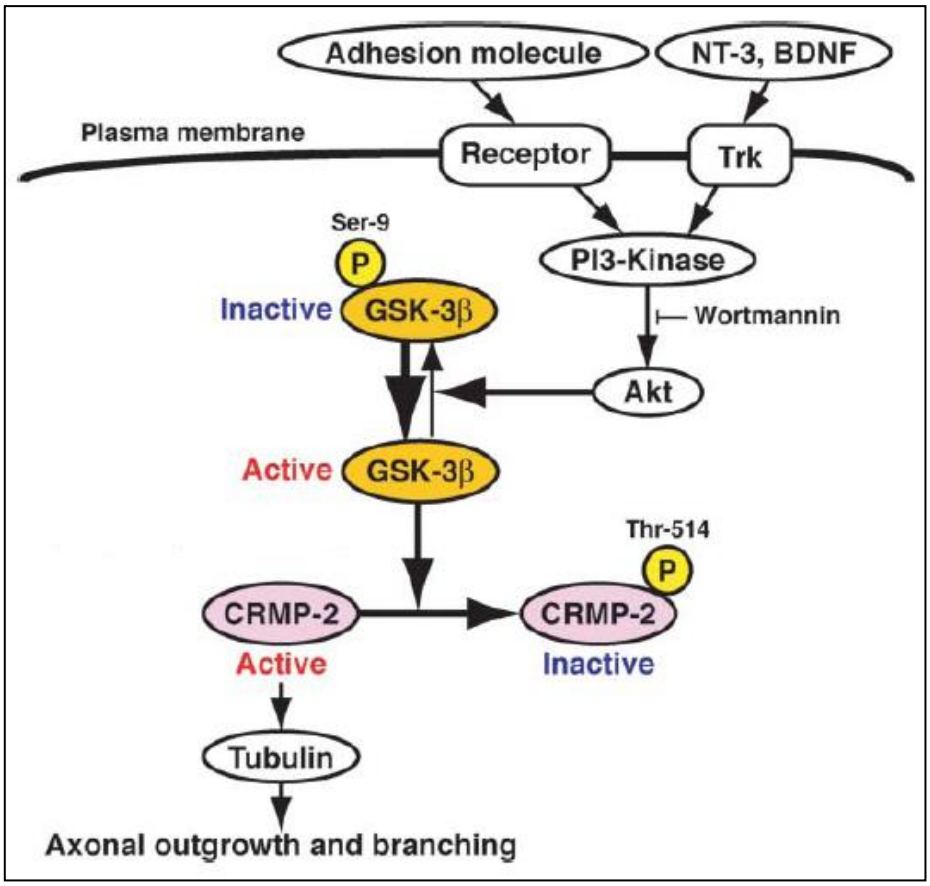

Figure 1.4 Activation of PI3K and GSK-3β phosphorylate CRMP-2

Adhesion molecule, NT-3 and BDNF activate PI3K and produces PIP3 and PDK1 which in turn phosphorylate Akt. Activated Akt phosphorylates GSK-3β inactivating the kinase activity of GSK-3β. Activated form of GSK-3β is able to phosphorylate CRMP-2 at Thr-514 preventing the axonal outgrowth and branching. Reproduced with permission from (Yoshimura et al., 2005) (License number 3565110517879).

LKB1/STRAD, SAD, MARK

Serine/threonine kinase 1, also known as liver kinase B1 (LKB1), homolog of Par4 is another group of kinases which is important for axon initiation. LKB1 binds to STRAD (STE20-related protein) and this complex promotes axon initiation during neuronal polarization (Shelly et al., 2007). Depleting either LKB1 or STRAD, using siRNA in dissociated hippocampal neurons, prevented axon differentiation while ectopic expression of LKB1 led to formation of multiple axons. One mechanism by which LKB1/STRAD could regulate neuronal polarization involves PKA-dependent phosphorylation of LKB1 at one of the neurites, which later forms the axon (Shelly et al., 2007). Another explanation is through the activation of synapses of amphids defective kinase, SAD-A/B kinases. It has been hypothesized, based on its role in presynaptic vesicular clustering in *C.elegan*, that SADA/B might specify axon identity by directing vesicular trafficking into the neurite becoming the axon (Crump et al., 2001). LKB1/STRAD also phosphorylates microtubule affinity regulated kinases (MARK1-4), which are required for axon specification because they phosphorylate microtubule-associated proteins such as Tau required for microtubule stability and axonal transport (Drewes et al., 1997, Matenia and Mandelkow, 2009).

1.2.3 TGFβ signalling pathway specifies an axon

Transforming growth factor beta (TGFβ) signalling pathway is one of the main extrinsic factors regulating neurogenesis. Treatment of embryonic hippocampal and cortical cells with TGFβ decreased the number of progenitors and increased the expression of neuronal markers, indicating that the TGFβ pathway reduces neural progenitors and promotes neuronal differentiation (Vogel et al., 2010). For the canonical Smad-dependent pathway, a TGFβ superfamily ligand initiates the pathway by binding to a type II TGFβ receptor (TβR2), which recruits and phosphorylates a type I TGFβ receptor (TβR1). The activated TβR1 then phosphorylates receptor-regulated Smads (R-Smad) which can now form a heterogenic complex with Co-mediator Smad (Co-Smad), Smad4. The activated R-Smad/Co-Smad complex translocates into the nucleus and regulates the transcription of target genes **(Figure 1.5)** (Shi and Massague, 2003, Dupont et al., 2009, Derynck and Zhang, 2003).

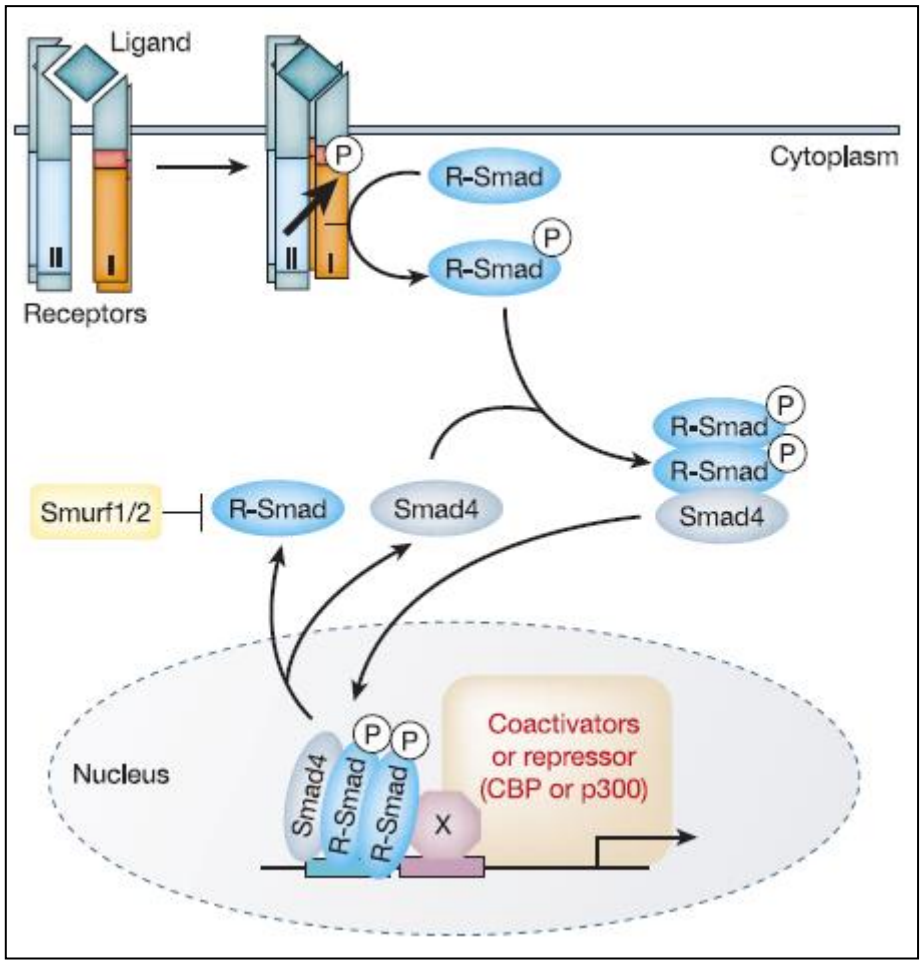

Figure 1.5 Smad-dependent TGFβ signalling pathway

At the cell surface, a TGFβ superfamily ligand binds to a type II TGFβ receptor (TβR2), which recruits and phosphorylates a type I TGFβ receptor (TβR1). The activated TβR1 phosphorylates R-Smads then form a complex with a common Smad4. Activated Smad complexes translocate into the nucleus, where they regulate transcription of target genes, through physical interaction and functional cooperation with DNA-binding transcription factors (X) and CBP or p300 coactivators. R-Smads and Smad4 shuttle between nucleus and cytoplasm. The E3 ubiquitin ligases Smurf1 and Smurf2 mediate ubiquitination and consequent degradation of R-Smads. Reproduced with permission from (Derynck and Zhang, 2003) (License number 3565160558824).

Multiple lines of evidence support the importance of the TGFβ pathway in axon development. Firstly, in *Drosophila* mushroom body neurons, loss of the TGFβ receptor results in axon over-extension (Ng, 2008). In the mouse brain, TGFβ is expressed throughout the CNS during development and there is high axonal expression of TGFβ receptors in migrating neurons of the developing cortex (Yi et al., 2010, Mecha et al., 2008). Deletion of the TGFβ receptor *in vivo* inhibited axon formation and disrupted the migration of neocortical neurons (Yi et al., 2010). This is further supported by *in vitro* observations where localized exposure of one neurite of symmetrical dissociated hippocampal neurons, to TGFβ ligand is sufficient to specify an axon (Yi et al., 2010). Besides axon specification, TGFβ pathway also regulates axonal growth, as TGFβ ligand treatment results in increased axonal length and branching in cultured neurons (Stegeman et al., 2013, Ishihara et al., 1994).

1.2.4 Microtubule-actin interactions and small GTPase signalling

There are multiple lines of evidence that suggest actin filaments influence microtubule dynamics. The reciprocal interactions between microtubules and actin are important for axon specification, as well as axon guidance and elongation. One of the main factors regulating the crosstalk between these two cytoskeletal elements in developing neurons is small GTPase signaling. Upon stimulation by an upstream signal, a guanine nucleotide exchange factor (GEF) converts the guanosine diphosphate (GDP)-bound inactive form into the guanosine triphosphate (GTP)-bound active form through GDP/GTP replacement. The GTP-bound form interacts with one or more specific downstream effector proteins. The GTP form exhibits a weak intrinsic GTPase activity for GTP hydrolysis, requiring a GTPase-activating protein (GAP) for efficient deactivation (Barnes and Polleux, 2009).

The Rho family of GTPases, including Rho, Rac and Cdc42, has been shown to regulate microtubule-actin interactions in developing neurons. For example, the inhibition of RHOK (rhodopsin kinase) in dissociated hippocampal neurons by expressing the HA-tagged Rho inhibitory toxin C3 (HA-C3) results in multiple axon formation (Da Silva et al., 2003). The disruption of neuronal polarity caused by the inhibition of RHOK could be related to its phosphorylation, and hence inactivation, of T-cell lymphoma invasion and metastasis, TIAM1 and TIAM2, which both are

GEFs for Rac, associated with microtubules involved in axon formation (Takefuji et al., 2007). Additionally, the inhibition of RHOK phosphorylates Par3, further enhancing Rac activation via TIAM1 (Nishimura et al., 2005). DOCK7 (dedicator of cytokinesis 7), a GEF for Rac, also regulates microtubule-actin interactions in developing neurons. Ectopic expression of DOCK7 induces multiple axon formation and conversely its depletion inhibits axon formation in hippocampal neurons *in vitro*. DOCK7 and Rac activation phosphorylates and inactivates the microtubule destabilizing protein stathmin in the nascent axon thus regulating axon formation (Watabe-Uchida et al., 2006). These opposing effects of Rho and Rac are important regulators of microtubule and actin dynamics which may specify axon formation.

GAPs also regulate neuronal polarization. One example is tuberous sclerosis complex 2 (TSC2), a GAP for Rheb GTPase, which is an activator for the mTOR kinase and associates with TSC2. TSC1 and TSC2 form a heterodimeric complex and function as TSC2 GAP to inhibit mTOR signalling (Wullschleger et al., 2006, Choi et al., 2008). Co-expression of TSC1 and TSC2 in dissociated hippocampal neurons has been shown to inhibit axon formation while their depletion by short hairpin RNA (shRNA) results in the formation of multiple axons. Knockdown of TSC1 and TSC2 is thought to promote axonal growth by increasing SAD activity and Tau phosphorylation (Choi et al., 2008).

1.3 Axon growth and extension

Axon elongation is dependent on two opposing forces generated at the growth cone. Firstly, it is the slow axonal transport of tubulin dimers and polymerization of microtubules which generates the pushing force from the axonal shaft. Secondly, the polymerization of actin at the leading edge of the growth cone and subsequent flow back towards the cell body (retrograde flow of actin), produces the pulling force at the front of the growth cone (Lewis et al., 2013, Conde and Caceres, 2009, Yang et al., 2012). In addition to microtubule and actin dynamics at the axonal growth cone, microtubule dynamics along the axon are the key player for sustaining axon elongation. This is due to the axonal transport of a variety of proteins, organelles and cytoskeletal elements along the microtubule through slow transport by motor

proteins. Disruption of the tubulin-dependent slow transport affects the polymerization of microtubules and thus axon elongation.

1.3.1 Microtubule dynamics regulate axon growth

Microtubule plus-end tracking proteins (+TIPs)

+TIPs are proteins that accumulate specifically at the plus end of the microtubule, regulate microtubule dynamics and growth direction, and associate with components of cell context. Adenomatous polyposis coli (APC) and end binding proteins EB1 and EB3 are examples of +TIPs. EB1 contains a calponin homology (CH) domain at the N-terminal that allows it to bind to the plus end of microtubules and a C-terminal that can associate with other +TIPs, including APC or motor proteins (kinesin and dynein) for axonal transport (Hayashi and Ikura, 2003, Gu et al., 2006, Conde and Caceres, 2009). EB1 has been implicated in axonal transport as it is required to target Kvβ2-mediated voltage-gated potassium (Kv1) channels to the axon, especially the growth cone for the generation of the action potential (Gu et al., 2006). Ectopic expression of APC has also been shown to inhibit axon formation and elongation (Zhou et al., 2004).

Microtubule de-polymerization proteins

The Stathmin family of genes encodes for stathmin-1, superior cervical ganglia neural-specific 10 protein (SCG10), SCG10-like protein (SCLIP) and stathmin-like gene (RB3) all of which are microtubule destabilising proteins (Grenningloh et al., 2004, Wen et al., 2010, Duncan et al., 2013). Stathmin-1 is a ubiquitous cytosolic protein whereas SCG10, SCLIP and RB3 are neuron-specific and membrane-associated (Grenningloh et al., 2004, Gupta et al., 2013). These proteins increase the rate of microtubule catastrophes, which are the transition from growth to shrinkage (**Figure 1.2**), either by acting directly at the plus end of the microtubule or by tubulin sequestration. This is thought to depend on the different termini of stathmin proteins as the N-terminus promotes microtubule catastrophes whereas the C-terminus exhibits tubulin-sequestering activity.

Microtubule polymerization proteins

These proteins are responsible for binding to tubulin heterodimers and promoting the assembly of microtubules. One example is CRMP-2 which regulates axon specification, as well as axon growth and branching (Inagaki et al., 2001, Fukata et al., 2002). Co-immunoprecipitation of CRMP-2 and α-tubulin or β-tubulin, from developing rat brain lysate, has shown that CRMP-2 interacts with both. It does this by linking the tubulin heterodimers to kinesin-1 which transports tubulin to the distal end of the growing axon (Kimura et al., 2005). The activity of CRMP-2 is regulated by different signalling pathways. For example, activation of the GSK-3β pathway phosphorylates CRMP-2 at Thr-514 and abolishes the interaction between CRMP-2 and tubulin heterodimers, inhibiting the elongation of the axon (Yoshimura et al., 2005).

Microtubule-associated proteins (MAPs)

One example of a MAP is Tau, which regulates microtubule stability and axonal transport. Tau protein is regulated by microtubule affinity regulated kinases (MARK1-4) (Matenia and Mandelkow, 2009, Timm et al., 2006). When Tau protein is phosphorylated by MARK, Tau protein detaches from the microtubule, resulting in destabilization of the cytoskeleton and tau aggregation (Matenia and Mandelkow, 2009, Timm et al., 2006). Recently, it has been shown that MARK4 is the crucial isoform of the MARK family implicated in the pathological phosphorylation of tau (Gu et al., 2013). Doublecortin (DCX) is another MAP that is present in the growing axon and enriched distally at the axonal growth cone (Tint et al., 2009). DCX has a strong bundling activity that promotes microtubule polymerization and stability (Gleeson et al., 1999, Francis et al., 1999, Horesh et al., 1999). High levels of DCX-microtubule binding are found at the axonal growth cone, promoting the polymerization of F-actin and regulating axon guidance (Tint et al., 2009, Fu et al., 2013).

Microtubule-dependent motor proteins

Axonal transport is crucial as proteins synthesized in the cell soma need to be transported to the axon or nerve terminal for proper neuronal function and survival. In the axon, transport occurs bi-directionally. Kinesin motor proteins are mainly responsible for transporting cargo from the cell body to the periphery (anterograde),

while dynein transports cargo from the periphery to the cell body (retrograde). There are two speed types of transport in the axon: slow transport for cytosolic proteins and cytoskeletal proteins, and fast transport for membranous organelles (Hirokawa et al., 2010). Generally, kinesin superfamily proteins (KIFs) are composed of a motor domain, which binds to the microtubule, a tail domain which is also known as the cargo binding region, and a stalk region where two kinesin monomers interact and dimerize. To date, 15 kinesin families have been identified, termed kinesin 1 to kinesin 14B. These families are grouped into three types depending on the position of the motor domain. N-kinesins and C-kinesins have a motor domain at the amino-terminal and carboxyl-terminal regions, respectively. M-kinesins, including KIF2A and KIF2C, have a motor domain in the middle and de-polymerize the microtubule (Hirokawa et al., 2010).

Among the kinesin motor proteins, kinesin-1, also known as KIF5, has been widely studied. KIF5 transports different cargo including mitochondria, synaptic vesicle precursors, potassium and sodium channels (Hirokawa et al., 2010). Multiple data show KIF5 is important for axon elongation. For example, deletion of the KIF5 family in the hippocampal neurons, using siRNA, inhibits the transportation of c-Jun N-terminal kinases-interacting protein-1 (JIP3) to the distal end of the axon, which in turn decreases axonal length (Sun et al., 2013). KIF5 also transports tubulin heterodimers to the distal end of the growing axon (Kimura et al., 2005).

1.3.2 JNK signalling regulates axon elongation

c-Jun N-terminal kinases (JNK) signalling regulates axon elongation (Sun et al., 2013). Using microfluidic chamber experiments it was shown that inhibition of the JNK pathway, with SP600125 inhibitor, at axon tips decreased axonal length. However, exposure of the JNK inhibitor at the cell body did not affect axonal length, suggesting that local activation of JNK at the axon tips facilitates elongation (Sun et al., 2013). Local activation of JNK at the axon tips is thought to occur through JIP3, as a mutated form of JIP3 was unable to activate cofilin. JNK/cofilin activation regulates actin filament dynamics, especially filopodia at the growth cone thereby promoting axon elongation (Sun et al., 2013). The role of the JNK pathway in axon elongation was further supported by another study (Dajas-Bailador et al., 2008),

which demonstrated that depletion of JIP1 in dissociated hippocampal neurons decreased axonal length. Promotion of axon elongation by JIP1 occurs through its interaction with c-Abl tyrosine kinase which is linked to neuronal receptors and cytoskeletal regulatory machinery (Dajas-Bailador et al., 2008).

1.4 The ubiquitin-proteasome system (UPS)

1.4.1 Ubiquitylation

As noted above a number of post-translational modifications regulate key aspects of axonal specification and maturation. Ubiquitylation is a post-translational process, which modifies a protein by the covalent attachment of ubiquitin. Apart from targeting a protein for proteosomal degradation, it also regulates various other cellular processes such as endocytosis, protein trafficking, cell cycle control, DNA repair, ribosome biogenesis and stress responses (Kim et al., 2003, Hamilton and Zito, 2013). Ubiquitin is a 76 amino acid protein found in all eukaryotes and is highly conserved. It marks intracellular proteins by forming an isopeptide bond between the carboxyl-terminal glycine and the amino group of lysine of the target protein. Attachment of ubiquitin to proteins is energy dependent and catalyzed by the action of an ubiquitin activating enzyme (E1), an ubiquitin conjugating enzyme, also known as ubiquitin-carrier enzyme (E2) and an ubiquitin ligase (E3) (**Figure 1.6**). In the first step, an E1 enzyme activates the carboxyl-terminal glycine residue of the ubiquitin molecule and the ubiquitin molecule is bound to a cysteine residue on the E1 enzyme. The activated ubiquitin molecule is then transferred to a cysteine residue on an E2. In the final step an E3 catalyzes the carboxyl-terminal linkage of the ubiquitin molecule to a lysine residue on the target protein. Typically, eukaryotic cells have only one E1 but multiple E2 and E3 enzymes. Although E2 enzymes show specificity for particular E3 ligases, it is the E3 ligases which confer substrate specificity and thus determine the selectivity of protein ubiquitylation. There are two major classes of E3 ligases characterised based on their ubiquitin-associated domains: the HECT (Homology E6 C-terminus) domain family and the RING-type (Really Interesting New Gene) family (Hershko and Ciechanover, 1998, Hegde, 2010, Hamilton and Zito, 2013).

The addition of a single ubiquitin to protein is termed mono-ubiquitylation. When multiple lysine residues of the substrate are also modified, multi-ubiquitylation occurs. Ubiquitin itself has seven lysine residues (K-6, K-11, K-27, K-29, K-33, K-48 or K-63) which can lead to chain formation or poly-ubiquitylation, with K-48 and K-63 being the most common linkages. Mono-ubiquitylation often serves as an endocytosis signal. K-48 poly-ubiquitylation usually targets a protein for degradation through the 26S proteasome-complex, which has a 20S catalytic core and two 19S regulatory caps (Hegde, 2010, Hamilton and Zito, 2013).

1.4.2 Deubiquitylation

The ubiquitylation status of intracellular proteins is also regulated by deubiquitylating enzymes (DUBs). DUBs catalyze the removal of ubiquitin from ubiquitin-protein conjugates. DUBs also function in processing the ubiquitin precursors to generate free ubiquitin monomers. To maintain cellular ubiquitin levels, DUBs disassemble polyubiquitin chains after protein degradation. Some DUBs also have a proofreading ability which is able to prevent inappropriate degradation of intracellular proteins. DUBs also play vital roles in biological processes such as protein trafficking, stability, localization and signalling (Hershko and Ciechanover, 1998, Millard and Wood, 2006, Kim et al., 2003). It has been proposed that some DUBs are involved in neurological diseases and oncogenesis (Rott et al., 2011, Schwickart et al., 2009, Perez-Mancera et al., 2012, Kim et al., 2003).

DUBs are classified into five classes according to their different catalytic domains: ubiquitin C-terminal hydrolase (UCHs), ubiquitin-specific proteases (USPs), Machado-Joseph disease protein domain proteases (MJDs), Ovarian tumor proteases (OTUs) and Jab1/MPN/Mov34 metalloenzyme (JAMM) motif proteases. UCH, USP, MJD and OTU are cysteine proteases whereas JAMM motif proteases are metallo proteases (Nijman et al., 2005). Approximately 95 DUBs, most of which belong to the USP family, have been putatively identified in the human genome. USPs have a core catalytic domain with strong homology in two regions called the Cysteine and Histidine boxes. The complete domain varies in size from 300-800 amino acids due to NH_2 and/or COOH terminal extensions and insertion between the two motifs (Nijman et al., 2005).

Most DUBs, especially of the USP class, are substrate specific. It has been suggested that both the active sites and domains outside of catalytic core contribute to their specificity. DUBs must be able to recognize different lengths of ubiquitin and lysine residues involved in ubiquitylation. The ubiquitylation status of the substrates (mono-, multi-ubiquitylation, linear and branch ubiquitin polymers) results in distinct functions and are recognized by different type of DUBs. Specificity of DUBs might also be aided by their interaction with different types of E3 ligases (Nijman et al., 2005).

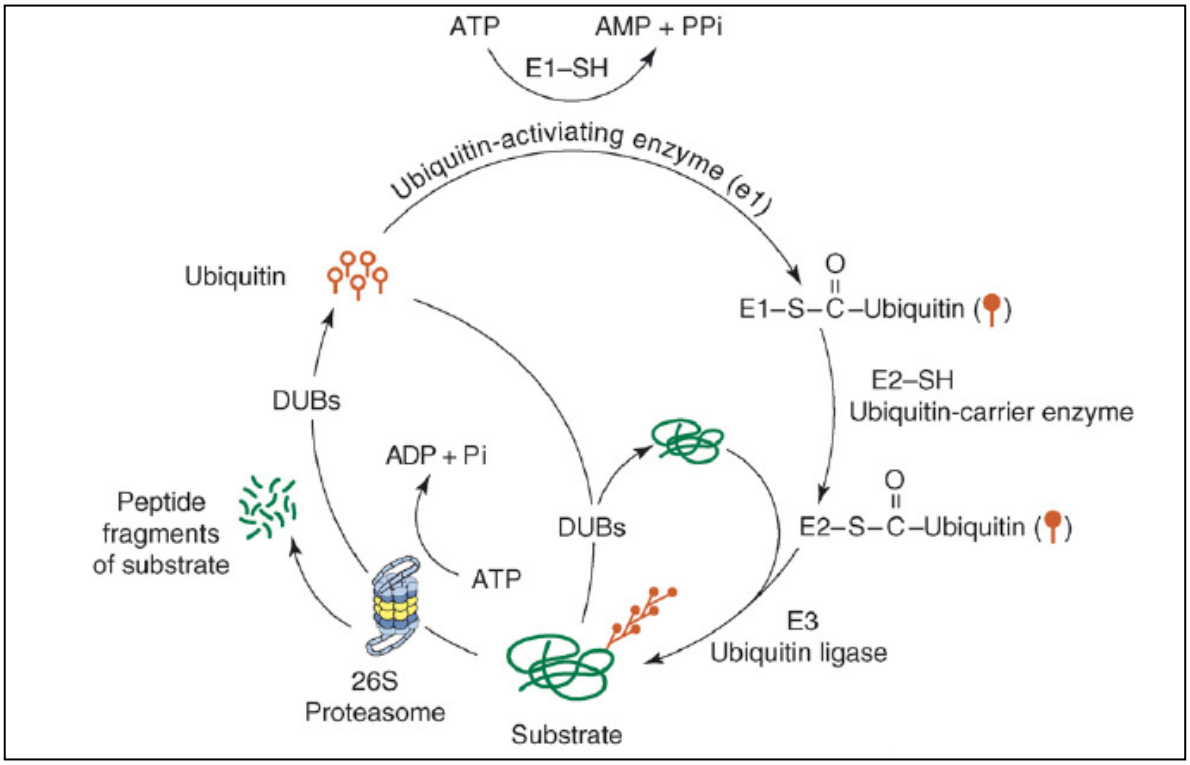

Figure 1.6 Ubiquitylation and deubiquitylation

Ubiquitin is attached to ubiquitin activating enzyme (E1) by forming a thiol ester link and is energy dependent. Ubiquitin is then transferred to ubiquitin conjugating enzyme/ubiquitin carrier enzyme (E2) and later to ubiquitin ligase (E3). E3 then adds ubiquitin to the substrate. Poly-ubiquitylated substrates are either degraded by the proteolytic 26S proteosome, which is energy dependent or deubiquitylated by the deubiquitylating enzymes (DUBs). Reproduced with permission from (Hegde and Upadhya, 2007) (License number 3564630696896).

1.4.3 The UPS in axon development

The UPS is thought to play an important role during axon development as there are multiple examples showing that local protein degradation is required for both axon specification and growth. For example, the inhibition of UPS, by treating the hippocampal neurons in culture with the proteasomal inhibitor MG132, results in the loss of axon-dendritic polarity (Yan et al., 2006). In addition, local UPS-mediated degradation of the inactive form of Akt and local stabilisation of activated Akt at a single neurite promotes axon formation and axon-dendrite polarity (Yan et al., 2006). Yet another report showed that the E3 ubiquitin ligase Smurf1 is able to stabilise Par6 and target RhoA for degradation in dissociated hippocampal neurons, promoting axonal formation and growth (Cheng et al., 2011a).

Ubiquitin-dependent mechanisms regulate *Drosophila* neuromuscular junction (NMJ) and synaptic function. This was the first evidence that a DUB was important for neurogenesis (DiAntonio et al., 2001). Neuronal overexpression of the *fat facets* gene (the homologue of mammalian Usp9X) in *Drosophila* leads to synaptic overgrowth, including a large increase in the number of synaptic boutons, an elaboration of the synaptic branching pattern, as well as disruption of synaptic function. Usp9X was later found in the synapses of rat CNS neurons, consistent with a role in synaptic development or function in mammals (Chen et al., 2003). The studies mentioned above strongly indicate that ubiquitylation and deubiquitylation activities are crucial for normal neuronal development and axon formation. This present study focused on the substrate-specific deubiquitylating enzyme, Usp9X and its role during axon formation.

1.4.4 Usp9X regulates axon development

At the cellular level, Usp9X is predominantly expressed in punctate structures in the soma, dendrites and axon, and highly enriched in the axonal growth cone in dissociated hippocampal neurons (Homan et al., 2014, Stegeman et al., 2013). It has recently been suggested to regulate axon development based on studies using Usp9X brain-specific knockout mice (Stegeman et al., 2013, Homan et al., 2014). Several alterations in neuronal projections were detected in multiple regions of the mouse brain. In the embryonic mouse brain, neuronal projections from the entorhinal cortex

to the hippocampus were reduced when Usp9X was absent (Stegeman et al., 2013). In the adult mouse brain, the size of the corpus callosum, which is the major axonal tract connecting the cerebral hemispheres, was markedly reduced in the absence of Usp9X (Stegeman et al., 2013). These findings are supported by *in vitro* evidence showing the absence of Usp9X disrupts normal neurite outgrowth. For example, 3, 5 and 7 *days in vitro* (DIV) cultures of hippocampal neurons in which Usp9X had been deleted displayed shorter axonal length compared to wild-type cultures, without the dendrite length being affected. Usp9X is also required for normal dendritic and axonal arborisation as the number of both axonal and dendritic termini was reduced in the Usp9X-null hippocampal neuronal cultures (Stegeman et al., 2013, Homan et al., 2014). Importantly, three Usp9X variants have been associated with X-linked intellectual disability in humans. These point mutations disrupt the ability of Usp9X to function properly in axonal growth and migration (Homan et al., 2014). All these data strongly indicate that Usp9X plays a role during axon formation and migration.

1.5 Usp9x substrates implicated in axon development

1.5.1 Usp9X and cell polarity

Usp9X has been linked to cell polarity and adhesion, which are two major determinants of cell morphology and hence function. In polarized epithelial cells, the apical membrane is separated from the basolateral membrane by tight junctions (TJs) and adherens junctions (AJs) (Farquhar and Palade, 1963). TJs are the most apical component of the junctional complex, and serve as a barrier to prevent solutes and water passage through the paracellular pathway. AJs on the other hand, connect to the actin cytoskeleton for further maturation of junctional adhesion (Kriegstein and Gotz, 2003). Usp9X regulates multiple substrates of which some are adhesion and polarity proteins, including AF-6 (Afadin), β-catenin and EFA6 (Taya et al., 1998, Taya et al., 1999, Theard et al., 2010).

Cell polarity is central to the self-renewal and cell fate decisions of neural progenitors (NPs). Usp9X has been shown to regulate NP polarity both *in vitro* and *in vivo*. Firstly, Usp9X is highly expressed in NPs in a polarized manner (Jolly et al., 2009). In embryonic stem cell derived NPs, over-expression of Usp9X promotes the

formation of polarized clusters of radial glial-like NPs. Adherens junction proteins and apical markers were concentrated at the centre of the cluster, and as such resemble the apical end-feet of NPs *in vivo*. This polarization of NPs promoted their self-renewal capacity and increased the number of both NPs and neurons *in vitro*.

In vivo, Usp9X is highly expressed in other progenitor populations including the pluripotent blastomeres of mouse pre-implantation embryos (Pantaleon et al., 2001). Depletion of Usp9X from two-cell mouse embryos results in failure of the embryos to develop to blastocysts. Usp9X deficiency not only resulted in slower blastomere cleavage rate, but inhibition of cell adhesion, as well as loss of cell polarity (Pantaleon et al., 2001). In addition, Nestin-Cre mediated deletion of Usp9X in mouse brain has been shown to affect adhesion and polarity proteins in embryonic NPs. Deletion of Usp9X results in decreased levels of adhesion proteins (N-cadherin, AF-6) and polarity proteins (aPKC, CD133) at E12.5, although these returned to normal at E14.5 and E16.5. However, the organisation of NPs in the ventricular and sub-ventricular zones remained perturbed in late stage E18.5 embryos (Stegeman et al., 2013). Somewhat surprisingly Usp9X depletion led to elevated expression of β-catenin at E12.5 and this elevated expression was maintained until at least E16.5 (Premarathne and Wood, unpublished). These observations support the hypothesis that Usp9X has an essential role in cell polarity and adhesion regulation.

AF-6 (Afadin)

Usp9X regulates acute lymphoblastic leukemia-1 (ALL-1) fusion partner from chromosome 6 (AF-6), a polarity and adhesion protein and Ras target (Kuriyama et al., 1996, Taya et al., 1998). The interaction between Usp9X and AF-6 has been suggested to recruit Usp9X to TJs in Madin-Darby canine kidney (MDCK) epithelia cells. At the plasma membrane, Usp9X co-localizes with AF-6 at the points of cell-cell contact and opposes the ubiquitylation of AF-6 (Taya et al., 1998, Murray et al., 2004). Deletion of AF-6 *in vivo* has been shown to weaken cell polarity and disrupt cell-cell adhesion in the ectoderm, particularly the nascent neuroectoderm (Zhadanov et al., 1999).

In cortical neurons, AF-6 accumulates in the budding growth cones of the axonal tips (Iwasawa et al., 2012). Elevated expression of AF-6 in cultured cortical neurons

increased axon number without affecting the axonal length (Iwasawa et al., 2012) and the Ras/AF-6 pathway has also been suggested to induce axonal branching in an actin-dependent manner (Mandai et al., 1997, Iwasawa et al., 2012).

β-catenin

Usp9X regulates the stability of β-catenin, which is an adhesion protein as well as part of the Wnt signalling pathway (Taya et al., 1999, Pantaleon et al., 2001, Chenn and Walsh, 2002). In the polarized intestinal epithelial cell line T84, Usp9X co-localizes with multiple adhesion proteins such as β-catenin, p120 catenin and Z0-1. Interestingly, Usp9X only interacts with β-catenin and E-cadherin in subconfluent cells where adhesion junctions are unstable and undergoing dynamic rearrangements (Murray et al., 2004). The E-cadherin-β-catenin complex plays an essential role in the establishment and maintenance of AJs and is targeted for degradation by the ubiquitin-proteasome pathway. Knockdown of Usp9X using antisense oligonucleotides in the pre-implantation mouse embryo resulted in a reduction of both AF-6 and β-catenin, an inhibition of cell-cell adhesion and a decrease in cell cleavage events (Pantaleon et al., 2001).

EFA6

In MDCK epithelial cells, Usp9X regulates TJ biogenesis by controlling the levels of the exchange factor for ARF6 (EFA6), a protein essential for TJ formation (Theard et al., 2010). Usp9X-mediated deubiquitylation of EFA6 is required for the establishment of TJs during a narrow temporal window, which precedes establishment of polarity (Theard et al., 2010). Depleting Usp9X was shown to disrupt TJ assembly but this could be rescued by over-expression of EFA6.

Overall, these studies show that Usp9X and its substrates, including cell adhesion and polarity components, play a role in apical-basal cell polarity. However, this regulation of cell polarity by Usp9X has been established in a variety of cell types but not neurons. Given the recent findings regarding the involvement of Usp9X for proper axon development (Stegeman et al., 2013, Homan et al., 2014), it is possible that Usp9X might regulate the formation of axon-dendritic polarization and this is worthy of further investigation. Although neurons do not contain adherens junctions, other factors associated with the actin/microtubule cytoskeleton play important roles

in maintaining neuronal polarity and axonal growth and it has recently been suggested that Usp9X regulates some cytoskeletal proteins (Homan et al., 2014).

1.5.2 Kinase, MARK4

As mentioned earlier in **Section 1.2.2**, the tumour suppressor kinase LKB1 forms a complex with STRAD and MO25, which is important for both axon specification and growth. These complexes activate MARK which in turn regulates microtubule stability and axonal transport through phosphorylation of Tau (Drewes et al., 1997, Mandelkow et al., 2004). One of these kinases, MARK4, is a substrate for Usp9X (Al-Hakim et al., 2008). The regulation of Par1/MARK4 by Usp9X was originally identified in *Drosophila*, where Usp9X deubiquitylates activated Par1. Disruption of this regulation leads to accumulation of activated Par1 and synaptic toxicity (Biernat et al., 2002). Interaction between Usp9X and MARK4 in HEK293 does not control the stability of MARK4, but instead regulates its phosphorylation and activation by the LKB1 tumour suppressor (**Figure 1.7**) (Al-Hakim et al., 2008). This may reflect the fact that MARK4 is decorated with K-29 and K-33, and not K-48, poly-ubiquitin chains (Al-Hakim et al., 2008).

Loss of LKB1 in cortical pyramidal neurons prevents axon formation whereas overexpression of LKB1 and STRAD in NPs or LKB1 alone in post-mitotic cells leads to the formation of multiple axons (Shelly et al., 2007, Asada et al., 2007). Therefore, loss of Usp9X might increase ubiquitylation of MARK4 and prevent phosphorylation by LKB1, hence preventing axon formation. This might contribute to the shorter axonal length in Usp9X knockout neurons (Al-Hakim et al., 2008, Trinczek et al., 2004).

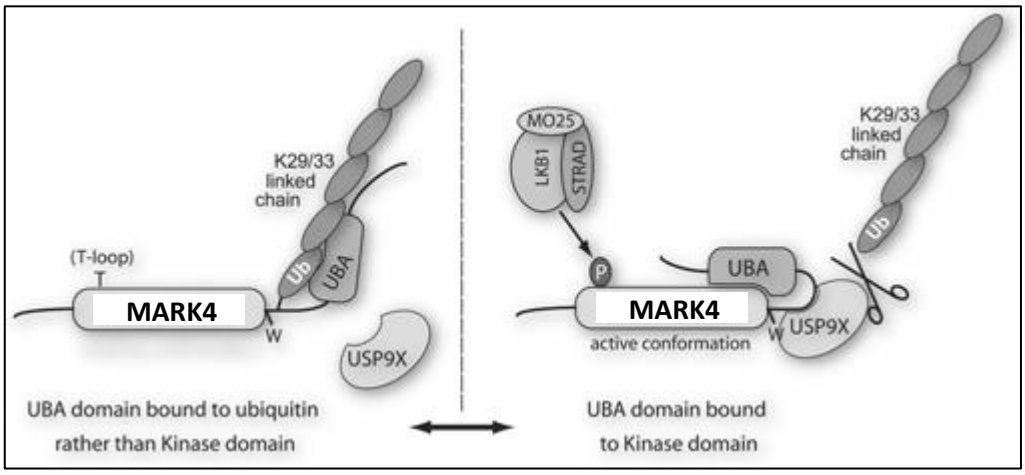

Figure 1.7 Usp9X de-ubiquitylates MARK4 and promotes the activation of kinase by LKB1

When MARK4 is ubiquitylated, the poly-ubiquitin chain is either Lys-29 or Lys-33. MARK4's ubiquitin-associated (UBA) domain binds to the ubiquitin chain. When MARK4 is de-ubiquitylated by Usp9X, the UBA domain binds to the kinase domain and the LKB1/STRAD/MO25 complex activates MARK4 by phosphorylating a conserved threonine residue located within the T-loop of the kinase domain. Reproduced with permission, from Al-Hakim AK, Zagorska A, Chapman L, Deak M, Peggie M, Alessi DR. (2008) Control of AMPK related kinases by USP9X and atypical Lys(29)/Lys(33)-linked polyubiquitin chains. *Biochemical Journal*, **411(2)** 249-260. © the Biochemical Society.

1.5.3 Usp9X, the TGFβ signaling pathway and axon development

As mentioned earlier in **Section 1.2.3**, the TGFβ signaling pathway regulates both axon specification and growth in cultured hippocampal neurons (Ishihara et al., 1994, Yi et al., 2010). Recently, Usp9X has been suggested to have a regulatory role in TGFβ-mediated axon formation. This is based on studies using dissociated hippocampal neuron from Usp9X knockout mice, which have shorter axonal length, decreased numbers of axonal branches and reduced ability to migrate (Stegeman et al., 2013, Homan et al., 2014). This is consistent with the findings by Yi et al. (2010) suggesting the involvement of Usp9X in the regulation of axon production via TGFβ signaling pathway. In addition, studies have shown that dissociated hippocampal neurons do not respond to exogenous TGFβ ligand when Usp9X is absent. This was demonstrated using both a transfected TGFβ luciferase reporter construct as well as

the endogenous target gene, brain-derived neurotrophic factor (BDNF) (Stegeman et al., 2013). In these experiments while wild-type neurons responded to increasing TGFβ concentrations with increased luciferase activity or BDNF mRNA levels, Usp9X-null neurons did not alter basal levels. Functionally, TGFβ treatment did not induce axonal growth in Usp9X null neurons as it did in the wild-type neurons. These data indicate that Usp9X is required for cultured hippocampal neurons to respond to TGFβ (Stegeman et al., 2013).

There are several possible molecular mechanisms whereby Usp9X might regulate the TGFβ pathway during axon development, two of which include the known Usp9X substrates, Smad4 and Smurf1, the common second messenger and an E3 ubiquitin ligase of the TGFβ pathway, respectively (Dupont et al., 2009, Xie et al., 2013). Another possibility is through the new putative Usp9X target, PJA1, identified in a yeast-2-hybrid screen and mass spectrometry following Usp9X affinity purification (Agrawal et al., 2012).

Smad4

Usp9X regulates TGFβ signalling pathway, at least in multiple systems, via Smad4 (Dupont et al., 2009). TGFβ-mediated neuronal differentiation has been shown to be Smad4-dependent (Vogel et al., 2010). Smad4 shuttles between the nucleus and cytoplasm, and its localization is regulated by Ectodermin and Usp9X. Ectodermin is an E3 ubiquitin ligase for Smad4. It ubiquitylates Smad4 at lysine 519 in the cell nucleus, preventing the binding of Smad4 to the activated form of Smad complex and thus inhibits the TGFβ pathway (Dupont et al., 2005). Subsequently, Smad4 was found to be deubiquitylated in the cytoplasm by Usp9X, in both mammalian cell lines and *Drosophila.* Deubiquitylation by Usp9X was shown to activate Smad4 rather than stabilise it, as the loss of Usp9X did not affect the levels of Smad4 (Dupont et al., 2009). Under normal conditions, activation of the TGFβ pathway results in the binding of free Smad4 in the cytoplasm with phosphorylated Smad2, 3 complex and translocation into the nucleus of the cells (Dupont et al., 2009, Vogel et al., 2010). It is proposed that when Usp9X is absent, Ectodermin targets Smad4 for ubiquitylation and prevents its binding to the phosphorylated Samd2, 3 complexes and thus reduces the percentage of nuclear Smad4 in the cells, inhibiting the activation of TGFβ signalling for axon development (**Figure 1.8**).

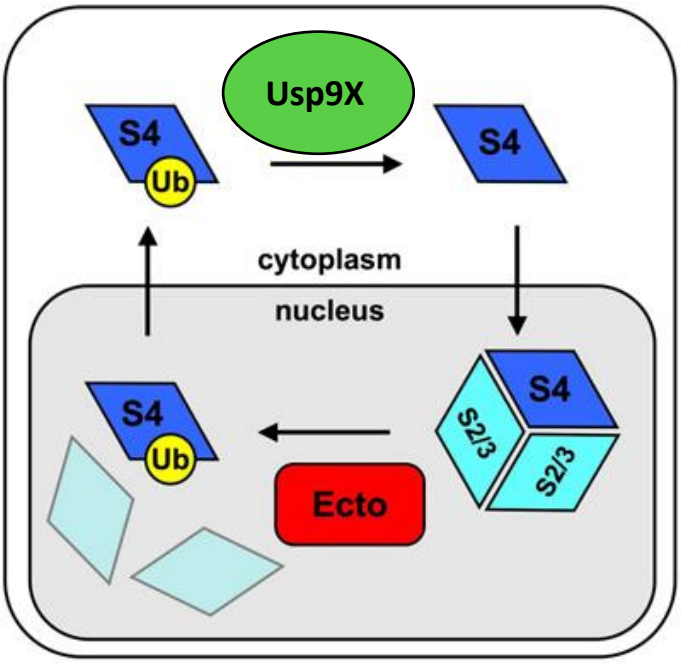

Figure 1.8 Ubiquitylation status of Smad4 is regulated by Ectodermin and Usp9X Ectodermin (Ecto) mono-ubiquitylates Smad4 (S4) in the nucleus and prevent its binding to the Smad 2/3 complex (S2/3) and inhibits the activation of TGFβ pathway. Usp9X in turn de-ubiquitylates Smad4 in the cytoplasm, Smad4 binds to the activated form of the Smad2/3 complex and translocates into the nucleus when the TGFβ pathway is activated. Reproduced with permission from (Dupont et al., 2009) (License number 3557950245638).

Smurf1

Smurf 1 is also a Usp9X substrate (Xie et al., 2013). Smurf1 was originally reported for its negative regulation of the TGFβ/BMP (bone morphogenetic proteins) pathways (Zhu et al., 1999, Ebisawa et al., 2001). Activation of the TGFβ pathway triggers the expression of the inhibitory Smad, Smad7. Smurf1 binds with Smad7 in the nucleus and translocates into the cytoplasm. This complex then binds to the TGFβ type-I receptor targeting it for degradation and thereby inhibiting the TGFβ pathway (Ebisawa et al., 2001). Smurf 1 (SMAD-specific E3 ubiquitin protein ligase 1) can be auto-ubiquitylated through its intrinsic HECT (homologous to E6AP carboxyl terminus) E3 ligase activity targeting it for proteasomal degradation. It can be targeted by other ubiquitin ligases as well such as SMURF2 and SCFFBXL15 (Fukunaga et al., 2008, Cui et al., 2011). Auto-ubiquitylation of Smurf1 is

antagonized by Usp9X resulting in its stabilisation (Xie et al., 2013). It is possible that in the absence of Usp9X auto-ubiquitylated Smurf1 will be degraded thereby preventing the negative regulatory effect of Smad7.

PJA1

E3 ubiquitin ligase Praja 1 (PJA1) has been shown to ubiquitylate embryonic liver fodrin (ELF), a tumor suppressor and Smad4 adaptor protein in TGFβ signalling pathway (Saha et al., 2006, Mishra et al., 2005). PJA1 also regulates neuronal differentiation by targeting NGARE, which is a class II melanoma antigen (MAGE) family member (Teuber et al., 2013). NGARE has been shown to be involved in the neuronal differentiation of PC12 cells (Feng et al., 2010). Elevated expression of PJA1 reduces the expression of NGARE and this in turn inhibits the neuronal differentiation of PC12 cells after induction with nerve growth factor (NGF) (Teuber et al., 2013). However, the role of PJA1 via TGFβ signalling pathway in axon formation remains unclear.

Based on a yeast-2-hybrid screen using a 14-week old human fetal brain library and full-length Usp9X as a bait, an interaction between Usp9X and PJA1 was predicted with high confidence (Wood, unpublished). An independent report also identified PJA1 by mass spectrometry from Usp9X affinity purification experiments suggesting that there is high probability that PJA1 is a Usp9X interacting protein, and possible substrate (Agrawal et al., 2012). Therefore, further experiments are required to determine if Usp9X regulation of axon specification and growth is mediated through TGFβ pathway regulation and, if so, to map precisely where in the pathway it occurs.

1.5.4 Usp9X-doublecortin (DCX): Neuronal migration

Doublecortin (DCX) is a microtubule-associated protein which is important for neuronal migration and differentiation (Francis et al., 1999, Gleeson et al., 1999, Horesh et al., 1999). It contains a microtubule binding domain which is composed of two repeats at amino acids 47-135 and 174-259 and a serine/proline rich region at its carboxyl terminal (Sapir et al., 2000, Taylor et al., 2000). DCX has been shown to bind to the microtubule cytoskeleton and cause bundling (Moores et al., 2006). Mutation of DCX is one of the major causes of lissencephaly in humans, where the

layers of the cerebral cortex are disorganised due to defective neuronal migration, and is associated with mental retardation and epilepsy (Gleeson et al., 1998). The first repeat binds to tubulin but not microtubules and enhances microtubule polymerization (Sapir et al., 2000). DCX is expressed in both the intermediate zone and the cortical plate of the developing cortex. In the adult brain, it is expressed only in neurons migrating from the subventricular zone to the olfactory bulb (Gleeson et al., 1999, Francis et al., 1999).

There are three variants within the C-terminal region of Usp9X that have been associated with X-linked intellectual disability. All the Usp9X variants disrupt the localization of Usp9X and DCX at the axonal growth cone and all three variants display defects in axonal growth and neuronal migration (Homan et al., 2014). Usp9X interacts with DCX at the C-terminal region. However, DCX is not a Usp9X substrate and their interaction is thought to transport Usp9X in the axon and other neuronal processes (Friocourt et al., 2005). The DCX/Usp9X complex is co-localized with microtubules at the distal portion of the neurites in differentiating neurons (Friocourt et al., 2005). Usp9X trafficking by DCX may facilitate interactions between Usp9X and other substrates or component protein essential for axonal and neurite development. The interaction between DCX and Usp9X may play some role in axon formation. For example, Usp9X could regulate the association of DCX with microtubules at the extremities of neuronal processes in migrating and differentiating neurons. There is also the possibility that the DCX/Usp9X complex regulates adhesion and membrane turnover, which are essential for neuronal migration and differentiation.

1.5.5 Usp9X regulates cytoskeletal proteins

Usp9X has been shown not only to associate with cytoskeletal elements in epithelial cells (Murray et al., 2004), but regulate neuronal cytoskeleton based on 2D proteomic analysis of 5 *days in vitro* (DIV) Usp9X-null cortical neurons (Homan et al., 2014). In this latter study, 28 proteins were identified that were deregulated in neurons in the absence of Usp9X, with 27 down-regulated and one up-regulated. Among these proteins the majority are structural proteins including tubulin subunits (tubulin βIII, βIIB, βIIC and α1A), microtubule dynamics related proteins (stathmin-

1, Dihydropyrimidinase-related protein 2 and 3, also known as CRMP2 and CRMP4) and actin filament dynamics related proteins (cofilin-1 and actin related protein 2/3 complex subunit 2 (Arpc2)) (Homan et al., 2014). Involvement of Usp9X in neuronal cytoskeleton regulation is further supported by yeast-2-hybrid data from 14-weeks fetal brain, which used full-length Usp9X as bait. This screen identified interactions between Usp9X with the microtubule plus-end tracking proteins (EB1) and microtubule based motor protein (Kif5B). In addition both the proteomic and yeast-2-hybrid analyses indicated that components of GTPase signalling pathway, for example guanine nucleotide-binding protein G (o) subunit alpha (GNAO), GTP-binding nuclear protein (RAN) and G protein-coupled receptor associated sorting protein 1 (GPRASP1), associate with Usp9X. As mentioned in **Section 1.2.4**, small GTPase signalling regulates microtubule-actin interactions and thereby axonal growth and specification. Taken together, these novel data suggest several possible mechanisms whereby Usp9X might regulate microtubule and actin dynamics during axon development.

1.6 Rationale and aims

Neurons are the core functional cells of the CNS. They are highly polarized with an axon and multiple dendrites, which are important for the directional information transfer in the CNS. The axon is the region of the neuron which transmits the signal and forms neural circuits. Improper axon formation and migration can lead to various neurocognitive diseases such as epilepsy and X-linked intellectual disability (Gleeson et al., 1998, Homan et al., 2014). Axon formation has three main phases: specification, growth and maturation. Axon specification and elongation have been linked to different neuronal signalling pathways, kinases and polarity proteins which are the main regulators for microtubule and actin dynamics.

Usp9X has recently been suggested to regulate axon development in several regions of the mouse brain including projections from the entorhinal cortex to hippocampus in the embryo and the corpus callosum in the adult (Stegeman et al., 2013). These findings are supported by *in vitro* evidence showing the absence of Usp9X disrupts normal neurite outgrowth. Loss of Usp9X in 3, 5 and 7 DIV hippocampal neurons resulted in shorter axons without the dendrite length being affected. Usp9X is also

required for normal dendritic and axonal arborisation as the numbers of both axonal and dendritic termini was reduced in cultured Usp9X-null hippocampal neurons (Stegeman et al., 2013, Homan et al., 2014). In addition three pathological Usp9X variants, associated with X-linked intellectual disability disrupt axonal growth and migration (Homan et al., 2014). These data strongly indicate that Usp9X is required for normal axon formation and migration. However, the molecular mechanism whereby it achieves this remains unclear.

It is hypothesized that Usp9X regulates axon initiation and/or elongation by regulating signalling pathways, polarity proteins and/or microtubule/actin dynamics.

The hypothesis was addressed in the following aims:

Aim 1: To determine if Usp9X regulates the initiation and /or elongation of the axon.

Aim 2: To study the regulation of signalling pathways by Usp9X, which control axon initiation and/or elongation.

Aim 3: To study the regulation of microtubule dynamics and kinases by Usp9X involved in axon initiation and /or elongation.

Cultured mouse hippocampal neurons isolated from a conditional knockout (cKO) mouse model of Usp9X were used. The hippocampus was dissected at E18.5 and neurons were grown in culture to address the aims of this project.

2. Materials and Methods

2.1 Animal ethics

Ethical clearance (AEC-BPS/10/11) was granted for animal experimentation by the Griffith University Animal Ethics Committee (AEC) and research was conducted in accordance with the approved protocol at the Eskitis Institute for Drug Discovery (ESK), Griffith University.

2.2 Mouse mating for Cre/Usp9X^{loxP}

To generate mice in which Usp9X was conditionally deleted from the brain, Usp9X$^{loxP/loxP}$ female mice were crossed with heterozygous Nestin-Cre males as described (Stegeman et al., 2013). Nestin-Cre results in the deletion of Usp9X from all neural precursors and their differentiated derivatives enabling the study for Usp9X at the early stage of neuronal development (Arbour et al., 2008, Tronche et al., 1999, Isaka et al., 1999, Stegeman et al., 2013). Conventional deletion of Usp9X cannot be used as it results in early embryonic lethality (Naik et al., 2014). Under this breeding regime, all the male offspring would receive an Usp9X loxP gene. Male offspring positive for Nestin-Cre were used as Usp9X cKO and male offspring negative for Nestin-Cre, as littermate controls in the experiments below (as per Stegemen *et al*, 2013). Conversely, female offspring would be either wild-type (Nestin-Cre negative) or heterozygous (Nestin-Cre positive) for Usp9X gene deletion. Given random X-inactivation occurs before Nestin-Cre activation, Nestin-expressing cells in females would express either wild-type levels of Usp9X (if the inactivated X chromosome carried the floxed allele) or be Usp9X-null (if the X chromosome carrying the wild-type Usp9X was inactivated and Cre deleted the floxed allele). As X-inactivation is random this would result in a chimeric culture of Usp9X positive and negative neurons. Therefore only males were analysed in the experiments.

2.3 Plasmids

pCMV-YFP-tagged Kif5B and pCMV-HA-tagged Kif5B plasmids (Rivera et al., 2007) were a kind gift from Professor Don Arnold, University of Southern California,

Los Angeles, USA. pBetaActin-Kif5C560-YFP was a gift from Dr. Gary Banker, Centre for Research on Occupational and Environmental Toxicology, Oregon Health & Science University, Portland (Jacobson et al., 2006). pEF-Dest V5-tagged FAM/Usp9X was available in-house (Murray et al., 2004). All of the plasmids were ampicillin resistant and expanded in JM109 *Escherichia coli* (*E. coli*) competent cells purchased from Promega. Cells were grown at 37°C in Luria Broth (LB-10g tryptone, 5g yeast extract, and 10g NaCl in 950 mL deionized water.), or on LB Agar bacterial plates (LB containing 4% (w/vol) dissolved bacteriological Agar), both containing 100µg/ml Ampicillin (Sigma-Aldrich). Transformation was achieved using heat-shock method as described in manufacturer's protocol (Gateway® Technology) (Pope and Kent, 1996). Large scale plasmid preps were achieved using Maxi-Prep Kit (Qiagen) as per the manufacturer's instructions. All the plasmids were verified by performing restriction enzyme digest (New England Biolabs).

2.4 DNA extraction and Genotyping

Mouse genotyping was performed on DNA extracted from tail tips and PCR was performed using RedExtract tissue PCR Kit (Sigma-Aldrich). The tail tip samples were incubated in the tissue preparation and extraction solutions as provided by the kit for 10 minutes at room temperature. The samples were heated to 95°C for 3 minutes and then mixed with neutralisation solution prior to PCR. 1.5µL of the DNA extract was then added to a PCR reaction containing primers and REDExtract-N-Amp PCR ReadyMix according to the manufacturer's protocol. 15µL of PCR reactions was loaded and PCR was performed on a BioRad thermal cycler. Primers were designed to detect Cre-recombinase and male embryos were identified using primers for SRY region of the Y chromosome. See table 2.1 for primer sequences, annealing temperatures and product lengths. Cycling conditions varied depending on primer melting temperatures and product length but generally were as follows for 35 cycles:

92 ºC for 5 seconds (denature DNA template)
X ºC for 15 seconds (primer annealing)
72 ºC for 30 seconds (extension)

Table 1.1 Primers were purchased from Sigma-Aldrich as 100μM solution

Primer	Sequence (5'→3') F:Forward; R:Reverse	Annealing temperature (°C)	Amplicon size (base pair)
Cre	F: CTGACCGTACACCAAAATTTGCCTG R: GATAATCGCGAACATCTTCAGGTTC	53	203
SRY	F: GAGGCACAAGTTGGCCCAGCA R: GGTTCCTGTCCCACTGCAGAAG	60	246

The PCR amplifications were run in 1 x TAE buffer (40 mM Trisacetate, 1 mM EDTA, pH 8) on a 1% agarose gel containing ethidium bromide (0.5μg/ml) at 100 volts for 15 minutes. 100bp DNA ladder (New England Biolab) was loaded to assist in determining the sizes of the products. Gels were then photographed under UV light (GelLogic200 Imaging System, Eastman Kodak Company).

2.5 Cell culture

Cell Counting

Cell counts were performed on single cell suspension by diluting 10μL of the suspension with 10μL of trypan blue (Sigma-Aldrich). 10μL of the mixture was then loaded onto the haemocytometer and counted under the 10X magnification using Olympus CKX41 microscope (Olympus).

Isolation and culture of primary hippocampal neurons:

Preparation of the hippocampal cell cultures was according to published protocols (Kaech and Banker, 2006). In brief, hippocampi were dissected from embryonic day 18 (E18) mice using ice cold dissection media (Hanks Buffered Salt solution (Invitrogen), 10mM Hepes (Invitrogen), 1mM sodium pyruvate (Invitrogen), 0.5% glucose (Sigma-Aldrich), 1 x penicillin/streptomycin (Invitrogen) and digested with pre-heated papain suspension (Washington, 20 units in 3mL dissection media) at 37°C for 20 minutes. The tissue was then dissociated with a fire-polished pasteur pipette in plating medium (Neurobasal medium (Invitrogen), 5% fetal bovine serum (Sigma-Aldrich), 2% B27 supplement (Invitrogen), 0.5mM glutamine (Invitrogen), and 1 × penicillin / streptomycin). Neurons were then plated onto glass coverslips (ProSciTech) coated with 1mg/mL of poly-L-lysine (Sigma-Aldrich) in Trizma

buffer pH 8.5, 0.1M at a low density with 2.5 x 10^4 cells / well for immunofluorescence and morphometric analysis or high density 5 x 10^4 cells / well for biochemical assays in 12-wells plate. Neuronal cultures were incubated at 37°C with 5% CO_2. After neurons attached to the substrate (normally around 4-6 hours after plating), the medium was exchanged to neuronal culture medium (Neurobasal medium, 2% B27 supplement, 0.5mM glutamine and 1× penicillin/streptomycin).

Cell lines:

Neuro2a cells were cultured in Dulbecco's Modification of Eagle's Medium (Invitrogen) supplemented with 5% fetal bovine serum while HEK293 cells were cultured in Dulbecco's Modification of Eagle's Medium/F12 media (Invitrogen). There were plated at 6 x 10^4 cells / well in 6-wells plate for biochemical assays.

2.6 TGF-β1 and BDNF treatment, Mitochondria analysis, Transfection, siRNA knockdown, Ubiquitylation assay

Examination of nuclear Smad4 in hippocampal neuronal culture was performed by treating neurons with 1 ng/mL TGF-β1 ligand (R&D System) three days after plating to activate the TGFβ pathway (Vogel et al., 2010). After four hours, neurons were fixed with 4% Paraformaldehyde (PFA) in 1X Phosphate Buffered Saline (PBS) for 10 minutes at room temperature in preparation for immunofluorescence (**Section 2.7**).

Hippocampal neurons were treated with 100ng/mL BDNF (Pepro Tech, INC) in neuronal culture media 6 hours after plating. Five random bright field images were taken at different time points for morphological studies as discussed in **Section 3.4**. For morphometric studies, at least 100 cells at each time-point were analysed per culture (3 Usp9X knockout versus 3 littermate control embryos). Statistical significance was determined using ANCOVA. The graph displays mean average of replicate experiments, error bars represent ±1 SEM.

For mitochondrial analysis, hippocampal neurons were treated with 400nM MitoTracker® Orange CMTMRos (Invitrogen) at 37°C according to the manufacturer's protocol, three days after plating. After 30 minutes, neurons were fixed for immunofluorescence. Neurons were double-labelled with βIII-tubulin and 80μm at both the distal and proximal ends of the axon were measured using ImageJ

software (Ooms et al., 2006). The number of mitochondria at both distal and proximal ends for each neuron was counted. Cultures were derived from 3 Usp9X knockout and 3 littermate control embryos. At least 20 neurons were analysed per culture. Statistical significance was determined using an unpaired Student's T test and $p < 0.05$ was considered to be statistically significant. Error bars represent ±1 SEM.

Transfection of hippocampal neurons - A total of 1 x 10^6 hippocampal neurons, in suspension (in plating media-Neurobasal medium 5% fetal bovine serum, 2% B27 supplement, 0.5mM glutamine, and 1 × penicillin / streptomycin), were transfected with either 2μg of Kif5C560-YFP or YFP-Kif5B or pMAX GFP plasmid with an Amaxa Mouse Neuron Nucleofector kit (Lonza) using parameters recommended by the company. The transfected neurons were plated into four wells of a 12-well plate and media was changed the following day before cells were fixed with 4% PFA for analysis.

For co-transfection, a total of 12μg of HA-Kif5B and V5-Usp9X plasmids at 1:1 ratio was transfected into HEK293 cells using Lipofectamine® reagent (Life Technologies) according to the manufacturer's protocol. Cells were plated onto a 10cm tissue culture dish and used for Co-immunoprecipitation (Co-IP) (**Section 2.12**) after two days.

For Usp9X knockdown using siRNA, HEK293 cells were treated with Usp9X siRNA or non-targeting siRNA using DharmaFECT reagent (Dharmacon) according to the manufacturer's protocol. DharmaFECT reagent 1 and final a concentration of 25nM or 100nM siRNAs were used for the experiments. ON-TARGETplus Human Usp9XsiRNA-SMARTpool target sequences (Dharmacon) consisted of the following - GAAAUAACUUCCUACCGAA, GUACGACGAUGUAUUCUCA, ACACGAUGCUUUAGAAUUU and AGAAAUCGCUGGUAUAAAU. As a negative control, a non-targeting siRNA UGGUUUACAUGUCGACUAA (Dharmacon) was used. Cell lysate were collected at 24, 48, 72 and 96 hours for immunoblotting (**Section 2.11** and **2.13**).

To inhibit the proteasome, three days *in vitro* hippocampal neurons or HEK293 cells, grown to 90% confluence in T-25 flask, were treated with the proteasome inhibitor

25nM epoxomicin (Sigma-Aldrich) dissolved in DMSO (Han et al., 2012, Stewart et al., 2010). After six hours, protein lysates were collected for immunoblotting analysis.

2.7 Immunofluorescence on cell cultures

Cells were fixed with 4% PFA in 1X PBS for 10 minutes, permeabilised and blocked in PBS containing 3% goat serum and 0.1% Triton X-100 at room temperature for 20 minutes. Primary antibodies were diluted in blocking solution containing PBS with 3% goat serum for overnight incubation at 4 ºC followed by secondary antibodies for one hour at room temperature in the dark. Cells were mounted with cover-slips using DAPI in Vectashield mounting media (Vector Lab) and sealed with nail polish. A negative control exposed to secondary but no primary antibody was included to determine autofluorescence for every staining. Antibody dilutions were used as described in Section 2.9. Images were photographed on either a Zeiss AxioImager Z1 or Olympus FV1000 Spectral microscope. For double-labelling of Usp9X and Kif5B in hippocampal neurons, images were photographed with Zeiss ELYRA Structured Illumination (SIM) super resolution microscopy and analysed by Dr Andreas Papadopulos, University of Queensland (see acknowledgements).

2.8 Tissue processing of brain sections

Brains were removed from the skulls of E18.5 mouse embryos and drop-fixed in 4% PFA for two hours at room temperature. Samples were cryo-protected in 15% sucrose at 4°C overnight, then in 30% sucrose at 4°C overnight, 1:1 ratio of 30% sucrose and O.C.T at 4°C overnight and finally frozen in Tissue-Tek O.C.T. compound (Sakura) then sectioned at 10μm on a Leica CM3050 S cryostat.

2.9 Histology, immunofluorescence and image acquisition of brain sections

For coronal analysis, sections from a comparable position along the rostral-caudal axis were used. Sections were matched by counting the number of coronal sections starting at the rostral-most edge of the brain and confirmed by closely matching any unchanged anatomical land marks (Stegeman et al., 2013). For immuno-fluorescence,

brain sections were permeabilised in 1% sodium dodecyl sulphate (SDS) in 1X PBS for 4 minutes at room temperature. After washing 3 times with PBS, the samples were blocked in 2% Bovine serum albumin (BSA) in 1X PBS for 20 minutes, incubated with primary antibodies in 2% BSA/PBS at 4 ºC overnight, then incubated with biotinylated secondary antibodies for 1h and in streptavidin-biotin-peroxidase complex (Vector Laboratories) for 1.5h at room temperature, and mounted with Vectashield mounting medium with DAPI (Vector Laboratories). Antibody dilutions were used as described in Section 2.9. Images were obtained on a AxioImager Z1 microscope (Carl Zeiss) or Olympus FV1000 confocal microscope.

2.10 Immunofluorescence antibody dilutions

Table 1.2 Primary antibody dilutions for immunofluorescence

Antibodies	Raised in	Dilution	Catalogue Number and Company
Usp9X	Rabbit Mouse	1:250 1:200	A301-351A Bethyl Lab MABE352 Millipore
Stahmin-1	Rabbit	1:250 1:400 (B/S)	Ab52630 Abcam
CRMP2	Rabbit	1:200 (B/S)	Ab129082 Abcam
Kif5B	Rabbit	1:200	Ab5629 Abcam
MARK4	Rabbit	1:100	sc-98357 Santa Cruz
AF-6	Mouse	1:200	#610732 BD Transduction
PJA-1	Rabbit	1:100 1:200 (B/S)	J2830 Sigma-Aldrich
Smad4	Rabbit	1:100	sc-7154 Santa Cruz
Smurf1	Rabbit	1:50	sc-130877 Santa Cruz
Syntaxin-1	Mouse	1:500	S066 Sigma-Aldrich
Total Akt	Rabbit	1:200	#4685S Cell Signaling Technology
phospho-Akt	Rabbit	1:200	#4048S Cell Signaling Technology
βIII-tubulin	Rabbit Mouse	1:1000 1:2000	Ab18207 Abcam T5076 Sigma-Aldrich

B/S: Brain sections

Table 1.3 Secondary antibody dilutions for immunofluorescence

Antibodies	Dilution	Catalogue Number and Company
Alexa Fluor® 594 goat α mouse	1:500	A11032 Invitrogen
Alexa Fluor® 594 goat α rabbit	1:500	A11012 Invitrogen
Alexa Fluor® 488 goat α rabbit	1:500	A11008 Invitrogen
Goat Anti-Rabbit IgG Antibody, Biotin Conjugate	1:200	A24541 Invitrogen
Alexa Fluor® 488 streptavidin	1:400	S32354 Invitrogen
Alexa Fluor® 488 phalloidin	1:50	A12379 Invitrogen

2.11 Protein extraction from cells and brains

Protein was extracted from brain tissue samples using SDS-PAGE general lysis buffer containing 10mM Tris pH 7.4, 1% SDS, 10% glycerol and Sigma-Aldrichfast Protease Inhibitor Tablets (Sigma-Aldrich) according to manufacturer's recommendations. Tissue was washed with cold PBS, homogenised in SDS-PAGE general lysis buffer, DNA was sheared with a 21 – 27 gauge needle, centrifuged at 12000g at 4ºC for 5 - 20 min to pellet cellular debris and supernatant was transferred to a new tube. Protein concentration was estimated using a Bicinchoninic acid (BCA) kit (Thermo Scientific) according to manufacturer's instructions.

For cultured cells, cells were exposed to lysis buffer containing Protease Inhibitor (Sigma-Aldrich) and lysate was removed from the culture surface using a cell scraper. DNA was sheared with a 27 gauge needle, centrifuged at 15000g at 4ºC for 20 minutes to pellet cellular debris and supernatant containing total protein was transferred into a fresh tube. Protein concentration was estimated using a BCA kit (Thermo Scientific) according to manufacturer's instructions.

2.12 Immunoprecipitation

Mouse brain lysate (yielding 1.0mg total protein) was harvested from wildtype E18.5 embryonic mouse brain or protein lysate harvested from transfected HEK293 cells as mentioned in **Section 2.5** using ice-cold non-denaturing lysis buffer (Thermo Scientific).

Co-immunoprecipitation (co-IP) was done using the Thermo Scientific Pierce co-IP kit following the manufacturer's protocol. Briefly, Usp9X (Bethyl Lab) or V5 (Invitrogen) antibodies were first immobilized for 2 hours using AminoLink Plus coupling resin. The resin was then washed and incubated with lysate overnight. After incubation, the resin was again washed and protein eluted using elution buffer. A negative control, provided with the IP kit to assess nonspecific binding, received the same treatment as the co-IP samples and was analysed by immunoblotting. For this project, co-imunoprecipitation was performed by Dr Mariyam Murtaza, Griffith University (See acknowledgement).

2.13 Immunoblotting

10 - 25ug of protein was mixed at 1:1 ratio with 1X SDS-PAGE loading buffer (30% glycerol, 10% SDS, 5% β-mercaptalethanol, 0.02% bromophenol blue, 250mM Tris HCl pH 6.8 in dH_2O) and loaded into a well on a 6%, 8% or 10% hand-casting Polyacrylamide Gels (Biorad). A pre-stained protein ladder (PageRuler Plus Prestained Protein Ladder –Fermentas) was used to determine position of target proteins and when time of electrophoresis. Protein was transferred from the gel to a nitrocellulose membrane (Amersham Biosciences) using a BioRad transfer apparatus (BioRad). The membrane was then blocked with 5% skim milk powder in PBS 0.1% Tween, incubated with primary antibodies at 4ºC overnight, then incubated with horse radish peroxidase secondary antibodies (Millipore) for one hour at room temperature and developed with Immobilon™ western chemiluminescent horseradish peroxide (HRP) substrate (Millipore) according to the manufacturer's instructions, before imaging on a VersaDoc 4000 MP Imaging System (BioRad). β-actin was used as a protein loading normalization control.

2.14 Immunoblot antibody dilutions

Table 1.4 Primary antibody dilutions for immunoblot analysis

Antibodies	Raised in	Dilution	Catalogue Number and Company
Usp9X	Rabbit	1:2000	A301-351A Bethyl Lab
Stahmin-1	Rabbit	1:5000	Ab52630 Abcam

CRMP2	Rabbit	1:10000	Ab129082 Abcam
Kif5B	Rabbit	1:1000	Ab5629 Abcam
Kinesin-1	Mouse	1:1000	MAB1614 Millipore
MARK4	Rabbit	1:500	sc-98357 Santa Cruz
AF-6	Mouse	1:500	#610732 BD Transduction
PJA-1	Rabbit	1:1000	J2830 Sigma-Aldrich
Total Akt	Rabbit	1:2000	#4685S Cell Signaling Technology
phospho-Akt	Rabbit	1:1000	#4048S Cell Signaling Technology
p44/42 MAPK (Erk1/2)	Rabbit	1:1000	#4695S Cell Signaling Technology
Phospho-p44/42 MAPK (Erk1/2)	Rabbit	1:1000	#4370S Cell Signaling Technology
Ubiquitin	Mouse	1:2000	#3936S Cell Signaling Technology
HA	Mouse	1:1000	#2367S Cell Signaling Technology
V5	Mouse	1:4000	P/N46-0705 Invitrogen
β-actin	Rabbit	1:2000	A5060 Sigma-Aldrich

Table 1.5 Secondary antibody dilutions for immunoblot analysis

Antibodies	Dilution	Catalogue Number and Company
Goat α mouse HRP	1:10000	AP 124P Millipore
Goat α rabbit HRP	1:10000	AP 132P Millipore

2.15 Statistics and Graphs

For all analyses a minimum of three Usp9X knockout mice versus three or more littermate controls were used. Differences between knockout mice and littermate controls were assessed statistically using a Student's *t* test unless otherwise stated. All error bars on graphs represent ±1 SEM. All graphs were generated using either Excel (Microsoft) or SPSS.

3. Usp9X regulation of axon development

3.1 Introduction

Usp9X brain-specific knockout mice display differences in neuronal projections in several brain regions suggesting that Usp9X may regulate axon development (Stegeman et al., 2013). In the embryonic mouse brain, neuronal projections from the entorhinal cortex to the hippocampus were reduced when Usp9X was absent (Stegeman et al., 2013). In the adult mouse brain, the size of the corpus callosum, which is the major axonal tract that connects the cerebral hemispheres, was markedly reduced in the absence of Usp9X. These findings are supported by *in vitro* evidence showing the absence of Usp9X disrupted normal neurite outgrowth. For example, reduction in the number of axonal and dendritic termini have been observed in Usp9X-null hippocampal neuronal cultures (Stegeman et al., 2013). The axon length in these cultures was also shorter compared to wild-type cultures, without the dendrite length being affected. However, these data were based on day 3, 5 and 7 hippocampal neuronal cultures at which time axons are established. As such, these experiments did not discriminate the effect, if any, of Usp9X loss on axon initiation and/or growth.

Hippocampal neuronal culture has been well characterised with neurons maturing progressively through distinct stages: from freshly plated "stage 1" cells to functionally mature "stage 5" neurons (Dotti et al., 1988, Craig and Banker, 1994, Polleux and Snider, 2010). The technique is detailed below but in principle it recapitulates two critical events of neuron maturation, namely, axon specification and its subsequent growth. This *in vitro* culture system has been widely used for visualizing the subcellular localization of endogenous or ectopically-expressed proteins, for imaging protein and organelle trafficking and to define the molecular mechanisms underlying the development of axon-dendrite polarity and axon growth (Shao et al., 2013, Devaux et al., 2012, Stagi et al., 2006, Cheng et al., 2011a, Gu et al., 2006). Therefore, hippocampal neuronal culture was chosen to examine the regulation of axon specification and growth by Usp9X.

The aim of this chapter was to examine the role of Usp9X, if any, in axon specification using cultured mouse hippocampal neurons isolated from a conditional

knockout (cKO) mouse model of Usp9X (Usp9x cKO). The hippocampus was dissected at E18.5 and neurons were grown in culture (see **Material and Methods 2.4**). Neurons were then characterised based on their morphology to determine the effect of Usp9X's absence on axonal development.

3.2 Nestin/Cre conditional knockout of Usp9X

The Cre/loxP recombinant system was used to generate the Usp9X cKO mouse model (Stegeman et al., 2013, Savitt et al., 2005, Perez-Mancera et al., 2012). In this system, the deletion of exon 3 from the Usp9X gene is dependent on the expression of Cre recombinase expressed from the Nestin promoter. As all neural progenitors of the CNS express Nestin-Cre, Usp9X will be deleted from the entire mouse brain in this model system (Arbour et al., 2008, Park et al., 2010, Stegeman et al., 2013). $Usp9X^{loxP/loxP}$ female mice were crossed with heterozygous Nestin-Cre males to develop the Usp9X cKO mouse model. With this breeding regime, all the male offspring would receive an Usp9X loxP gene. Male offspring positive for Nestin-Cre were used as Usp9X cKO and male offspring negative for Nestin-Cre, as littermate controls in the experiments below (as per Stegemen *et al*, 2013). Conversely, female offspring would be either wild-type (Nestin-Cre negative) or heterozygous (Nestin-Cre positive) for Usp9X gene deletion. Given that random X-inactivation occurs before Nestin-Cre activation, Nestin-expressing cells in females would express either wild-type levels of Usp9X (if the inactivated X chromosome carried the floxed allele) or be Usp9X-null (if the X chromosome carrying the wild-type Usp9X was inactivated and Cre deleted the floxed allele). As X-inactivation is random this would result in a chimeric culture of Usp9X positive and negative neurons. Therefore only males were analysed in the experiments detailed below.

Dissection of hippocampi for culture was performed in parallel with genotyping. To confirm the genotype of each embryo, two PCRs were performed on tail DNA. The first PCR detected a 246 base pair male specific SRY gene fragment (**Figure 3.1A**). The second PCR detected the Cre gene with a 207 base pair fragment (**Figure 3.1B**). Only neurons from Cre-positive (Usp9X cKO) and Cre-negative (littermate control) males (Sry-positive) were plated for experiments.

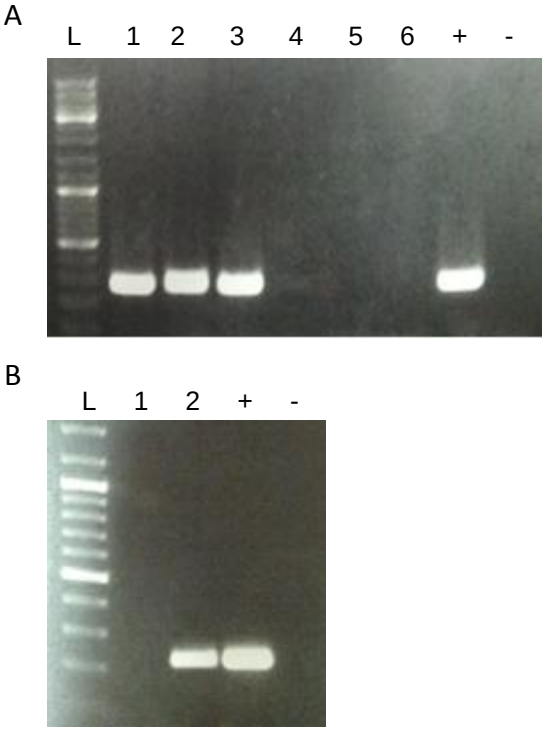

Figure 3.1 Genotyping of Nestin-Cre conditional knockout of Usp9X

Genotyping was performed with PCR using embryo tail DNA. (A) Genotyping for SRY. Lane 1-6 represents six different E18.5 embryos from the same litter, screened with primers for the male-specific SRY region of the Y chromosome. Embryos 1-3 are males (246 base pairs) and 4-6 are females. (B) Genotyping for Cre. Lane 1-2 represents the first two SRY-positive males from the same litter (in A). Only embryo 2 screened positive for Nestin-Cre transgene (207 base pairs) and was therefore a Cre-positive male and potentially Usp9X depleted. L: DNA molecular weight marker, +: Positive control (tail DNA from a known adult Cre-positive male); -: no-template negative control.

3.3 Early stages of neuronal development at 1, 2, and 3 days *in vitro*

Usp9X has been shown to be involved in axonal growth and branching. Loss of Usp9X results in shorter axons in hippocampal neurons following 3, 5 and 7 days in culture (Stegeman et al., 2013). As the role of Usp9X in axonal growth was previously investigated in hippocampal neurons, which is a highly homogenous population (Stegeman et al., 2013) to study the role of Usp9X in the early stages of neuronal maturation and development, the morphology of neurons from littermate controls and Usp9X cKO mice was observed for the first 3 days of culture in a pilot study. Representative bright field images were taken for wild-type and Usp9X-null neurons at 1, 2 and 3 days in culture as shown in **Figure 3.2**.

After 1DIV, approximately 50% of wild-type neurons were observed to possess a single long projection, being the axon, and the remaining 50% of neurons had neurites of equal length surrounding the nucleus. However, most Usp9X-null neurons possessed a few short neurites surrounding the nucleus (**Figure 3.2**). At 2DIV almost all of the wild-type neurons had axons. For Usp9X-null neurons, approximately half the neurons possessed axons while the remainder were symmetrical with multiple neurites. After 3DIV the majority of wild-type and Usp9X-null neurons possessed an axon. However, the axon of the Usp9X-null neuron appeared to be shorter than those of the wild-type neurons (**Figure 3.2**). This pilot study confirmed the requirement of Usp9X for supporting axonal length at 3DIV as reported previously (Stegeman et al., 2013) and justified further investigation.

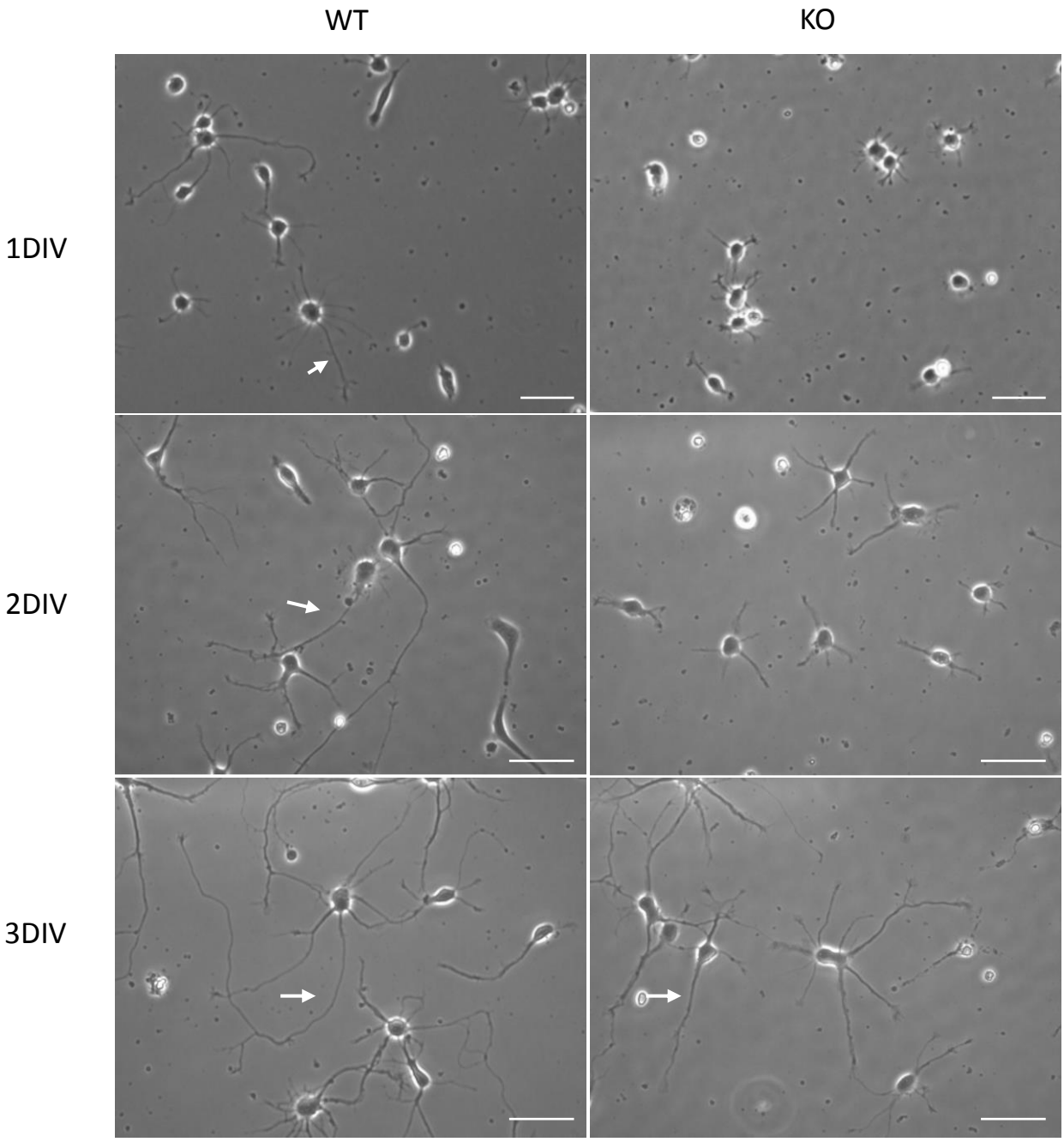

Figure 3.2 Delayed axon specification and shorter axonal length in cultured Usp9X-null hippocampal neurons

Hippocampal neurons isolated from E18.5 wild-type (WT) and Usp9x-null (cKO) embryos were cultured up to 3 days *in vitro* (DIV). Axons (arrows) were apparent in wild-type littermate control neurons at 1DIV but only 3DIV in Usp9X-null neurons. Scale bar 50μm.

3.4 Characterisation of different stages for hippocampal neurons

The observed differences in axonal length between Usp9X-null and wild-type hippocampal neurons from the pilot study (**Figure 3.2**), suggested that Usp9X may affect axon specification. The stages of the axon development is well characterised according to Dotti et al (1998) and Hirai et al (2011). Classification details are presented in the legend to **Figure 3.3**. Generally, stage 1 neurons extend a prominent lamella around the cell body (**Figure 3.3A**). Stage 2 neurons extend short symmetrical neurites (**Figure 3.3B**). During the transition from stage 2 to 3, neurite symmetry is broken and one neurite elongates and is specified to become an axon (Dotti et al., 1988, Hirai et al., 2011). To examine the role of Usp9X for axon specification, cultured hippocampal neurons were classified into three stages based on the morphology and parameters for neurite measurement as shown in **Figure 3.3**. The length of the neurites and diameter of the nucleus was manually traced in each cell and analysed using the public domain ImageJ software (Ooms et al., 2006). Only neurons, which were bright, isolated, possessed more than three neurites for stage 2 neurons and multiple neurites but only one long projection were included in the analysis.

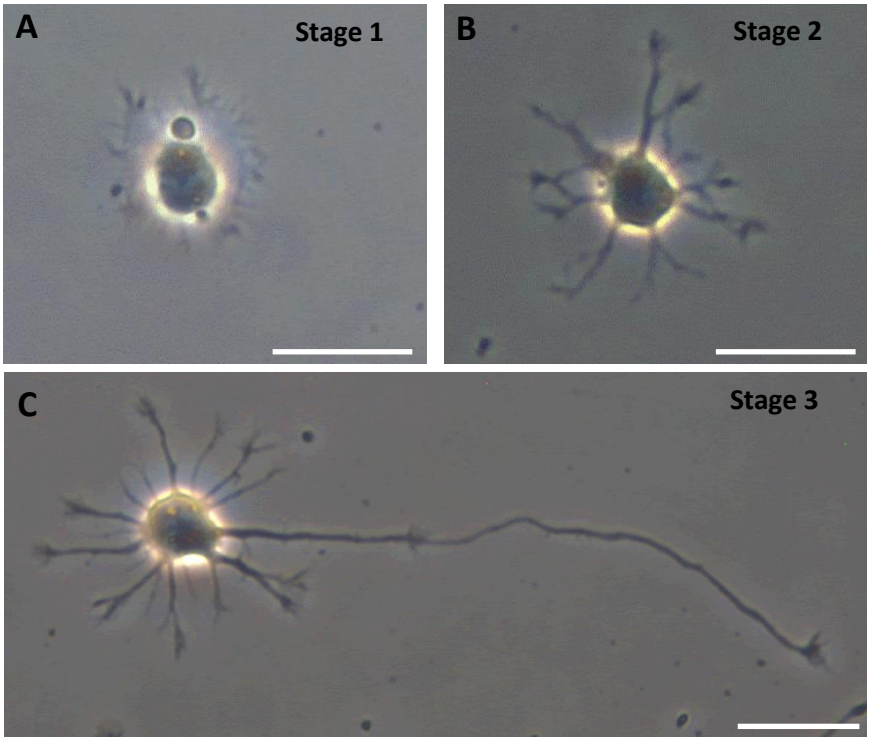

Figure 3.3 Morphological characterisation of neurites defining different stages of neuronal maturation

Phase-contrast images of cultured hippocampal neurons from a E18.5 Usp9x^{flox} Cre-negative littermate control embryo. (A) Stage 1 neurons possess fillopodia and lamellipodia surrounding the nucleus. Neurite length is less than the diameter of the nucleus (about five hours after plating for). (B) At Stage 2 the neuron is symmetrical, with several neurites of equal length, which the length of neurite is greater than the diameter of the nucleus (approximately 12 hours after plating). (C) Stage 3 neurons are polarized, with a single neurite as the longest projection, which is defined as at least 30% longer than the second longest neurite (from 24 hours onwards after plating). This single long projection is known as the axon. Scale bar 100μm.

3.5 Loss of Usp9X results in delayed axon specification

To rigorously examine the role of Usp9X in axon specification, wild-type and Usp9X-null hippocampal neurons were compared over the first 48 hours of culture and categorised into three stages as described in **Figure 3.3**. Five random bright field images were taken for each culture at different time points over the first 48 hours. 100 wild-type and Usp9X-null neurons (derived from 4 Usp9X cKO and 4 littermate controls) at each time point were categorised into the three stages based on their morphology and neurite length, as shown in **Figure 3.4**. The analysis was also performed by Dr. Mariyam Murtaza who was blinded to the sample genotpye. Overall, the percentage of stage 1 and stage 2 neurons decreased across time while the percentage of stage 3 neurons increased over time for wild-type neurons (**Figure 3.4A**). For Ups9X null neurons, stage 1 neurons also decreased across time but more slowly as compared to the wild-type neurons. Most strikingly, Usp9X-null neurons tended to remain at stage 2 longer than wild-type neurons before slowly progressing into stage 3 (**Figure 3.4B**).

Although there was no significant difference in the percentage of stage 1 neurons at 5 hours of culture (**Table 3.1**), there were significantly more Usp9X-null neurons remaining at stage 1 over the 48-hour time course of this experiment (**Table 3.1**). However, following this initial delay there was no significant difference in the rate at which Usp9X-null neurons exited stage 1 and entered stage 2 (ANCOVA *p*=not

significant; **Figure 3.5A**). While the number of stage 2 neurons similarly increased between 5 hours and 12 hours (**Table 3.1**), the number of Usp9X-null neurons remaining in Stage 2 was markedly higher after 12 hours (ANCOVA p=0.002; **Figure 3.5B, Table 3.1**). A significant delay in the increased percentage of Usp9X-null neurons entering stage 3 was observed between 5 and 12 hours, however the rate at which Usp9X-null neurons entered stage 3 over time was not significantly different from wild-type neurons (ANCOVA p=0.06; **Figure 3.5C**).

These differences between wild-type and Usp9X-null neurons in their progression to stage 3 neurons indicate that Usp9X is required for normal axon specification. From 12 hours onward Usp9X-null neurons significantly lagged behind wild-type counterparts in progression from stage 1 to 2 (p=0.002; **Figure 3.5B**, **Table 1**). A larger effect of Usp9X loss was observed during stage 2 to 3 progression where Usp9X-null neurons required over 36 hours longer to specify an axon (p=0.001) (**Table 3.1**).

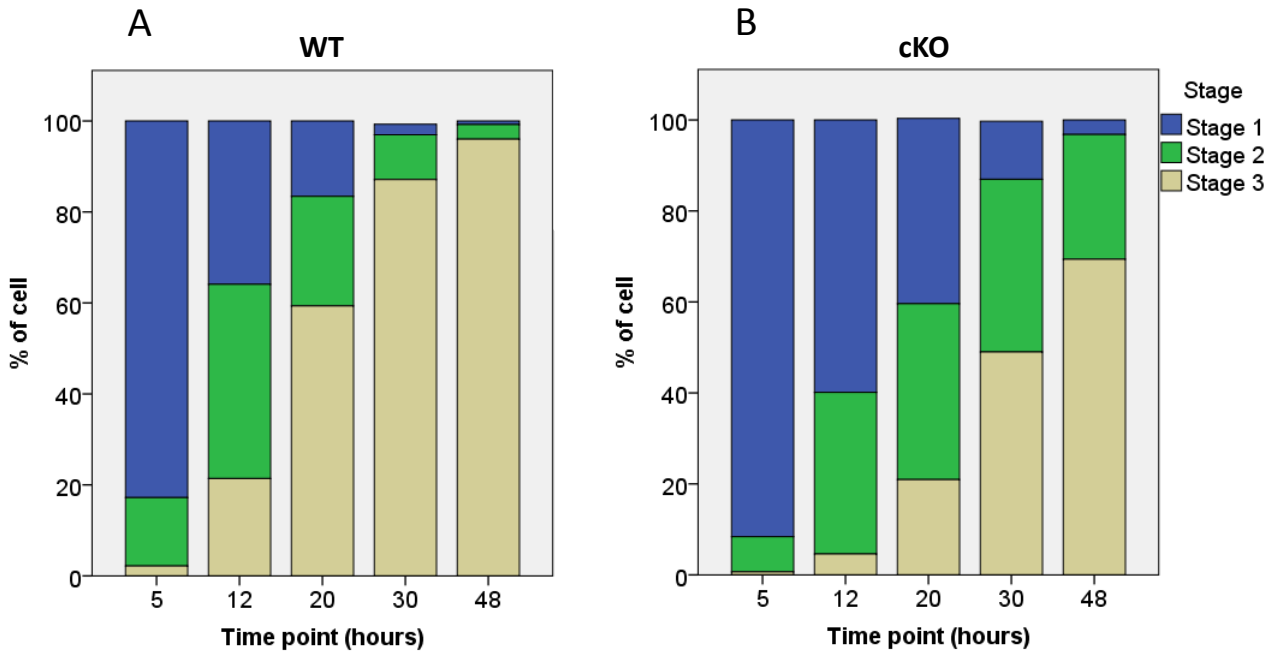

Figure 3.4 Overall distribution of wild-type and Usp9X-null neurons across different time points

(A) For wild-type neurons, the percentage of stage 1 and 2 decreased across time while stage 3 neuron increased across time. (B) For Ups9X null neurons, stage 1 neurons decreased across time but slower compared to wild-type neurons. Usp9X-null neurons remained at stage 2 longer before progressing to stage 3 at a similar rate to the wild-type neurons. WT: wild-type littermate control, cKO: Usp9X knockout.

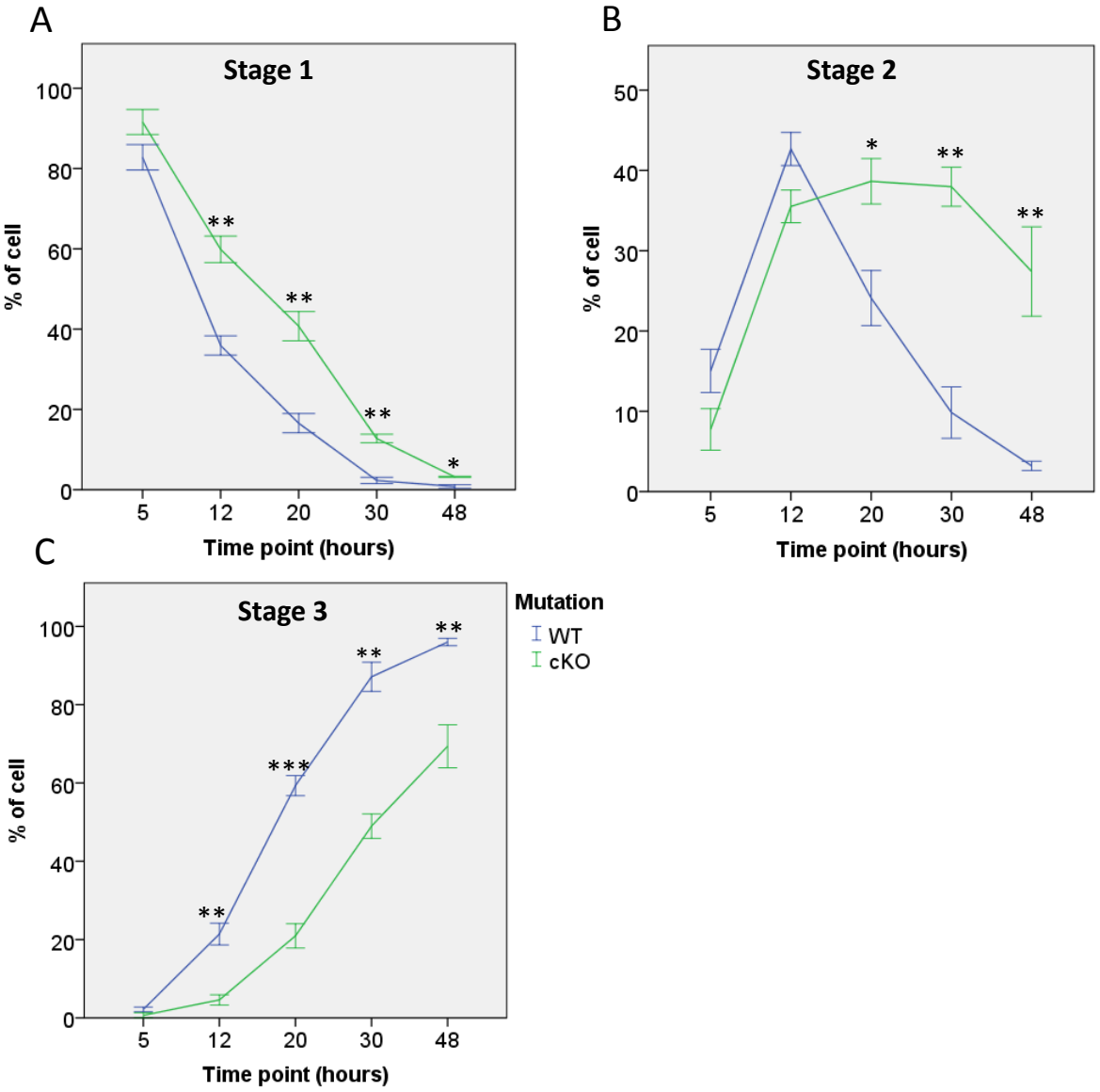

Figure 3.5 Progression of hippocampal neuronal cultures from stage 1 to stage 3 is delayed in Usp9X-null neurons *in vitro*

Time course of the percentage of stage 1 (A), stage 2 (B) and stage 3 (C) wild-type and Usp9X-null neurons. After an initial delay the rate of progression from stage 1 to stage 2 neurons were similar between wild-type and Usp9X-null neurons ($p>0.05$). The progression from stage 2 to stage 3 neurons was delayed in Usp9X-null cultures ($p<0.001$), but progressed similarly to wild-type neurons after this initial lag phase ($p=0.06$). n = 100 neurons at each time point from four Usp9X cKO and four littermate control embryos have been analysed with ANCOVA. WT: wild-type; cKO: Usp9X knockout. Error bars= standard error of the mean.

Table 1.6 Percentage of cells for each stage across different time points for wild-type and Usp9X-null neurons

Time point (hr)	Stage	Average % of cell		SE		
		WT	cKO	WT	cKO	P [a]
5	1	82.75	91.33	3.22	3.18	0.124
12	1	35.75	59.67	2.50	3.28	0.002
20	1	16.50	41.00	2.47	3.79	0.002
30	1	2.25	12.67	0.75	1.20	0.001
48	1	0.75	3.00	0.48	0.00	0.011
5	2	15.00	8.00	2.68	2.65	0.130
12	2	42.50	35.67	2.02	2.03	0.067
20	2	24.00	38.67	3.39	2.96	0.027
30	2	10.00	38.00	3.19	2.65	0.001
48	2	3.00	27.33	0.41	5.36	0.003
5	3	2.25	0.07	0.63	0.67	0.149
12	3	21.25	4.67	2.69	1.33	0.004
20	3	59.50	21.00	2.63	3.06	0.000
30	3	87.00	49.00	3.81	2.89	0.001
48	3	96.00	69.33	0.91	5.70	0.003

[a] Student's t-test P value

n=100 neurons from four mice per genotype have been analysed. WT: wild-type; cKO: Usp9X knockout; SE: Standard error of mean.

Studies have shown that the kinesin-1 motor domain (Kif5C560) and shootin-1 proteins can be used as markers for axon specification (Jacobson et al., 2006, Toriyama et al., 2006, Toriyama et al., 2010). Live cell imaging showed that these proteins are expressed in multiple growth cones, at the neurite tips, when the cells are symmetrical. However, when the symmetry of the neuron is broken, these proteins eventually accumulate predominantly in a single neurite, which later forms the axon (Jacobson et al., 2006, Toriyama et al., 2006, Toriyama et al., 2010). To study the delayed axon specification in real time using live cell imaging, wild-type and Usp9X-null neurons were transfected with a plasmid expressing a YFP-tagged truncated form of Kif5C560 (Jacobson et al., 2006). However, despite several attempts no YFP-fluorescence was detected and, due to time constraints this experiment was not continued.

3.6 Loss of Usp9X results in shorter axonal length at 48 hours

It has been previously shown that loss of Usp9X results in shorter axonal lengths in hippocampal cultures as early as 3DIV and this difference is maintained at least up to 7DIV (Stegeman et al., 2013). To determine if differences in axonal length are detectable earlier, the longest projection of stage 3 wild-type and Usp9X-null neurons was measured at 48 hours after plating. The axonal length of Usp9X-null neurons (mean length = 65μm) was significantly shorter than those of wild-type neurons (mean length = 95 μm; $p<0.001$), indicating that Usp9X is required for proper neuronal outgrowth (**Figure 3.6**).

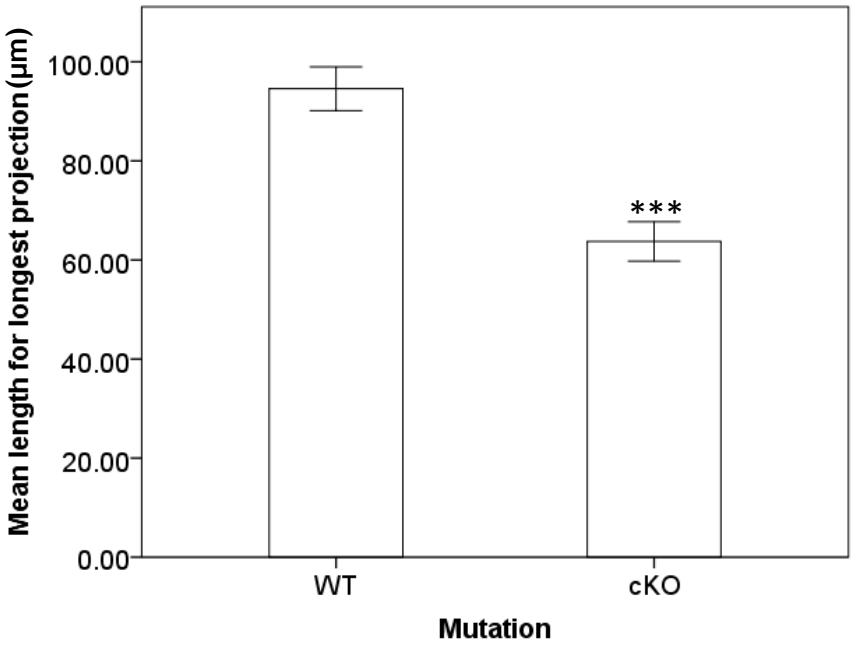

Figure 3.6 Loss of Usp9X reduces axonal length at early time points

The length of axons was measured 48 hours after plating and analysed using ImageJ. *** = Student's t-test $p < 0.001$. WT = wild-type littermate control; cKO = Usp9X-null neurons.

3.7 Loss of Usp9X does not affect the number of neurites

It has been previously shown that loss of Usp9X reduced the number of axon and dendritic termini in hippocampal cultures as early as 3 days *in vitro* and maintained up to 7DIV. However, the reduction of dendritic termini was not significantly different at 5 days *in vitro* (Stegeman et al., 2013). To determine if differences are detectable earlier, the number of neurites for stage 3 wild-type and Usp9X-null neurons was counted at 48 hours after plating. As shown in **Figure 3.3**, a neurite is defined as a minor projection with a length at least equal to, or longer, than the diameter of the cell excluding the longest projection, known as the axon (Ferrari et al., 2010). The mean number of neurites for wild-type neurons was 3.5 and Usp9X-null neurons 3.6, indicating that Usp9X does not affect the number of neurites formed at early stages of neuronal development (**Figure 3.7**).

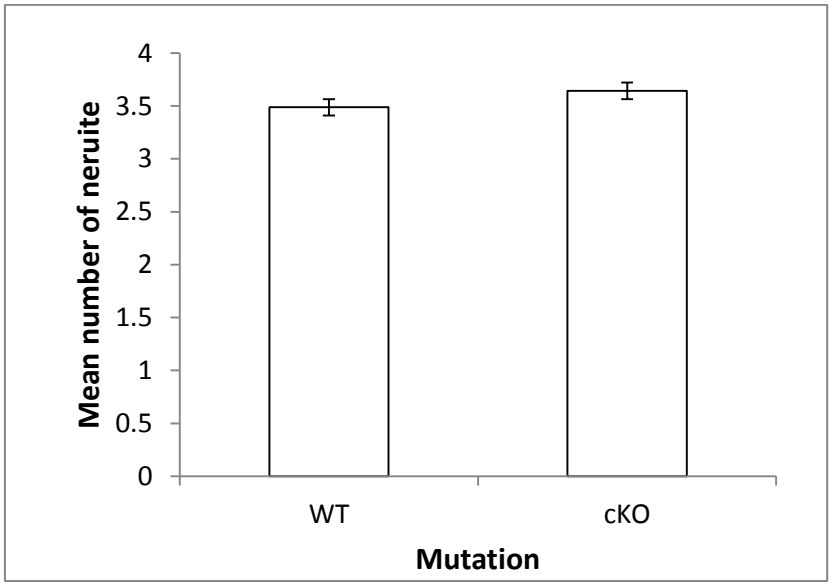

Figure 3.7 Loss of Usp9X does not affect the number of neurites

The number of neurites for stage 3 neurons was measured at 48 hours after plating and analysed using Student's t-test p =0.62. WT = wild-type littermate control; cKO = Usp9X-null neurons.

3.8 Discussion

Usp9X is required for normal axonal elongation and branching both *in vivo* and *in vitro* (Stegeman et al., 2013, Homan et al., 2014). The experiments presented here confirm that axons of Usp9X-null neurons were shorter at day 3 of culture compared to wild-type neurons (**Figure 3.2**), consistent with Stegeman *et al* (2013) who reported shorter axonal length at day 3, 5 and 7 days of culture when Usp9X is absent. Results in this chapter also indicated that differences in axonal length occurred as early as 2 days in culture, as the longest neuronal projections were significantly reduced by 30% without affecting the number of neurites when Usp9X is absent (**Figure 3.6** and **3.7**). Most significantly these experiments establish that Usp9X is also required for axon specification based on the dramatically delayed neuronal progression from stage 2 to 3 ($p<0.001$) (**Figure 3.5B**). Finally, Usp9X may also facilitate initial neurite formation as Usp9X-null neurons displayed delayed progression from fillopodia and lamellipodia presenting stage 1 neurons to those with neurites (stage 2).

Usp9X may also regulate axon growth. Data from 2DIV (this chapter) and 3, 5 and 7 DIV (Stegeman et al., 2013), for wild-type neurons, detected an axonal length of 95µm, 180µm, 440µm and 480µm, respectively. These same experiments indicate axonal length in Usp9X-null neurons at these time points of 60µm, 120µm, 270µm, and 280µm, respectively. The calculated "elongation rate" for Usp9X-null neurons over each 24 hour time frame was slower at 2.5µm/hour, 3.1µm/hour and 0.2µm/hour, compared to wild-type neurons' 3.5µm/hour, 5.4µm/hour and 0.8µm/hour, suggesting that the shorter axonal length in Usp9X neurons was an additive effect of both delayed axon specification and a slower elongation rate. Therefore, in the future, to more precisely examine axonal growth rate, live cell imaging should be performed.

The Kinesin-1 motor domain, Kif5C560 has been used as marker for axon specification (Jacobson et al., 2006). In this previous study, live cell imaging began 24 hours post-transfection to trace the transition from neuronal stage 2 to stage 3 (Jacobson et al., 2006). Several attempts were made to introduce the Kif5C560-YFP or pMAX-GFP plasmids into cultured hippocampal neurons by nucleofection at the time of plating. However, at 24 and 48 hours post-transfection, only GFP but no YFP fluorescent was observed, suggesting that transfection with YFP-tagged truncated

Kif5C failed. Given that Kif5C560-YFP was a gift from Dr. Gary Banker and only restriction digested with endonucleases, the sequence for the plasmid is required for sequencing in the future. Alternatively, Shootin-1 is another marker for axon specification which could be used in the future (Toriyama et al., 2006, Toriyama et al., 2010).

Usp9X is also required for neuritogenesis, the first step of neuronal differentiation. The dissociated neurons first form lamellipodia and filopodia structures after plating, which are both highly regulated by actin and microtubule dynamics and so for neurite formation (Dehmelt et al., 2003, Dent et al., 2007). However, the factors regulating neurite initiation have not been widely examined as compared to axon specification and growth. Given this is the first evidence showing that Usp9X might regulate neuritogenesis, which is consistent with its role in regulating cytoskeletal proteins (Homan et al., 2014), the role of Usp9X in this process is worth exploring. Neurite formation is the very first step of neuronal differentiation and a defect in this process might affect later stages of neuronal development.

In summary, loss of Usp9X resulted in delayed neuronal progression from stage 2 to stage 3, indicating that Usp9X regulates axon specification. Usp9X regulates the early stages of axonal development without affecting the number of neurites but does delay their formation. Regulation of axon specification by Usp9X might be mediated through its role in different neuronal signalling pathway including the TGFβ (Dupont et al., 2009, Xie et al., 2013) and mTOR (Agrawal et al., 2012) pathways and/or microtubule and actin dynamics (Homan et al., 2014) which are important determinants of axon-dendritic polarisation. Further evaluation of possible Usp9X substrates in hippocampal neuron cultures is presented in **Chapter 4**.

4. Evaluation of potential Usp9X substrates regulating axon specification and growth

4.1 Introduction

Loss of Usp9X delays axon specification (**Chapter 3**) and reduces the length and branches of the axon in cultured hippocampal neurons (Stegeman et al., 2013, Homan et al., 2014). These studies implicate Usp9X as a critical component in both axon specification and growth. However, the molecular mechanism by which Usp9X regulates axon development remains to be elucidated. This chapter investigates the possible molecular mechanism underlying Usp9X's role in axon specification and growth.

There are three main phases of axon development: (i) specification and neuronal polarity; (ii) growth or extension and, (iii) differentiation and maturation (Lewis et al., 2013, Barnes and Polleux, 2009). Multiple intrinsic and extrinsic factors such as TGFβ (Yi et al., 2010), Notch (O'Keefe et al., 2011) and mTOR (Morita and Sobue, 2009, Li et al., 2008) regulate the establishment of neuronal polarity, as well as actin/microtubule dynamics which are involved during neuronal growth. Interestingly, Usp9X has been associated with each of these signalling cascades as well as the regulation of actin/microtubule dynamics.

To identify proteins interacting with Usp9X during neural development our lab has previously conducted a yeast-2-hybrid screen of a human fetal (14week) brain library, using full length Usp9X as bait. From this screen, cDNA sequences encoding peptide fragments for PJA1 (an E3 ubiquitin ligase of the TGFβ pathway), Mindbomb 1 (a E3 ubiquitin ligase regulating the Notch pathway), Kif5B (microtubule-based motor protein) and EB1 (regulating microtubule dynamics) were identified, with reasonable confidence, as potential targets interacting with the full length Usp9X. In a separate series of experiments, 2D proteomic analysis was carried out on Usp9X-null cortical neurons following 5DIV culture. A total of 28 proteins were differentially expressed between wild-type and Usp9X null neurons of which 27 were down-regulated (Homan et al., 2014). From these data sets, we prioritised for further investigation, those targets implicated in the establishment of cytoskeletal structure and signalling pathways relevant to axon development. The primary aim of the experiments in this

chapter was to efficiently screen a number of potential Usp9x substrates, before proceeding with a more detailed analysis of any that were differentially regulated, in the absence of Usp9x, during axon specification and/or growth. The combined "Results and Discussion" for each candidate is presented below.

4.2 Distribution of total level Usp9X in hippocampal neurons

In this chapter, all experiments have been conducted on 3DIV Usp9X cKO and wild-type (WT) hippocampal neurons unless otherwise stated, as this is the stage when most of the neurons are polarised.

Embryos were genotyped to identify males (Sry positive), either Cre-negative (WT controls) or Cre-positive (Usp9X-null). To confirm the genotyping, the distribution and total level of Usp9X protein was examined by immunofluorescence and immunoblotting. Based on both techniques, the total level of Usp9X in cKO neurons compared to controls was negligible (**Figures 4.1** and **4.2**). Punctate staining for Usp9X has previously been shown in different cell types and *in vivo* (Jolly et al., 2009, Theard et al., 2010). In control neurons, Usp9X localised in punctate in the soma, dendrites and axon. Additionally, high Usp9X levels were observed at the axonal growth cone (**Figure 4.3**), which is consistent with recent studies (Homan et al., 2014, Stegeman et al., 2013).

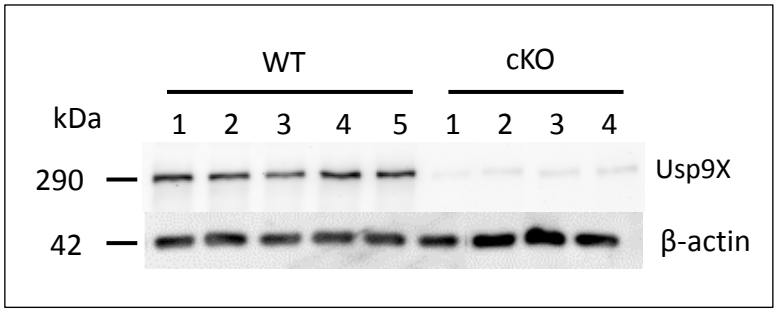

Figure 4.1 Total level of Usp9X in 3 day *in vitro* hippocampal neurons
Total level of Usp9X protein was negligible for all Usp9X knockout (cKO) samples, confirming genotyping results. WT: wild-type; cKO: Usp9X conditional knockout. n=5 wild-type embryos and 4 Usp9X cKO embryos were used for analysis.

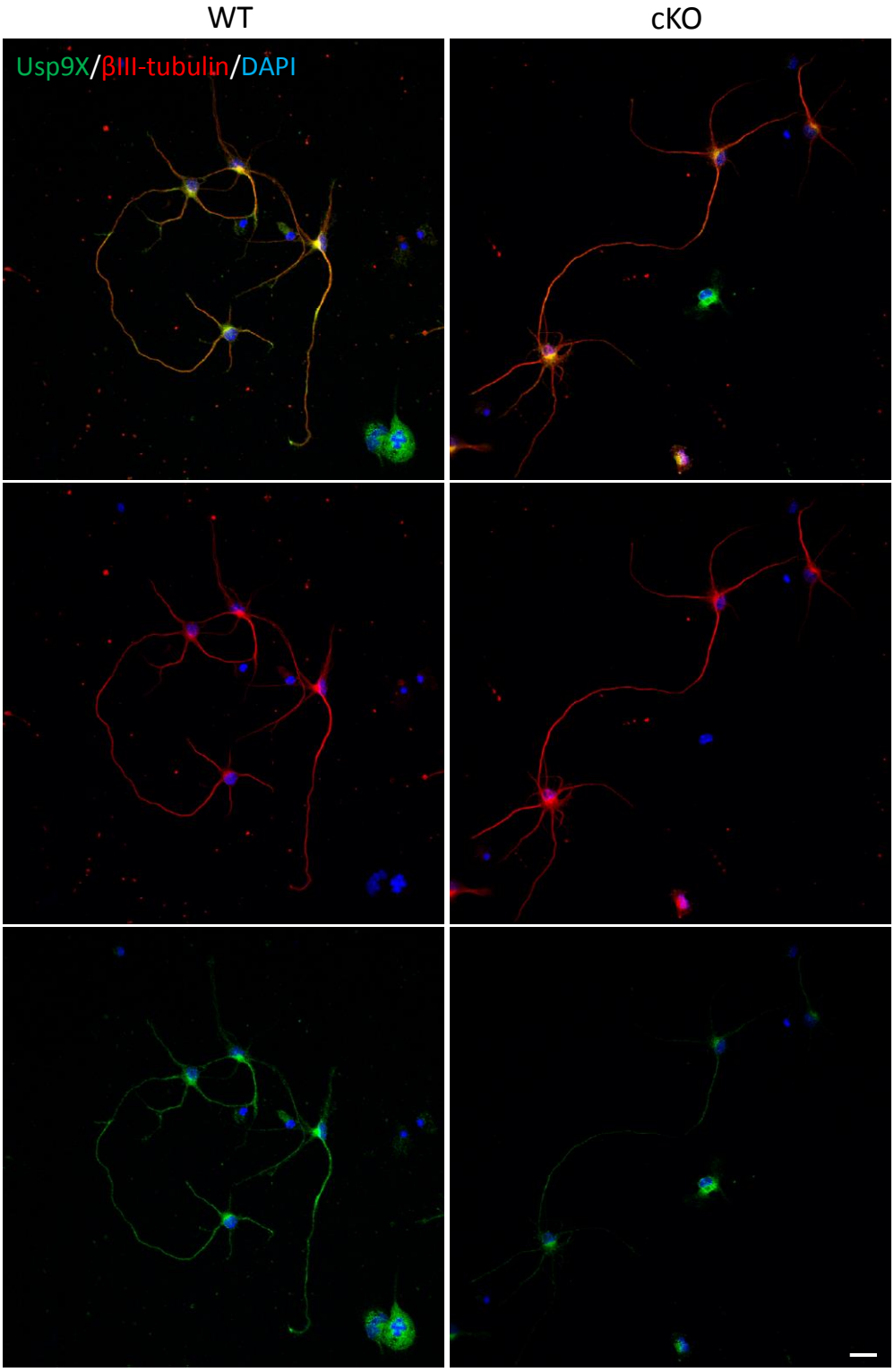

Figure 4.2 Usp9X protein level was negligible in 3 day *in vitro* Usp9X-null hippocampal neurons

Very little Usp9X protein was detected by immunofluorescence, using antibodies directed toward both the N- and C-terminal domains of Usp9X, in neurons derived from Cre-positive males (cKO). Usp9X (green; anti-Usp9x C-terminal antibody from Bethyl Laboratiries); Nuclear marker DAPI (blue). WT: wild-type; cKO: Usp9X knockout. Scale bar: 20μm.

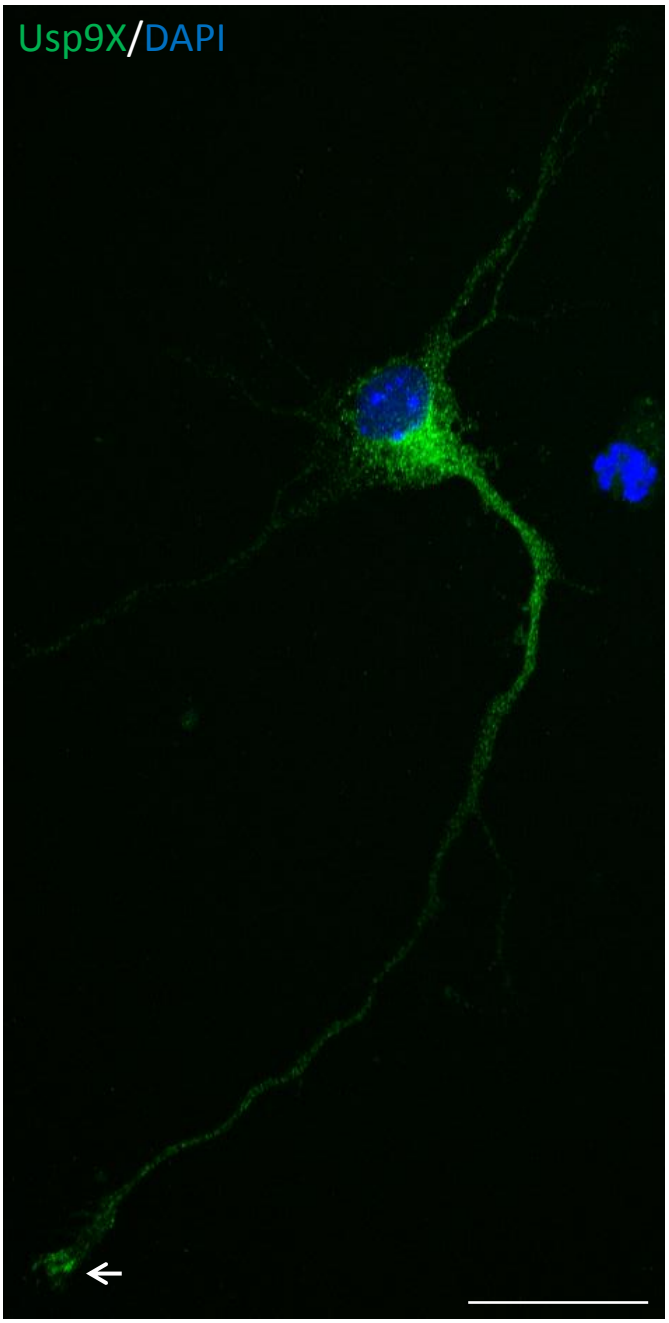

Figure 4.3 Usp9X is present in puncta within the soma, axon, dendrites and is enriched at the axonal growth cone in stage 3 wild-type hippocampal neuron Arrow indicates Usp9X enrichment at the axonal growth cone. Usp9X (green); Nuclear marker DAPI (blue). Scale bar: 20μm.

4.3 Actin / microtubule dynamics regulate axon development

The major cytoskeletal components for axons and dendrites are microtubules and actin filaments (**Section 1.1.1**). The microtubule is the key determinant of the polarised axon-dendrite compartment of the neuron. It is a long filament formed from the polymerization of α- and β-tubulin subunits which occurs only at the growing end ("plus end"), hence it is polarised (Conde and Caceres, 2009). It is the local stabilization of microtubules in a single neurite that specify axon identity (Witte et al., 2008). Within the axon, dynamic microtubules are located at the distal end of axon and the stable microtubules at the proximal region (near the soma).

There are different proteins associated with the actin / microtubule cytoskeleton that form the framework of the developing axon (Hur et al., 2012, Conde and Caceres, 2009, Lewis et al., 2013). As a loss of Usp9X from hippocampal neurons reduces the level of some cytoskeletal structural proteins involved in these processes their status was investigated in individual Usp9X-null neurons (Homan et al., 2014).

4.3.1 Stathmin-1

Reduced stathmin-1 protein levels were detected in a proteomic analysis of cultured Usp9X-null hippocampal neurons (Homan et al., 2014). Stathmin-1 is a microtubule destabilising protein (Wen et al., 2010). It increases the rate of microtubule catastrophes, which is the transition from growth to shrinkage, either by acting directly at the plus end of the microtubule or by tubulin sequestration (Grenningloh et al., 2004, Conde and Caceres, 2009, Gupta et al., 2013). Two studies have examined the distribution of stathmin-1 in cultured cortical neurons (Di Paolo et al., 1997, Gavet et al., 2002). While both detected cytosolic stathmin-1, mainly in the cell soma (Di Paolo et al., 1997) one also showed stathmin-1 expression extending into dendrites, axon and growth cones (Gavet et al., 2002).

To examine if stathmin-1 distribution was affected in Usp9X-null neurons, hippocampal neurons were fixed at 3DIV, when most neurons are at stage 3. The distribution of stathmin-1 in 30 wild-type and 30 Usp9X-null neurons (derived from three embryos of each genotype) was compared. In wild-type neurons, stathmin-1 was detected in the cell soma, dendrites and axon which is consistent with the

previous report (Gavet et al., 2002). The neurons were co-stained with phalloidin, which is a marker of filamnetous actin, which revealed enrichment of stathmin-1 in both dendritic and axonal growth cones. However, there was no observable difference observed in stathmin-1 distribution in the absence of Usp9X (**Figure 4.4** and **4.5**). The total level of stathmin-1 in Usp9X-null hippocampal neurons was examined by immunoblot (**Figure 4.6A**). The amount of protein loaded for all Usp9X-null samples was under-loaded due to a technical error. Nonetheless, densitometric analysis of stathmin-1 levels, compared to β-actin, revealed that there was no statistical significant difference between wild-type and Usp9X-null neurons (**Figure 4.6B**; Student's *t* test, $p = 0.19$).

At the same time a preliminary examination of stathmin-1 expression in E18.5 Usp9X cKO mouse brain sections was also conducted. However, no obvious difference was observed (**Figure 4.7**). *In vivo* brain sections may not be an ideal system to examine the expression and distribution for the proteins of interest. This is due to the multiple layers of cells for a section, making it difficult to visualise or examine the expression of the protein in a specific sub-cellular compartment, for instance, the axonal growth cone. Also, loss of Usp9X might result in only subtle changes in the proteins and would be difficult to be detected in the brain section. A reduction in stathmin-1 protein level was identified from 2D proteomic data derived from dissociated cultured Usp9X-null neurons (Homan et al., 2014). Therefore, *in vitro* hippocampal neurons were used to analyse the expression and distribution for protein of interest. However, after examining 30 neurons from a total of 3 wild-type and 3 Usp9X cKO brains, no evidence of an alteration on stathmin-1 was detected. Therefore examination this potential "substrate" was not pursued further.

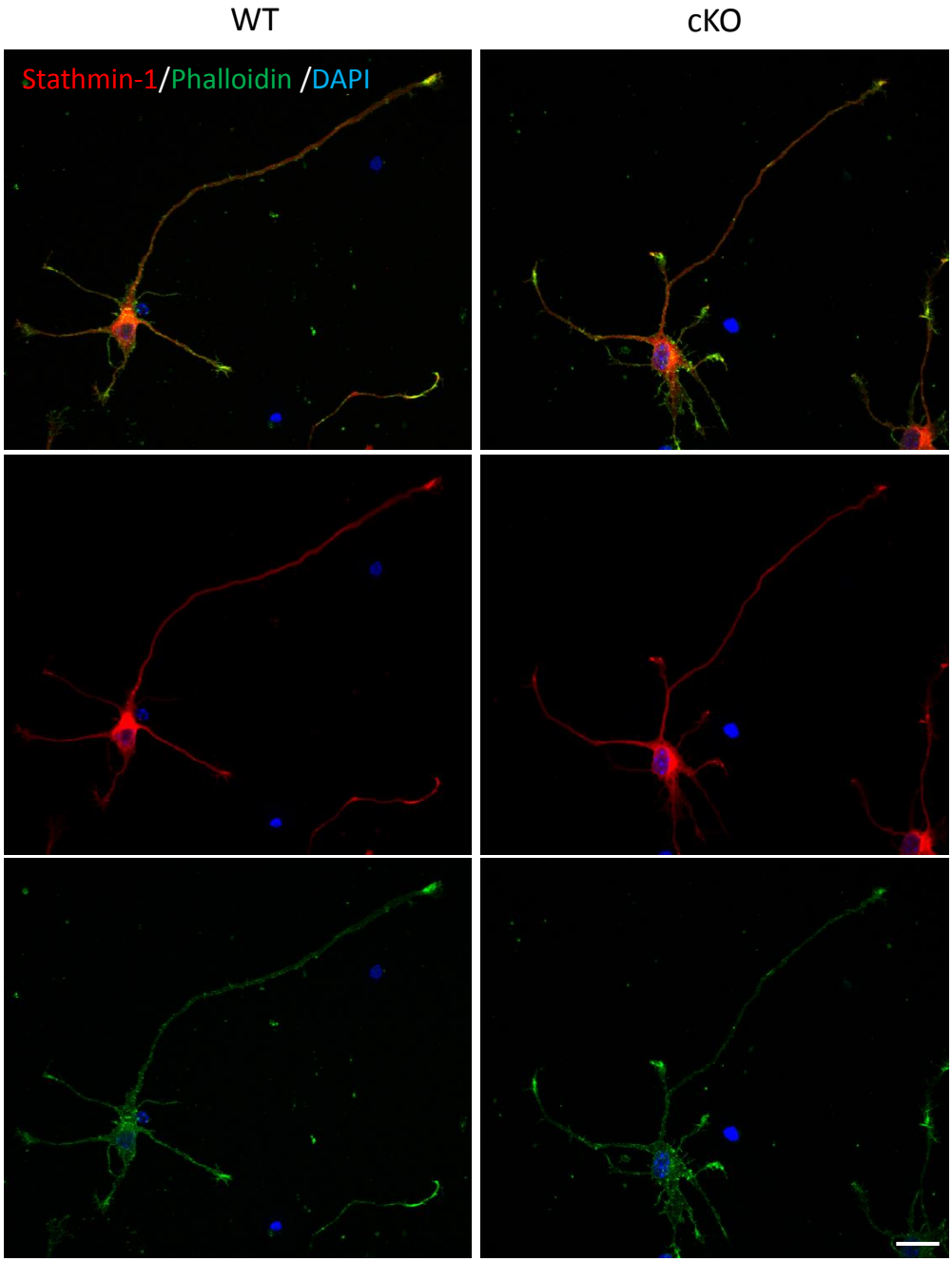

Figure 4.4 Distribution of stathmin-1 for both wild-type and Usp9X-null hippocampal neurons were similar

Stathmin-1 (red) was expressed in cell soma, dendrite and axon. It was highly enriched at the growth cone for dendrites and axon. 30 neurons derived from three embryos per genotype were compared. Stathmin-1 (red); Phalloidin (green); Nuclear marker DAPI (blue). WT: wild-type; cKO: Usp9X knockout. Scale bar: 20μm.

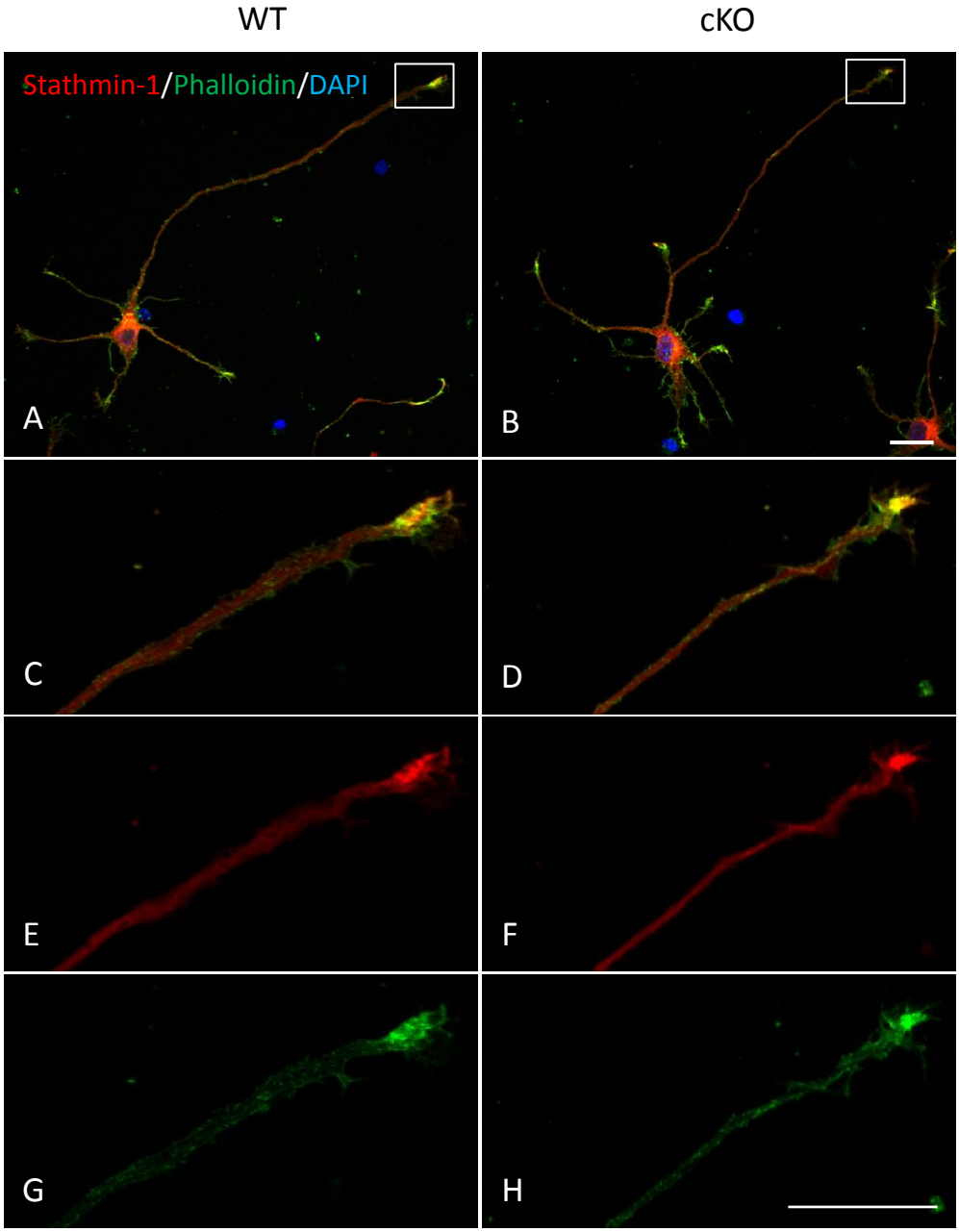

Figure 4.5 Stathmin-1 was highly enriched in the axonal growth cone in both wild-type and Usp9X-null hippocampal neurons

Immunofluorescent staining for stathmin-1 (red) and phalloidin (green). Cell nuclei were stained DAPI (blue). Higher magnification images (C-H) for the axonal growth cones (white boxes in A and B) were taken. WT: wild-type; cKO: Usp9X knockout. Scale bars represent 20μm.

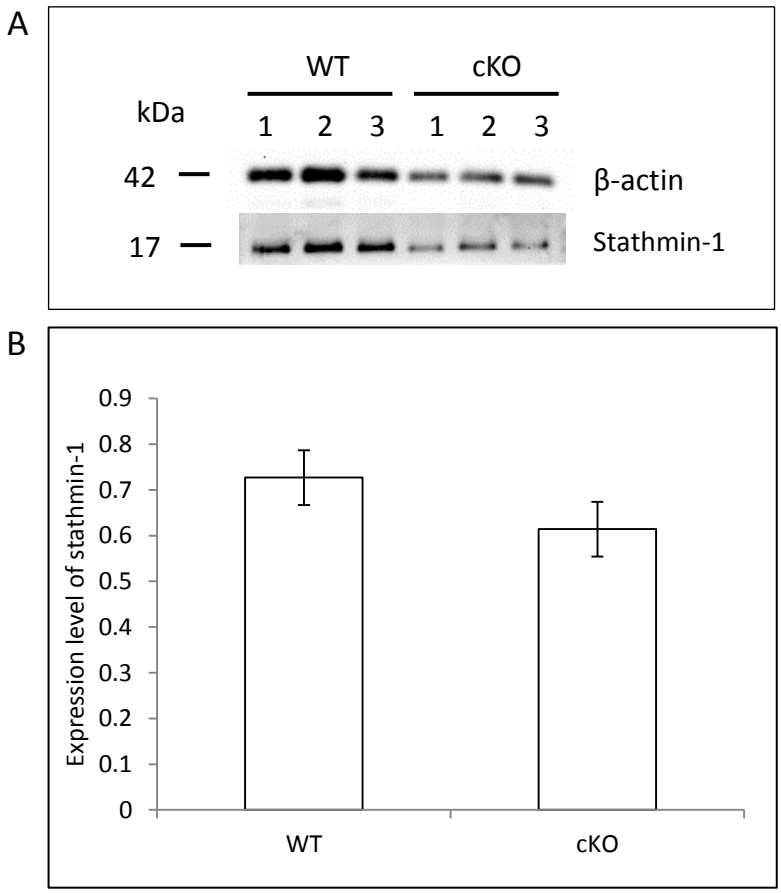

Figure 4.6 Total stathmin-1 level is not significantly depleted in cultured Usp9X-null hippocampal neurons

(A) Immunoblot analysis of stathmin-1 protein levels in hippocampal neuronal cultures from wild-type (WT) and Usp9X-null (cKO) embryos. (B) Densitometry was performed for stathmin-1 and normalised against β-actin. There was no statistical significant difference in the total level of stathmin-1. WT: wild-type; cKO: Usp9X knockout. Student's *t* test $p = 0.19$ (n=3 embryos per genotype). Error bars represent standard error of the mean.

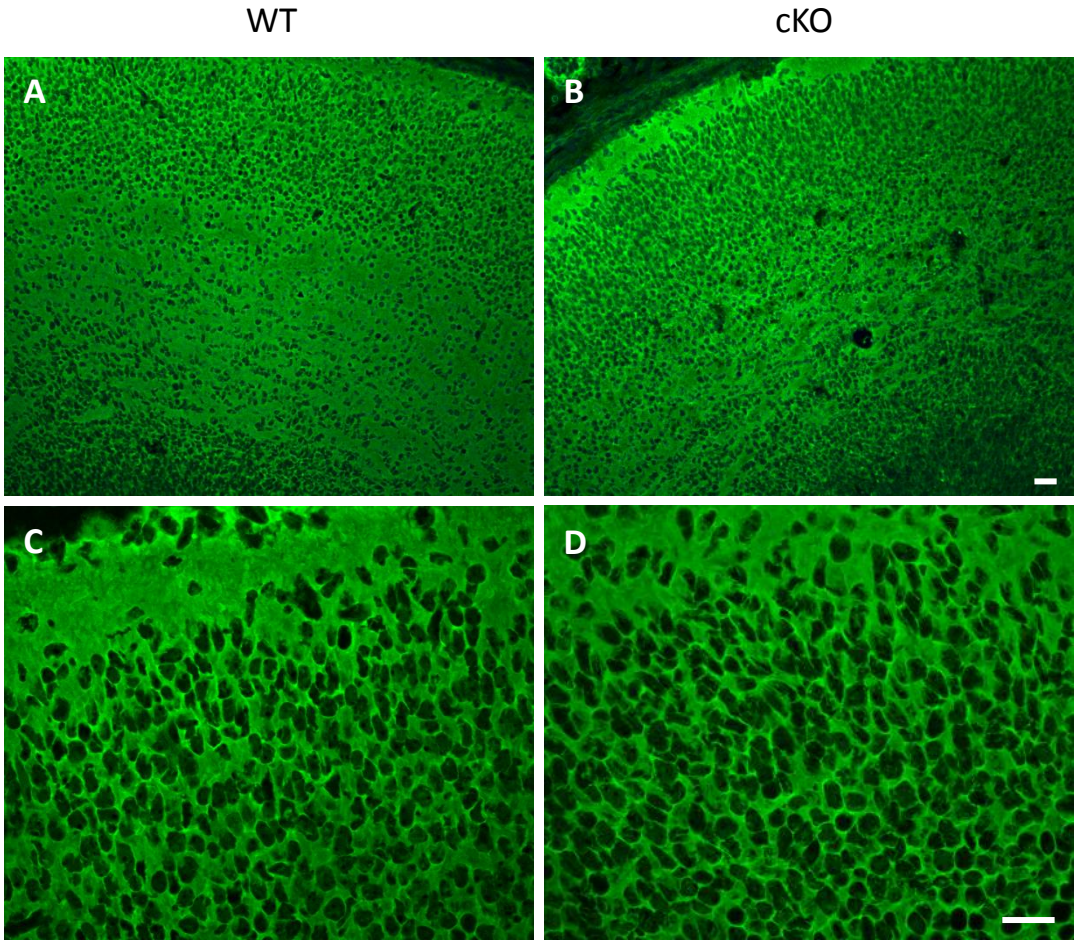

Figure 4.7 Stathmin-1 expression in the cortical region of E18.5 mouse brain

Low (A,B) and high (C,D) magnification images showed that stathmin-1 (green) was ubiquitously expressed in the cortical region of E18.5 mouse brain for wild-type and Usp9X-null models (n=1 embryo). WT: wild-type; cKO: Usp9X knock-out. Scale bar: 20μm.

4.3.2 Collapsin response mediator protein-2 (CRMP-2)

A decrease in collapsin response mediator protein-2 (CRMP-2) protein levels was reported in Usp9X-null neuronal cultures (Homan et al., 2014). CRMP-2 not only regulates axon specification, but also axon growth and branching, by binding to tubulin heterodimers thereby promoting microtubule assembly (Fukata et al., 2002, Inagaki et al., 2001). Previous reports have demonstrated that CRMP-2 is expressed in the cell soma, dendrites and axon and is highly expressed at the distal end of the axon in stage 3 hippocampal neurons (Yoshimura et al., 2005, Inagaki et al., 2001).

To examine if the distribution of CRMP-2 was affected when Usp9X was absent, hippocampal neurons were subjected to immunofluorescence analysis after three days *in vitro*. 30 neurons from both control and Usp9X cKO models (n = 1 embryo of each genotype) were compared. CRMP-2 was found to be expressed in the cell soma, dendrites and the axon in the hippocampal neurons. There was no obvious difference in the CRMP-2 subcellular distribution between the wild-type and Usp9X-null neurons at low magnification (**Figure 4.8**).

However, high expression of CRMP-2 at the distal end of the axon, as previously reported (Inagaki et al., 2001, Yoshimura et al., 2005), was not detected even in wildtype neurons. This could be due to the different CRMP-2 antibodies used here. The previous studies used C4G antibody, which binds to the unphosphorylated form of CRMP-2 (Gu et al., 2000, Inagaki et al., 2001, Yoshimura et al., 2005). For this project, 3F4 antibody, which recognises phosphorylated CRMP-2 at Thr-509, Ser-518 and Ser-522 was used. 3F4 antibody binds completely to the epitope when all the three sites are phosphorylated and has been widely used to study the neurofibrillary tangles, which accumulate in neurons in Alzheimer's disease (Yoshida et al., 1998, Ryan and Pimplikar, 2005, Gu et al., 2000). Attempts to obtain small samples of the C4G antibodies were unsuccessful. Therefore the further analysis of CRMP-2 in the absence of Usp9x was paused while other candidates were pursued. In the future, to examine the role of CRMP-2 and its possible interaction with Usp9X during axon development, C4G antibody and antibody p-CRMP-2 (at Thr-514 only) should be used for complete analysis (Yoshimura et al., 2005, Tan et al., 2013).

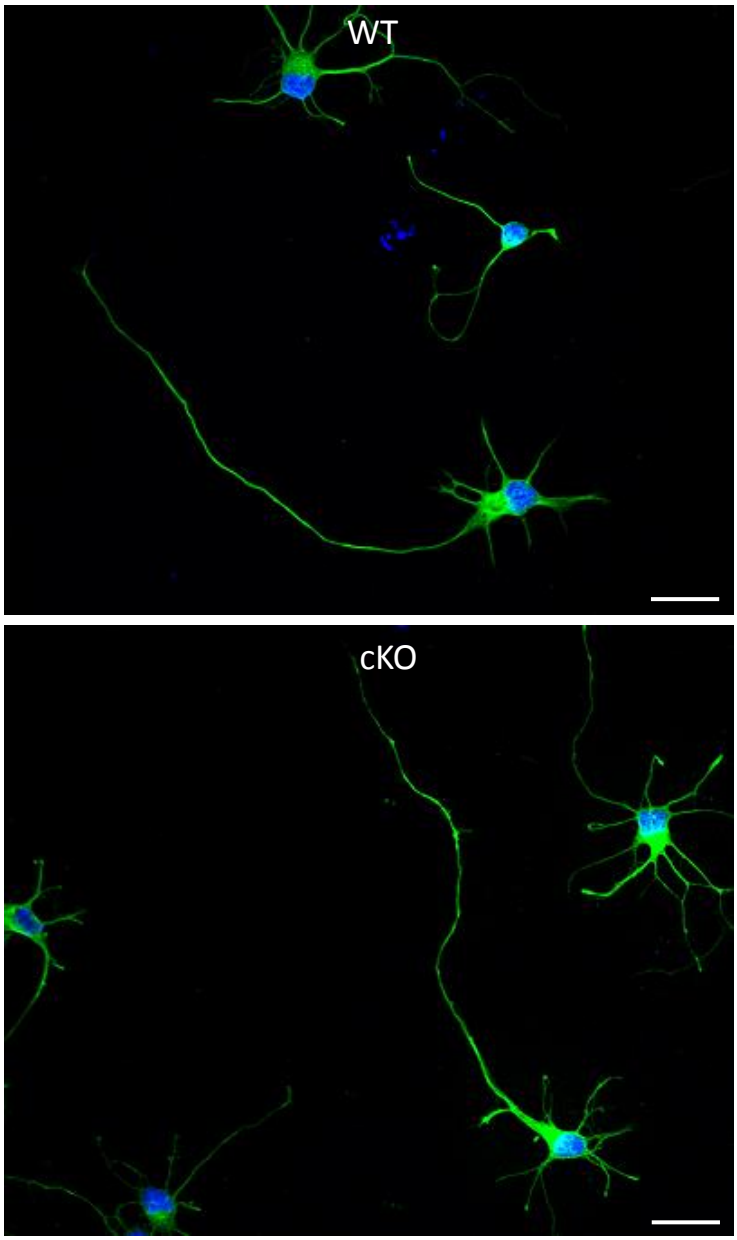

Figure 4.8 CRMP-2 expression is similar in wild-type and Usp9X-null hippocampal neurons

Subcellular distribution of CRMP-2 for wild-type and Usp9X-null neurons was observed to be similar. 30 neurons derived from a mouse embryo per genotype. CRMP2 (green); Nuclear marker DAPI (blue). WT: wild-type; cKO: Usp9X knockout. Scale bar: 20μm.

4.3.3 Kif5B

The yeast-two-hybrid screen of human fetal brain library identified Kif5B as interacting with Usp9X. In neurons, Kif5B has been demonstrated to anterogradely transport mitrochondria, synaptic vesicle precursor, voltage-gated potassium and sodium channels along the microtubules (Saxton and Hollenbeck, 2012, Cai et al., 2007, Rivera et al., 2007, Su et al., 2013). Kif5B is present in the soma, dendrites and axon of cortical neurons in dissociated culture (Rivera et al., 2007). To examine if the subcellular distribution of Kif5B is affected in the absence of Usp9X, hippocampal neurons were fixed after three days *in vitro* culture. The cellular distribution of Kif5B was compared between 30 wild-type and 30 Usp9X-null neurons (derived from 4 mice per genotype). In wild-type neurons, Kif5B was detected in the cell soma, dendrites and axon as reported (Rivera et al., 2007). Interestingly, there was an extensive reduction of Kif5B protein observed when Usp9X was absent (**Figure 4.9**). To further confirm the reduction of Kif5B in 3DIV Usp9X-null hippocampal neurons, immunoblotting, using the same Kif5B antibody was attempted several times. However, this antibody did not recognise Kif5B protein in the neuronal culture and brain lysate as shown in **Figure 5.4**. The nature of the interaction between Kif5B and Usp9X was pursued further and will be presented in detail in **Chapter 5**.

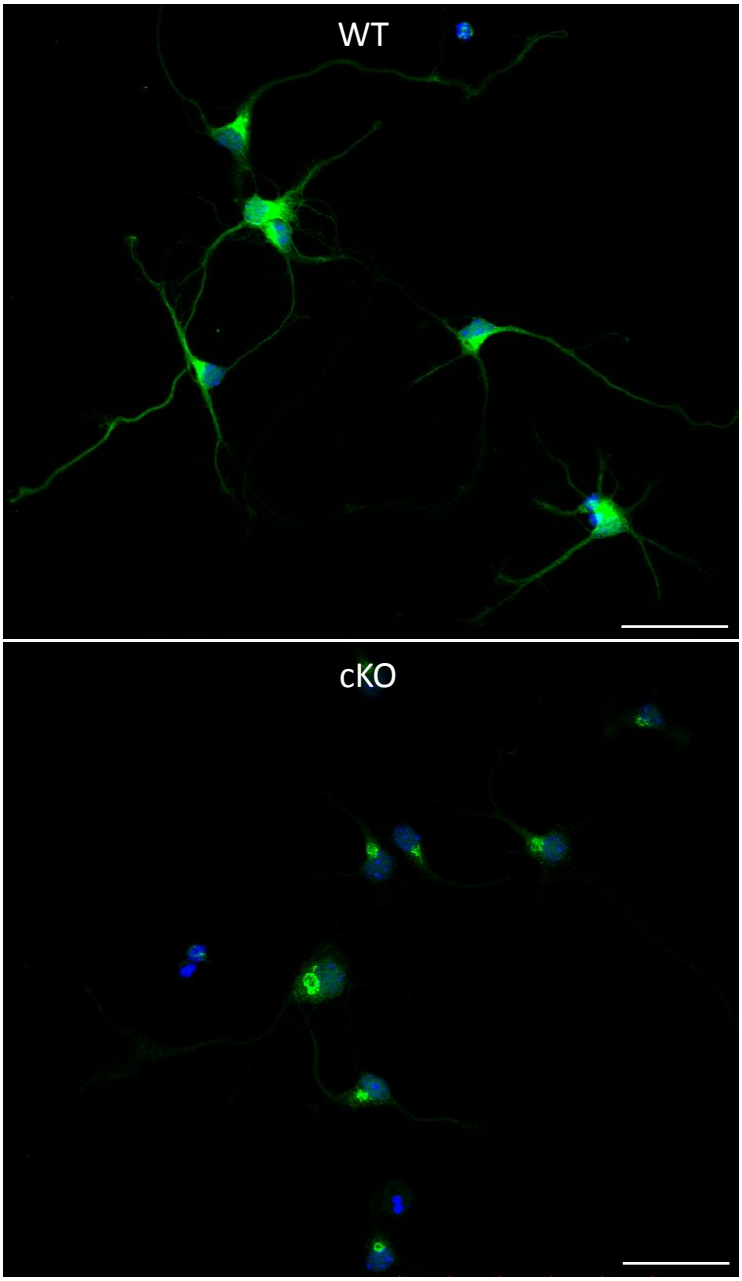

Figure 4.9 Kif5B is reduced in 3 day *in vitro* Usp9X null hippocampal neurons Kif5B was present in the soma, dendrites and axon of the wild-type neurons. There was a significant reduction of Kif5B in all three compartments when Usp9X was absent. 30 neurons derived from four mice per genotype were compared. Kif5B (green); Nuclear marker DAPI (blue). WT: wild-type; cKO: Usp9X knockout. Scale bar: 20μm.

4.3.4 Microtubule affinity regulated kinase (MARK4)

MARK4, which phosphorylates tau resulting in microtubule destabilisation, is an Usp9X substrate (Trinczek et al., 2004, Al-Hakim et al., 2008). Interaction of Usp9X and its substrates is cell context and developmental stage specific. Deubiquitylation of MARK4 by Usp9X in kidney cells (Hek293) does not control the stability of MARK4, instead it regulates its phosphorylation and activation by the LKB1 tumour suppressor (Al-Hakim et al., 2008). Therefore, we proposed that loss of Usp9X might increase the ubiquitylated form of MARK4 and this in turn increase the phosphorylation of Tau, resulting in microtubule instability. This could in turn contribute to the shorter axonal length in Usp9X knock-out neuronal cell.

To examine if loss of Usp9X affected the subcellular distribution and total protein level of MARK4, immunofluorescence and immunoblotting were performed. The cellular expression of MARK4 was observed in the soma, dendrites and axon. There was no observable difference in the cellular distribution of MARK4 in Usp9X-null neurons (**Figure 4.10**). Densitometry was performed on immunoblots to analyse MARK4 band intensity in wild-type and Usp9X-null neurons. The expression for MARK4 was normalised with β-actin. There was no statistical significant difference in the total level of MARK4 between wild-type and Usp9X-null neurons after analysing with Student's t test with $p=0.07$ (**Figure 4.11**).

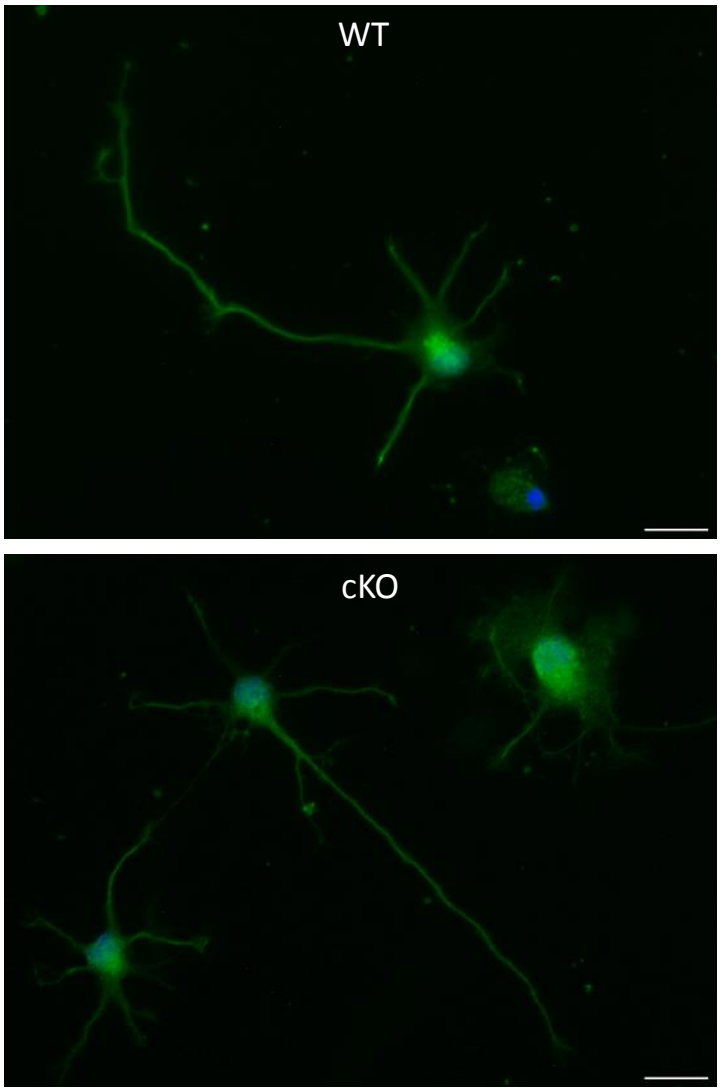

Figure 4.10 Subcellular distribution for MARK4 was similar between wild-type and Usp9X-null hippocampal neurons

MARK4 was observed in the soma, dendrites and axon of hippocampal neurons. There was no obvious difference in the cellular distribution of MARK4 between wild-type and Usp9X-null neurons. 30 neurons for a mouse per genotype have been compared. MARK4 (green); Nuclear marker DAPI (blue). WT: wild-type; cKO: Usp9X knockout. Scale bar: 20μm.

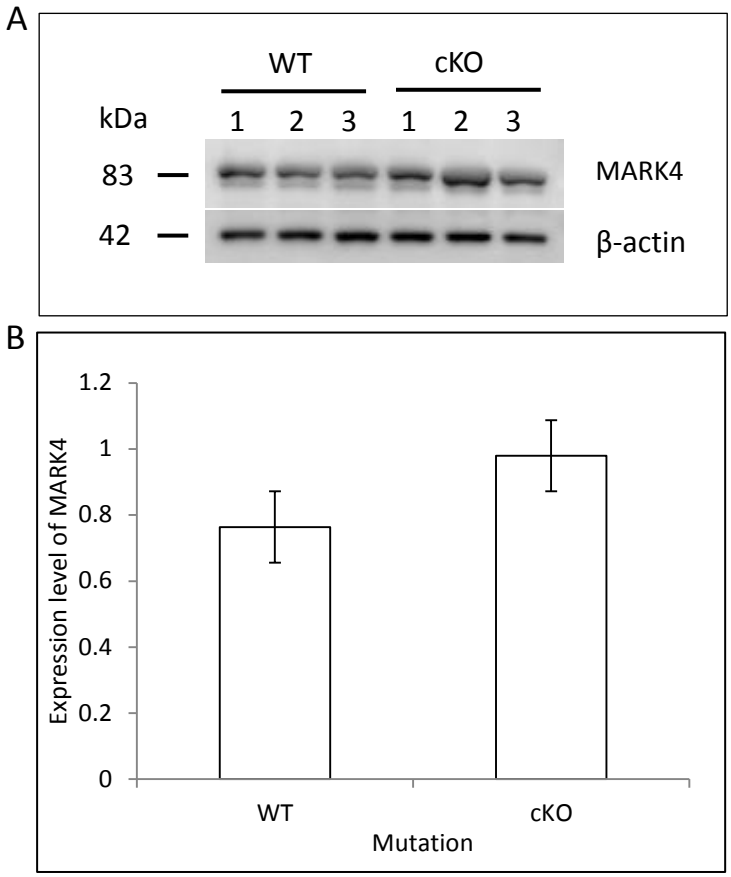

Figure 4.11 Total level of MARK4 is not significantly altered in 3 day Usp9X-null *in vitro* hippocampal neurons

(A) Immunoblot analysis of MARK4 protein levels in hippocampal neuronal cultures from wild-type (WT) and Usp9X-null (cKO) embryos. (B) Densitometric analysis comparing MARK4 levels for wild-type and Usp9X-null neurons normalised against β-actin. There was no statistical significant difference in the total level of MARK4 between wild-type and Usp9X-null neurons in the hippocampal neurons. WT: wild-type; cKO: Usp9X knockout. Student's *t* test $p = 0.07$ (n=3). Error bars represent standard error of the mean.

4.3.5 AF-6

Another possibility for the involvement of Usp9X during axon development is through AF-6. AF-6 is a substrate for Usp9X in polarised Madine Darby canine kidney II (MDCKII) cells and its activity is mediated, in large part, by Ras (Taya et al., 1998). In cortical neurons, AF-6 is distributed in the soma, dendrites and axon. It accumulates at the site of budding growth cones of the axonal tips (Iwasawa et al., 2012). Overexpression of AF-6 in cultured cortical neurons increased axon number without affecting axonal length (Iwasawa et al., 2012). The Ras / AF-6 pathway has been suggested to induce axonal branching in an actin-dependent manner (Mandai et al., 1997, Iwasawa et al., 2012).

To study if the impaired axonal growth and branching in the Usp9X-null neurons was due to the reduced or altered AF-6 expression, the subcellular distribution of AF-6 was examined in hippocampal neuronal culture. AF-6 was present in the soma, dendrites and axon. Higher expression of Af-6 was observed at the growth cone of the axon. However, there was no observable difference observed in AF-6 distribution in the absence of Usp9X (**Figure 4.12**). Based on these preliminary results, loss of Usp9X did not affect the cellular distribution of AF-6. Therefore, further examination for AF-6 was not continued.

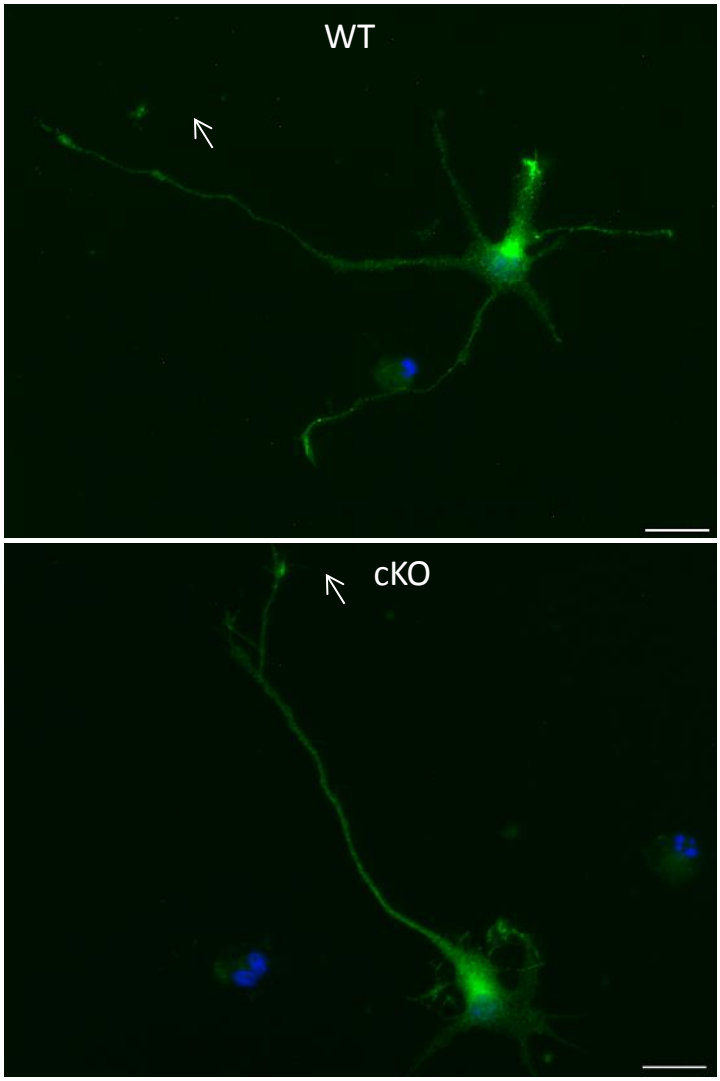

Figure 4.12 Cellular distribution of AF-6 is unaltered in Usp9X cKO hippocampal neurons

AF-6 (green) was observed in the soma, dendrites and axon of the neurons. It was accumulated at the growth cone of the axon tips. There was no observable difference in the cellular expression of AF-6 between wild-type and Usp9X-null neurons. White arrow indicates the high AF-6 expression in the tips of the axon. 30 neurons from a mouse per genotype have been compared. AF-6 (green); Nuclear marker DAPI (blue). WT: wild-type; cKO: Usp9X knockout. Scale bar: 20μm.

4.4 Axon development and the TGFβ signalling pathway

The TGFβ pathway has been shown to reduce the number of neural progenitors and promote neuronal differentiation (Vogel et al., 2010). This pathway also regulates both axon specification and growth in cultured hippocampal neurons (Ishihara et al., 1994, Yi et al., 2010). These results are consistent with the findings in dissociated hippocampal neurons of Usp9X knock-out mice which have delayed axon specification and shorter axonal length, suggesting the involvement of Usp9X in the regulation of axon production via TGF-β signaling pathway (Stegeman et al., 2013). Previous studies have also shown that hippocampal neurons transfected with TGFβ luciferase reporter construct do not respond to increasing concentrations of TGFβ when Usp9X was absent (Stegeman et al., 2013). At the mRNA level, BDNF, which is an endogenous target gene of TGFβ, showed no response to TGFβ ligand compared to wild-type neurons (Stegeman et al., 2013). At the cellular level, exogenous TGFβ treatment increased axonal length and number of axon and dendritic termini in the wild-type neurons but not in the Usp9X-null neurons. These results demonstrate that Usp9X is required for neurons to respond to TGFβ ligand (Stegeman et al., 2013).

There are several possible molecular mechanisms whereby Usp9X might regulate the TGFβ pathway during axon development. Two include the known Usp9X substrates, Smad4 and Smurf1, the common second messenger and an E3 ubiquitin ligase of the TGFβ pathway, respectively (Dupont et al., 2009, Xie et al., 2013). Another possibility is through the known TGFβ pathway target gene, BDNF (Sometani et al., 2001, Stegeman et al., 2013) and yet another is through the new putative Usp9X target, found in the yeast-2-hybrid and mass spectrometry following Usp9X affinity purification, PJA1 (Agrawal et al., 2012). The expression of each of these components of the TGFβ-pathway and potential Usp9X substrates was investigated in cultured hippocampal neurons.

4.4.1 Brain-derived neurotrophic factor (BDNF)

TGFβ ligand treatment increases axonal length and branching in cultured neurons (Ishihara et al., 1994, Stegeman et al., 2013). One of the target genes for TGFβ pathway is brain-derived neurotrophic factor (BDNF) as treatment of TGFβ ligand in cultured cortical neurons increased BDNF mRNA and protein levels (Sometani et al., 2001). A recent study reported that Usp9X is necessary for neurons to respond to TGFβ ligand. At the mRNA level, BDNF showed no response to TGFβ ligand when Usp9X was absent. At the cellular level, the axon of the Usp9X null neurons failed to show the TGFβ ligand-induced increase in axonal length (Stegeman et al., 2013). Treatment with exogenous BDNF triggers the specification of axons in developing hippocampal neurons in culture (Shelly et al., 2007). Endogenous BDNF also acts as an autocrine factor triggering its own secretion, which promotes axon specification and growth in hippocampal neurons (Cheng et al., 2011b).

To examine if BDNF treatment could rescue the delayed axon specification and growth in the absence of Usp9X, wild-type and Usp9X-null neuronal culture were treated with 100ng/ml BDNF added into the culture medium. Neurons were categorised into the three different developmental stages based on morphological study and measurement of the length of their neurites as described in Figure 3.3 (Dotti et al., 1988). However, neither wild-type or Usp9X-null neurons showed any response to exogenous BDNF (**Figure 4.13**). Given the previous report demonstrating that BDNF promotes axon specification, the failure of wild-type neurons to respond (**Figure 4.13**) suggested that the experiment was not working in our hands (Shelly et al., 2007, Cheng et al., 2011b).

BDNF treatment induces the activation of extracellular signal-regulated kinase, Erk1/2 signalling (Alonso et al., 2004, Slack et al., 2005). To confirm the activity for the recombinant BDNF protein, hippocampal neurons were treated with 100ng/mL of BDNF in neuronal culture media 6 hours after plating. The total level for Erk1/2 and p-Erk1/2 was examined by performing immunoblot. The treatment of BDNF resulted an increment for the total level of p-Erk1/2 (**Figure 4.14**), suggesting the recombinant BDNF was working and the unsuccessful experiment shown in **Figure 4.13** was not due to the exogenous BDNF used.

The unsuccessful experiment was possibly due to the method of BDNF treatment application. Localised exposure of one neurite of the undifferentiated neuron to BDNF has been shown to promote axon specification. To expose BDNF to single neurites, BDNF coated beads or BDNF stripes coated plate can be used to induce axon specification (Cheng et al., 2011a, Cheng et al., 2011b). However, these resources and technologies were not available and so this experiment was not investigated further.

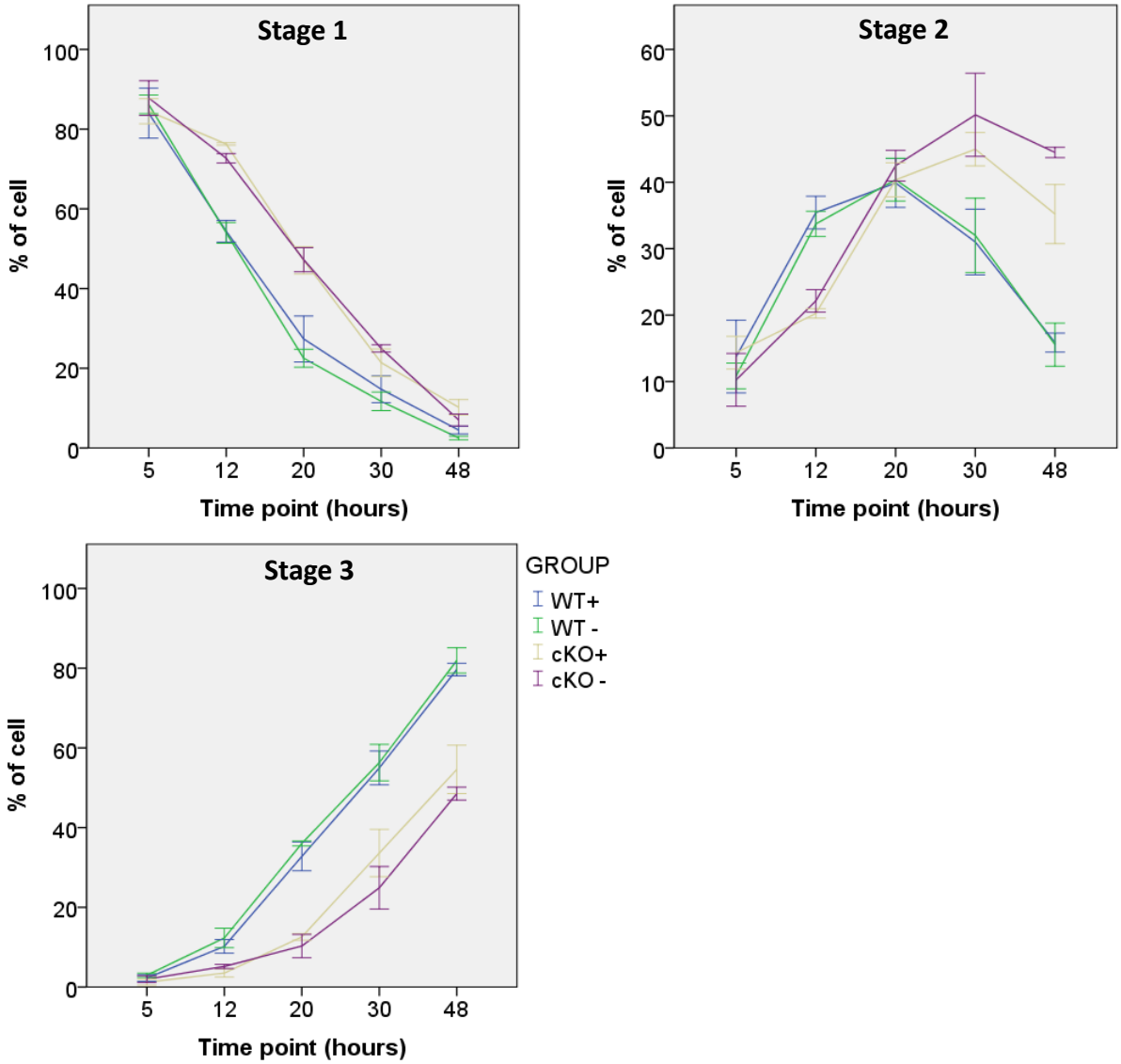

Figure 4.13 Developmental progression of Usp9X-null hippocampal neuronal cultures treated with BDNF

Percentage of stage 1 (A), stage 2 (B) and stage 3 (C) wild-type and Usp9X-null neurons treated and untreated with 100ng/ml of BDNF over time. No differential response to BDNF was detected in wild-type or Usp9x-null neurons. 100 neurons treated and untreated with BDNF derived from three mice per genotype have been compared. WT: wild-type; cKO: Usp9X knockout; +: BDNF treated; -: BDNF untreated.

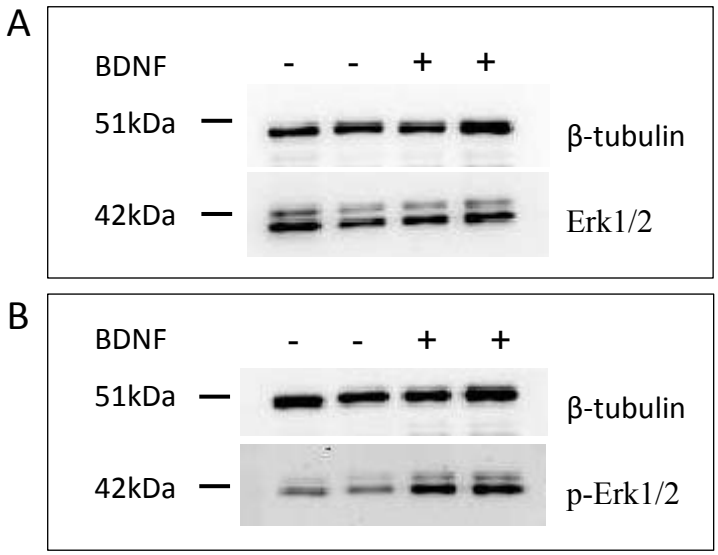

Figure 4.14 Treatment of BDNF in hippocampal neurons triggers the activation of Erk1/2 signalling

BDNF treatment did not affect the total level of Erk1/2 (A) but it increased the total level of p-Erk1/2 (B) indicating the recombinant BDNF protein was active. -: untreated; +: treated with BDNF.

4.4.2 Praja1 (PJA1)

The yeast-2-hybrid assay predicted, with high confidence, an interaction between, Usp9X and PJA1. This is consistent with another report, which identified PJA1 by mass spectrometry from Usp9X affinity purification experiments suggesting that there is high probability that PJA1 interacts with Usp9X (Agrawal et al., 2012). PJA1 is an E3 ubiquitin ligase, which has been studied in gastric cancer and shown to ubiquitylate the TGFβ signalling pathway adaptor protein Smad4 (ELF) (Saha et al., 2006, Mishra et al., 2005). Recently, PJA1 has been reported to target neurotrophin receptor interacting MAGE homologue, NGARE (Teuber et al., 2013). Over-expression of PJA1 reduces the expression of NGARE and this in turn inhibited the nerve growth factor – induced neuronal differentiation of PC12 cells (Feng et al., 2010, Teuber et al., 2013). Given that PJA1 is a possible substrate of Usp9X and that its role in axon development remains unclear, immunofluorescence was performed to study the distribution of PJA1 in stage 3 neurons. PJA1 was present in the soma,

dendrites and axon of both wild-type and Usp9X deficient neurons, suggesting loss of Usp9X did not affect the cellular distribution of PJA1 (**Figure 4.15**).

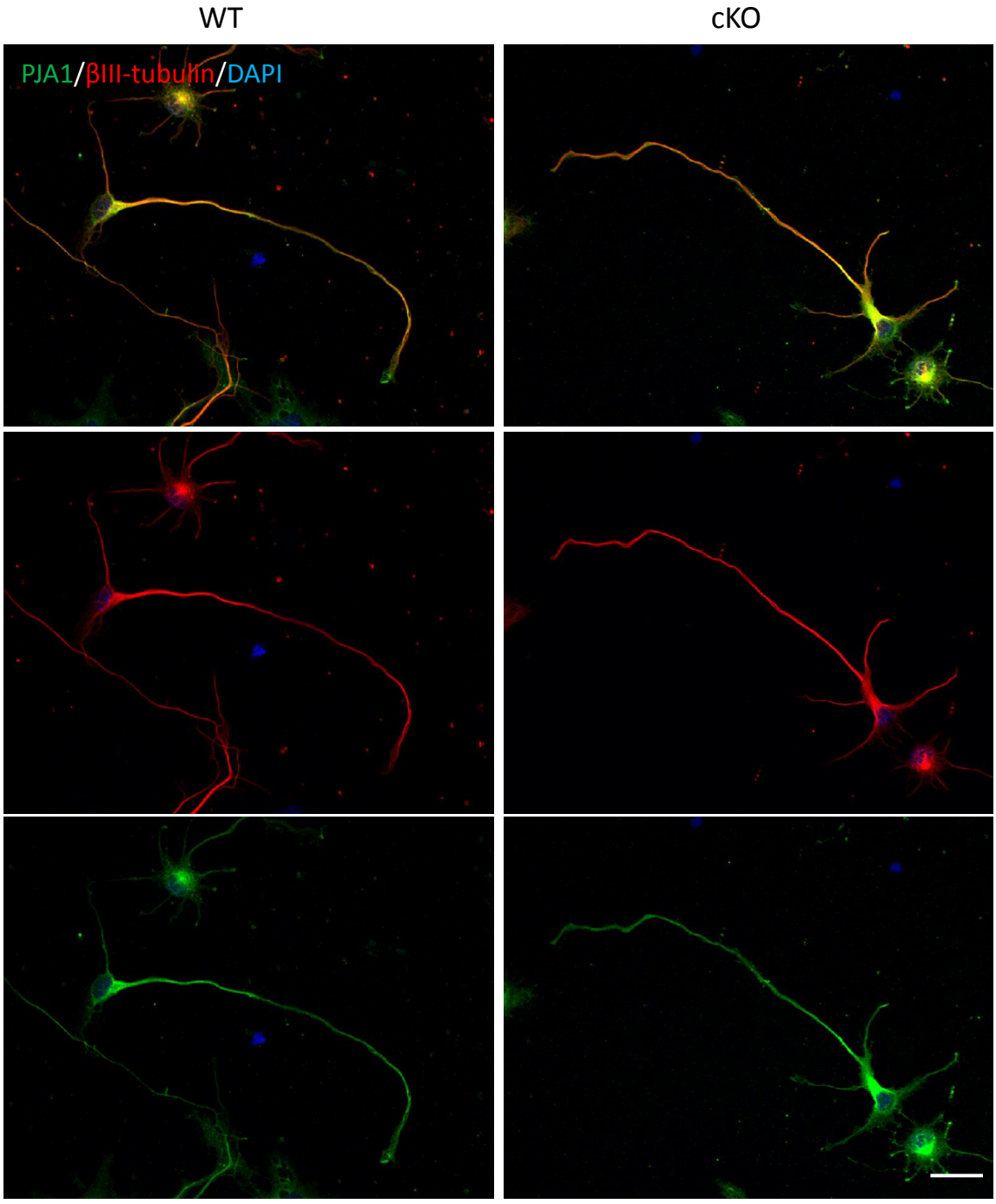

Figure 4.15 Loss of Usp9X does not affect the cellular distribution of PJA1

PJA1 (green) was observed in the cell soma, dendrites and axon of wild-type (WT) neurons but was reduced at the distal end of the axon for some of the Usp9X-null neurons. 30 neurons for three mice per genotype have been compared. Double

arrows show reduced PJA-1 at the distal end of the axon. WT: wild-type; cKO: Usp9X knock-out. Scale bar: 20μm.

4.4.3 Smad4

Usp9X regulates the TGFβ signalling pathway via Smad4 in the developing *Drosophila* wing, Xenopus gastrula and cultured human cells (Dupont et al., 2009). Smad4 shuttles between the nucleus and cytoplasm to facilitate TGFβ signalling. Its cellular localisation is regulated by Ectodermin and Usp9X. Ectodermin is an E3 ubiquitin ligase which ubiquitylates Smad4 in the nucleus of the cell, preventing the binding of Smad4 to the activated form of Smad complex, causing its relocation to the cytoplasm and thus inhibits the TGFβ pathway (Dupont et al., 2005). On the other hand, Smad4 is deubiquitylated in the cytoplasm by Usp9X. Deubiquitylation by Usp9X was shown to activate Smad4 rather than stabilise it as the loss of Usp9X did not affect the levels of Smad4 (Dupont et al., 2009). TGFβ-mediated neuronal differentiation has been shown to be Smad4-dependent (Vogel et al., 2010).

To examine whether exogenous TGFβ results in the translocation of Smad4, wild-type hippocampal neurons were treated with 1ng/ml TGFβ ligand after three days *in vitro* (Vogel et al., 2010). After four hours, neurons were fixed and stained with anti-Smad4 antibody for immunofluorescence. Smad4 was observed mainly in the cytoplasm for both the TGFβ treated and untreated cultures. Increased nuclear Smad4 was not observed in the TGFβ treated culture, at least by immunofluorescence (**Figure 4.16**).

Under normal conditions, activation of the TGFβ pathway results in the binding of free Smad4, in the cytoplasm, by phosphorylated Smad2,3 complex and translocation into the nucleus of the neurons (Dupont et al., 2009, Vogel et al., 2010). However, as shown in Figure 4.16, treatment of TGFβ did not trigger this translocation. One possible reason could be that the cultures were not first treated with Alk4, 5,7 inhibitor SB431542 to block the endogenous TGFβ signalling, before replacement with exogenous TGFβ1 ligand (Vogel et al., 2010, Dupont et al., 2009).

It is proposed that when Usp9X is absent, Ectodermin targets Smad4 for ubiquitylation, preventing its binding to the phosphorylated Samd2,3 complex. This

reduces the percentage of nuclear Smad4 in cells, inhibiting the activation of TGFβ signalling for axon development (Dupont et al., 2005, Dupont et al., 2009). However, due to the inability to get the control experiments working and time constraint, the regulation of Usp9X for the stability of Smad4 and its consequences for cytoplasm / nuclear Smad4 was not further investigated. In the future, cytoplasmic and nuclear Smad4 expression levels could be investigated by performing subcellular fractionation for immunoblotting.

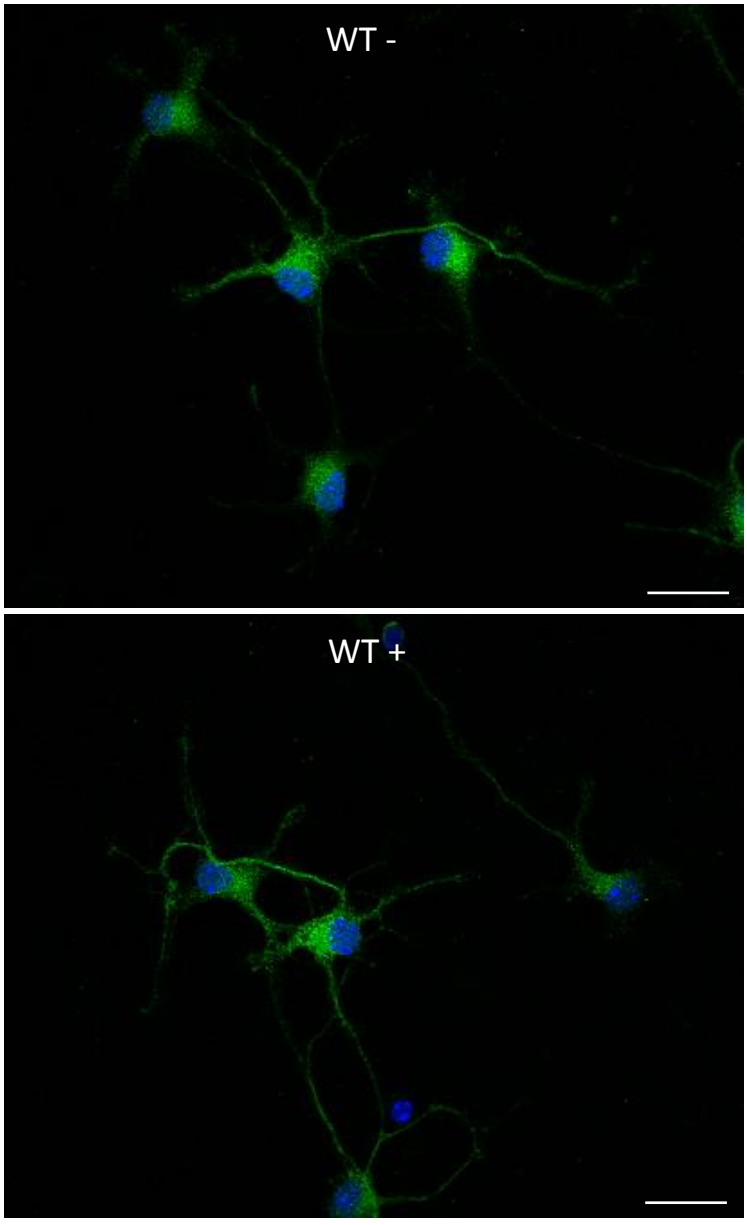

Figure 4.16 TGFβ treatment did not trigger the translocation of Smad4 from the cytoplasm to the nucleus

Higher nuclear Smad4 was not observed in the culture after treated with 1ng/ml of TGFβ ligand. n=20 neurons per treatment have been compared. Smad4 (green); Nuclear marker DAPI (blue). WT: wild-type; -: untreated with TGFβ ligand; +: treated with TGFβ ligand. Scale bar: 20μm.

4.4.4 Smurf-1

Another component of the TGFβ pathway, Smurf-1, has been shown to be a substrate for Usp9X (Xie et al., 2013). Smurf-1 (SMAD-specific E3 ubiquitin protein ligase 1) can be auto-ubiquitylated through its intrinsic HECT (homologous to E6AP carboxyl terminus) E3 ligase activity and targeted for proteosomal degradation. Smurf-1 was originally reported for its negative regulation of TGFβ/BMP (bone morphogenetic proteins) pathways (Zhu et al., 1999, Ebisawa et al., 2001). Activation of the TGFβ pathway triggers the expression of the inhibitory Smad, Smad7. Smurf-1 binds with Smad7 in the nucleus and translocates into the cytoplasm. This complex then binds to the TGFβ type-I receptor targeting it for degradation thereby inhibiting activation of the TGFβ pathway (Ebisawa et al., 2001).

To examine the effect, if any, of Usp9X loss on the status of Smurf-1, its cellular expression was examined at 3DIV hippocampal neurons culture by immunofluorescence. Smurf-1 was observed in the soma, dendrites and axon for both wild-type and Usp9X-null neurons. There was no observable difference in Smurf-1 expression level or localisation between wild-type and Usp9X-null neurons (**Figure 4.17**), suggesting that Usp9X does not regulate Smurf-1 in hippocampal neurons.

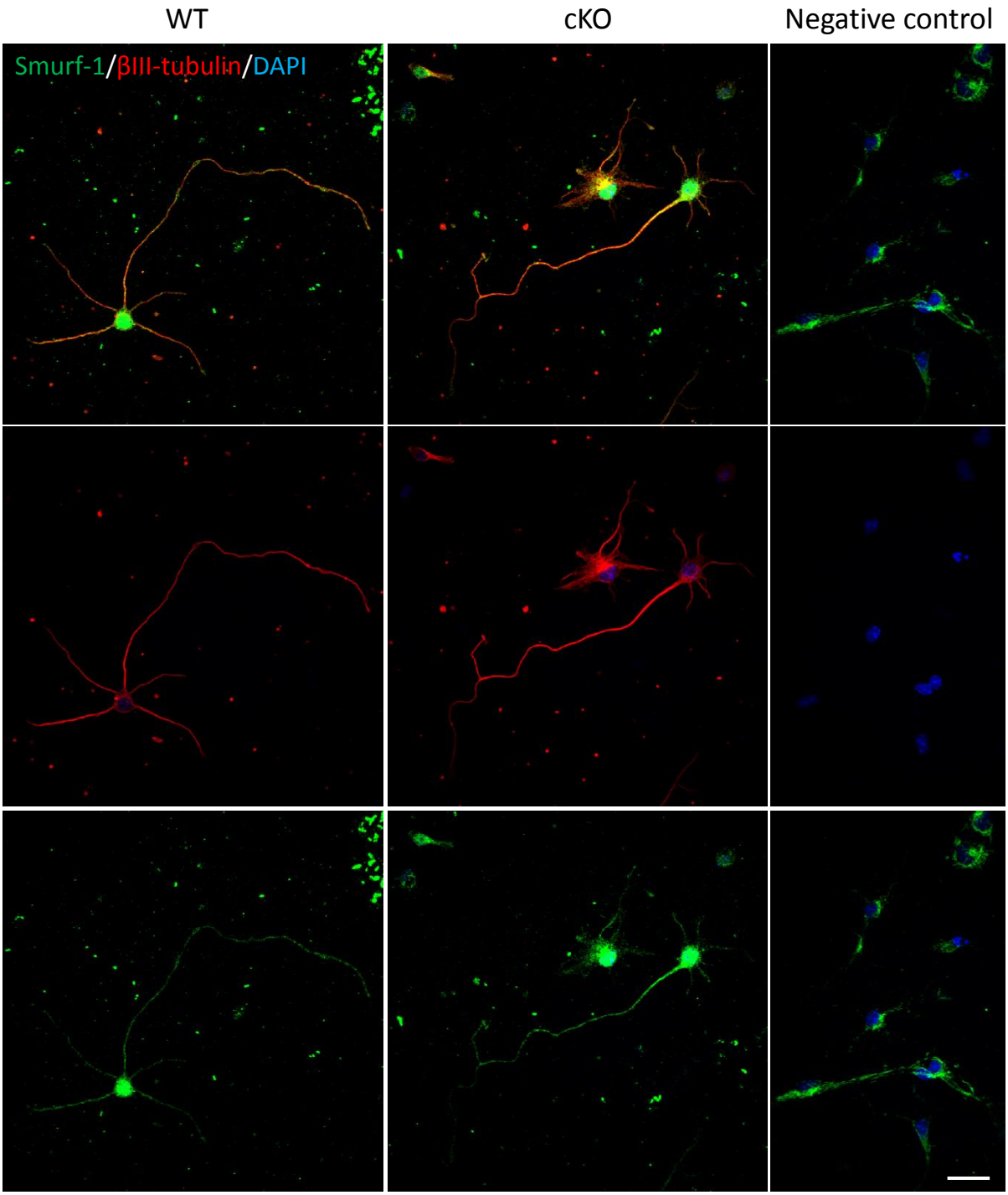

Figure 4.17 Subcellular expression of Smurf-1 for wild-type and Usp9X-null hippocampal neurons was similar

Smurf-1 (green) was present in the soma, dendrites and axon of the hippocampal neurons in both wild-type and Usp9X-null neurons. There was no observable difference in expression level of Smurf-1 in wild-type and Usp9X-null neurons. 30 neurons for two embryos per genotype have been compared. Immunofluorescent staining of Smurf-1 (green); βIII-tubulin (red); Nuclear marker DAPI (blue). WT: wild-type; cKO: Usp9X knockout. Scale bar: 20μm.

4.5 Axon development and mTOR2 activity

Usp9X regulates components of the mTOR pathway affecting both mTORC1 and mTORC2 signalling pathways in myoblasts (Agrawal et al., 2012). Genetic ablation of mTORC2 activity reduces the differentiation potential of C2C12 myoblasts (Shu and Houghton, 2009). mTORC2 signalling phosphorylates Akt at the hydrophobic motif at Ser473. mTORC2 is involved in actin organisation in cells (Jacinto et al., 2004) and it has been shown that Akt and p-Akt are present in the soma and axonal tips but not in dendrites of stage 3 neurons (Yan et al., 2006). Given that in C2C12 mouse skeletal myoblasts, Usp9X negatively regulates mTORC2 activity upon initiation of differentiation, the effect of loss of Usp9X on the cellular distribution and/or total level of Akt and p-Akt for stage 3 hippocampal neurons was examined (Agrawal et al., 2012).

Total Akt was observed in the soma, dendrites and axon with no observable difference in both wild-type and Usp9X-null neurons (**Figure 4.18**). For the immunoblots, densitometry was performed to analyse the intensity of total Akt and p-Akt for wild-type and Usp9X-null neurons and was normalised with β-actin. No statistically significant difference was observed for total Akt (p = 0.699) and p-Akt (p = 0.077) after analysed with Student T-test (n=3) (**Figure 4.19** and **4.20**).

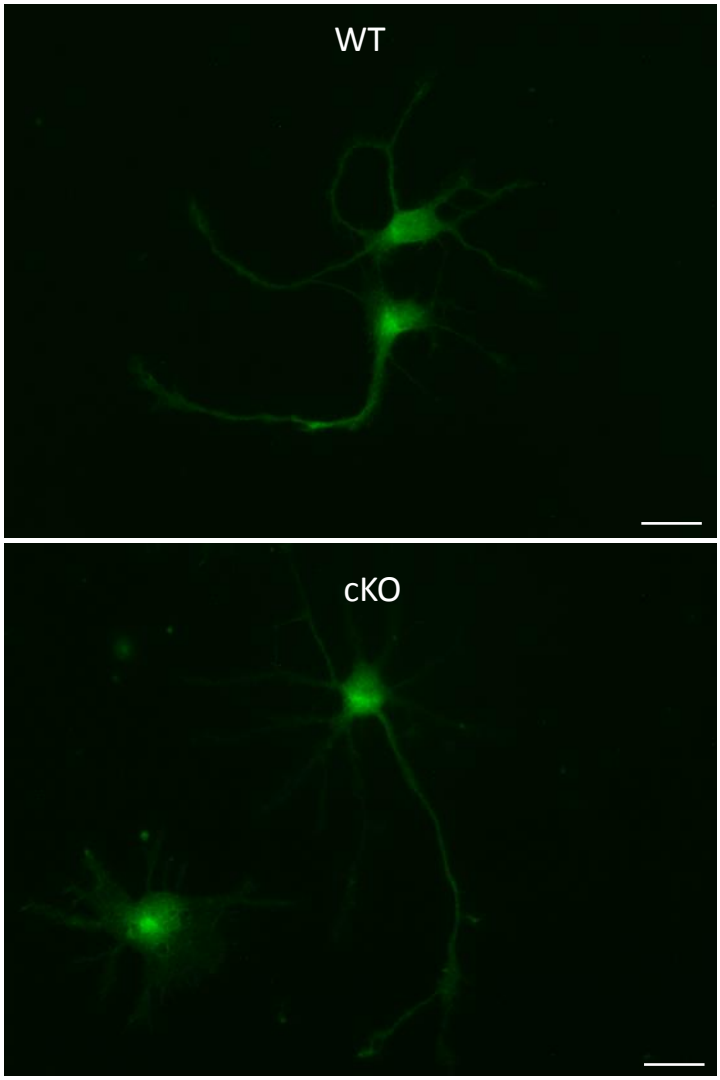

Figure 4.18 Subcellular distribution of total Akt for wild-type and Usp9X-null hippocampal neurons was similar

Total Akt (green) was present in the soma, dendrites and axon of the hippocampal neurons. There was no observable difference for the cellular distribution of total Akt in both wild-type and Usp9X-null neurons. n=30 neurons for an embryo per genotype were compared. WT: wild-type; cKO: Usp9X knockout. Scale bar: 20μm.

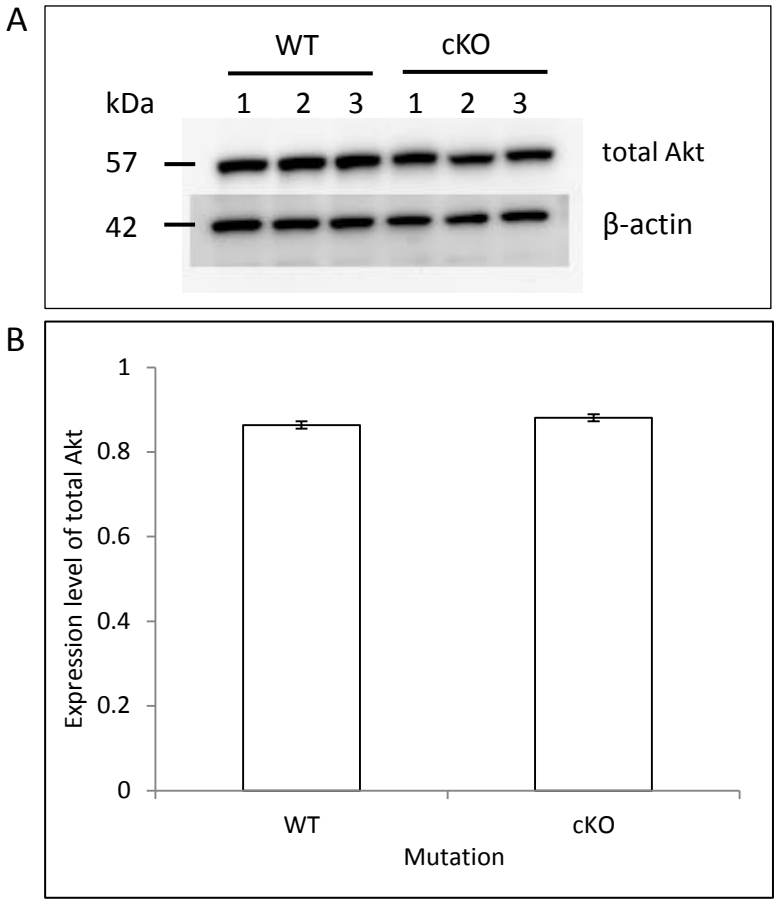

Figure 4.19 Level of total Akt was similar between wild-type and Usp9X null hippocampal neuronal cultures

(A) Immunoblot analysis of total Akt protein levels in hippocampal neuronal cultures from wild-type and Usp9X-null embryos. (B) Densitometric analysis of comparing the level of total Akt for wild-type and Usp9X-null neurons normalised against β-actin. There was no statistical significant difference in the level of total Akt between wild-type and Usp9X null neurons in the hippocampal neurons. WT: wild-type; cKO: Usp9X knock-out. Student's *t* test $p = 0.699$ (n=3 embryos). Error bars= standard error of the mean.

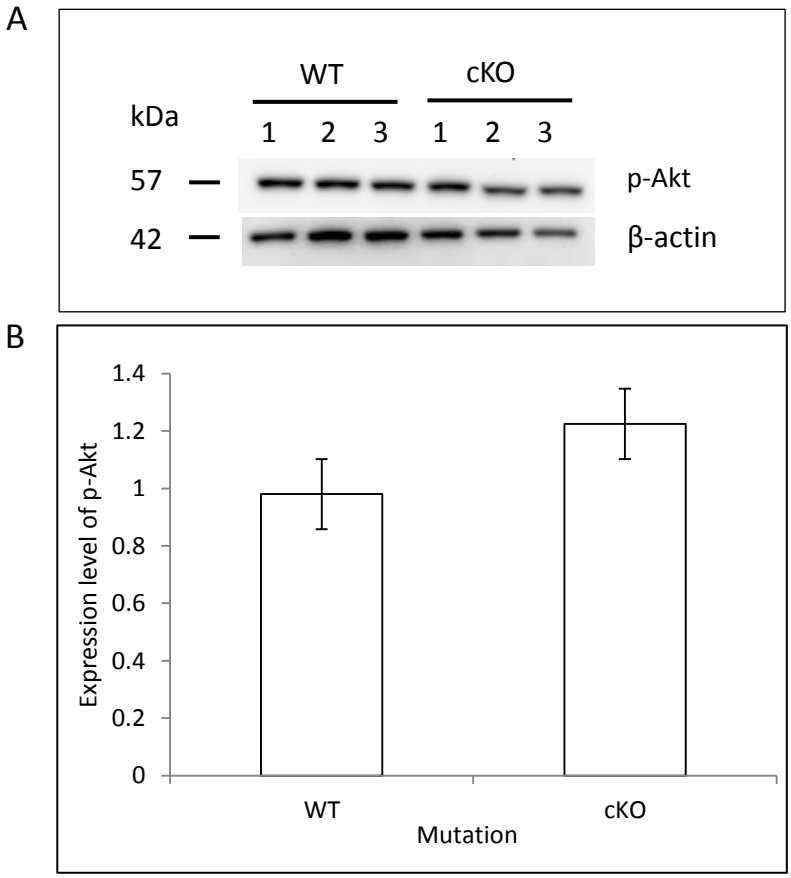

Figure 4.20 Level of phospho-Akt was not significantly altered in 3 day Usp9X-null *in vitro* hippocampal neurons

(A) Immunoblot analysis of p-Akt protein levels in hippocampal neuronal cultures from wild-type and Usp9X-null embryos. (B) Densitometric analysis of comparing p-Akt levels for wild-type and Usp9X-null neurons normalised against β-actin. There was no statistical significant difference in the total level of p-Akt between wild-type and Usp9X null neurons in the hippocampal neurons. WT: wild-type; cKO: Usp9X knockout. Student's *t* test $p = 0.077$ (n=3 embryos). Error bars= standard error of the mean.

4.6 Summary

In this chapter, regulation of Usp9X in cytoskeletal dynamics (stathmin-1, CRMP-2, Kif5B, MARK4 and AF-6); TGFβ signalling (BDNF, PJA1, Smad4 and Smurf-1); mTOR2 activity (Akt and p-Akt) for axon development have been examined. Based on the data presented, Kif5B is a putative substrate for Usp9X that warrant further investigation in axon growth. The shorter axonal length observed in Usp9X-null hippocampal neurons is consistent with the reduced Kif5B. Firstly, Kif5B is one of the kinesin-1 motor proteins, transporting different cargo including mitochondria, synaptic vesicle precursors, potassium and sodium channels along microtubules (Saxton and Hollenbeck, 2012, Cai et al., 2007, Rivera et al., 2007, Su et al., 2013, Hirokawa et al., 2010). Overall, KIF5 has been shown to regulate axon elongation as the deletion of KIF5 family using siRNA in hippocampal neurons decreases their axonal length (Sun et al., 2013). Based on the data presented in this chapter, Kif5B was dramatically reduced in 3DIV Usp9X-null hippocampal neurons (**Figure 4.9**), suggesting that the shorter axonal length could be due to the reduced level of Kif5B in the absence of Usp9X in the cultured neurons. Further examination for the interaction between Kif5B and Usp9X and their involvement during axon formation is presented in **Chapter 5**.

5. Evaluating the regulation of Kif5B by Usp9X

5.1 Introduction

In neurons, proper organelle and protein trafficking is important for polarization and synaptic formation. Kinesin-1 superfamily proteins (KIF5s) are heterodimers which are composed of two identical heavy chains and two identical light chains. There are three different isotypes of kinesin-1 motors proteins known as Kif5A, Kif5B and Kif5C which mediate the plus-end directed transport of different protein cargos along the microtubule. Kif5A (~117kDa) and Kif5C (~107kDa) are expressed highly in neurons while Kif5B (~109kDa) is ubiquitously expressed (Kanai et al., 2000).

Kif5A, has been shown to specifically regulate the transport of the $GABA_A$ receptor in dissociated hippocampal neurons and, conditional knock-out of Kif5A in the mouse brain causes epilepsy (Nakajima et al., 2012). Until now, little is known about the specific cargo proteins transported by Kif5C. A study has reported that Kif5C knock-out mice appear normal, however, the mutant mice had smaller brains and a relative loss of motor neurons compared with sensory neurons (Kanai et al., 2000).

Kif5B has been most widely studied among the three kinesin-1 motor proteins. Deletion of Kif5B in mice caused embryonic lethality by E11.5 (Tanaka et al., 1998). It has been demonstrated to regulate the axonal transport of mitochondria, which are the important energy producers for highly elongated cells like neurons (Saxton and Hollenbeck, 2012, Tanaka et al., 1998). Kif5B also transports anterogradely to the nerve terminal different precursor proteins important for presynaptic plasticity (Cai et al., 2007). It also promotes the forward transport and axonal localisation of the voltage-gated potassium and sodium channels (Su et al., 2013, Rivera et al., 2007).

The yeast-two hybrid screening of a human fetal brain library identified a direct interaction between Kif5B and Usp9X. In addition, a dramatic reduction in Kif5B protein was observed using immunofluorescence in cultured Usp9X null hippocampal neurons (**Figure 4.6**). These results suggest that Kif5B is regulated by

Usp9X and their interaction might be important for axon specification (**Chapter 3**) and growth (Stegeman et al., 2013, Homan et al., 2014).

The interaction of Kif5B and Usp9X (yeast-2-hybrid screen) and loss of Kif5B protein in the absence of Usp9X raises the possibility that Kif5B may be an Usp9X substrate. However, there is no evidence in the literature that Kif5B is ubiquitylated. Therefore, the aim of the study presented in this chapter was to examine the nature of the Usp9X and Kif5B interaction.

5.2 Reduced Kif5B expression in Usp9X null hippocampal neurons

A direct interaction between two independent clones encoding an overlapping region the kinesin-1 motor protein, Kif5B and full length Usp9X was identified in a yeast-2-hybrid screen of human fetal brain (S. Wood personal communication). Kif5B is present in the soma, dendrites and axon of cortical neurons in dissociated culture (Rivera et al., 2007). To examine if the cellular expression and localisation of Kif5B was affected in the absence of Usp9X, hippocampal neurons were fixed after 3DIV and 5DIV culture and stained with Kif5B antibody. The majority of the neurons at 3DIV were polarised. 30 wild-type and 30 Usp9X-null neurons were compared (4 mice per genotype). Kif5B was expressed ubiquitously in wild-type neurons as reported (Rivera et al., 2007). However, a dramatic reduction in Kif5B protein level was observed, by immunofluorescence, in both 3DIV and 5DIV Usp9X-null neurons (**Figure 5.1**). This confirmed our previous observations in 3DIV neurons (**Figure 4.9**).

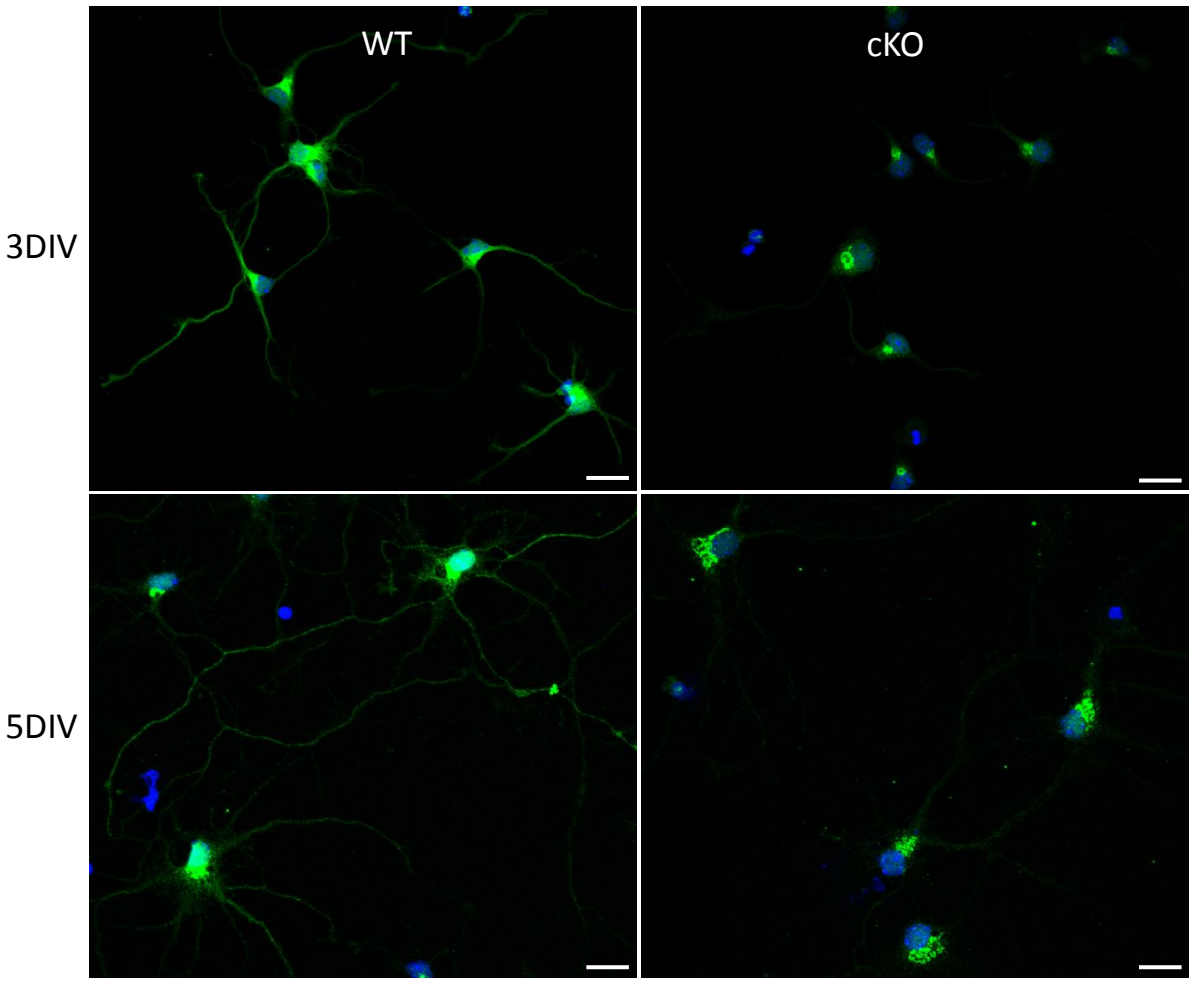

Figure 5.1 Kif5B protein levels are reduced in 3DIV and 5DIV Usp9X-null hippocampal neurons

In wild-type neurons, Kif5B was detected in the soma, dendrites and axon. There was an obvious reduction of Kif5B expression detected when Usp9X was absent in both 3DIV and 5DIV hippocampal neurons. Low levels of Kif5B were still detected in the soma of Usp9X knock-out neurons. n=30 neurons from four mice per genotype. Kif5B (green); Nuclear marker DAPI (blue). WT: wild-type; cKO: Usp9X knockout. Scale bar: 20μm.

To examine if the absence of Usp9X affected the level or localisation of Kif5B at earlier stages of the hippocampal neuronal development, both wild-type and Usp9X-null *in vitro* cultures were fixed at 24 hours and stained with Kif5B antibody. Only stage 2 symmetrical neurons (**Figure 3.3B**) were analysed. Firstly, the subcellular distribution of Usp9X was examined in stage 2 wild-type hippocampal neurons. Usp9X was distributed in the soma and evenly in all neurites (**Figure 5.2**). Kif5B was also distributed in the soma and neurites of the stage 2 neurons but there was no observable difference in the Usp9X-null hippocampal neurons at stage 2 (**Figure 5.3**).

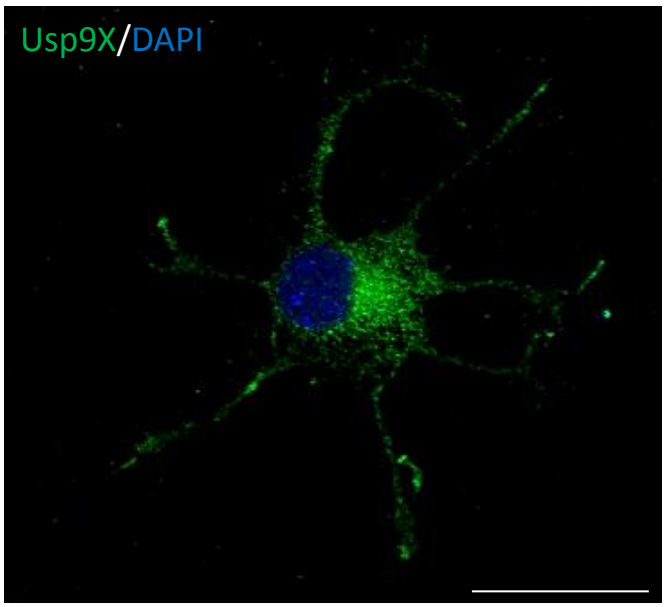

Figure 5.2 Usp9X is distributed evenly in the soma and all neurites in stage 2 hippocampal neurons

Usp9X (green); Nuclear marker DAPI (blue). Scale bar: 20μm.

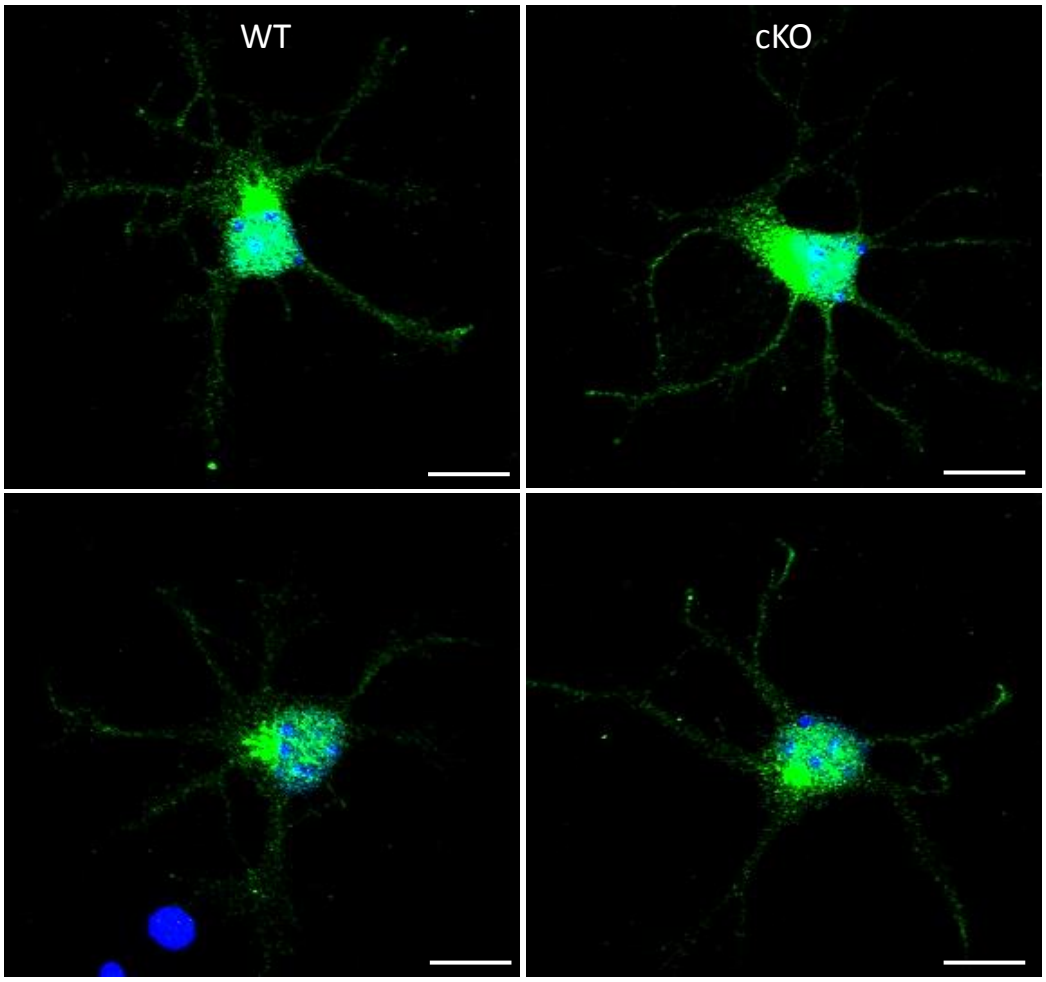

Figure 5.3 Loss of Usp9X does not affect the expression of Kif5B in stage 2 hippocampal neurons

There was no observable difference in the expression of Kif5B (green) in stage 2 wild-type and Usp9X-null neurons. WT: wild-type; cKO: Usp9X knockout. Scale bar: 10μm.

To confirm that the expression level of Kif5B was decreased in 3DIV and 5DIV of Usp9X-null culture, immunoblotting analysis was conducted using the same Kif5B antibody used for immunofluorescence (**Figure 5.1**). This antibody (Abcam) was specific for Kif5B according to the company datasheet. However, this antibody detected several bands. In addition, although this antibody detected a band at the predicted size for Kif5B, of approximately 110kDa, in whole cell lysate from Hek293 and Neuro2a cell lines, it did not detect any band in the lysate from hippocampal neuronal cultures (**Figure 5.4**) or mouse brain lysate (data not shown).

As shown in **Figure 5.4**, the band recognised by this Kif5B antibody (Abcam) in Neuro2a cells has higher molecular weight than in HEK293 cells.

A pan-kinesin-1 antibody (Millipore) was also used for immunoblotting. The pan-kinesin-1 antibody recognises the kinesin heavy chain of the kinesin-1 protein and can detect all kinesin-1 isotypes including Kif5A, Kif5B and Kif5C. Their predicted sizes are 117kDa, 109kDa and 107kDa respectively (Vidal et al., 2012, Kanai et al., 2000). As shown in **Figure 5.5**, the kinesin-1 antibody recognised a single dominant band in all cell lines tested including HEK293, Neuro2a and ReNcells VM as well as hippocampal neuronal cultures. ReNcell VM is a human neural stem cell line, which derived from 10-week ventral mesencephalon fetal brain tissue (Donato et al., 2007). The band detected by kineisn-1 antibody in Neuro2a cells and hippocampal neurons ran a bit higher than HEK293 and ReNcell VM cells (**Figure 5.5**). As mentioned earlier only Kif5B is expressed in non-neuronal cells therefore the band in HEK293 cells is Kif5B. In addition microarray analysis of ReNcells VM indicate they express Kif5B but not Kif5A (S.Wood personal communication). These data suggest that the pan-kinesin-1 antibody may primarily detect Kif5A in hippocampal neurons (**Figure 5.5**).

Not withstanding reservations about the ability of the pan-kinesin-1 antibody to detect Kif5B, it was used to detect KIF5 proteins in wild-type and Usp9X-null neurons. There was no statistically significant difference in the total level of kinesin-1 observed between wild-type and Usp9X-null neurons in 3DIV and 5DIV cultures (**Figure 5.6** and **5.7**). Although there was a trend to lower KIF5 protein at 3DIV after densitometry analysis (**Figure 5.6**) this is most probably due to a technical error, where one of the 3DIV Usp9X-null hippocampal neuron samples was under loaded.

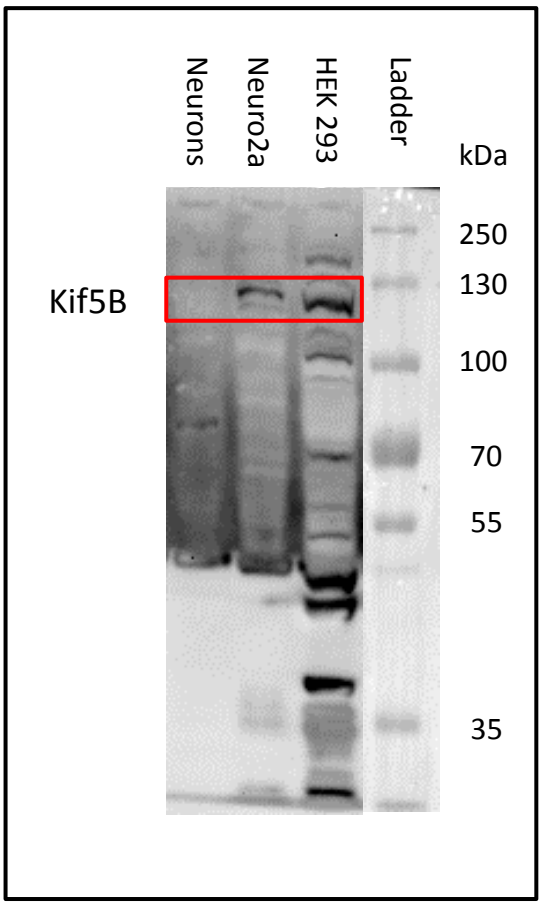

Figure 5.4 Kif5B antibody (Abcam) did not recognise Kif5B protein in hippocampal neurons in culture

Cellular expression of Kif5B (~109kDa) in HEK293 and Neuro2a cell lines was recognised by Kif5B antibody (Abcam). However, this antibody did not detect any specific band in the hippocampal neuronal culture. Data for β-actin, loading control was not shown as the membrane after probing with Kif5B antibody was too dirty for β-actin antibody to recognise bands at 42kDa.

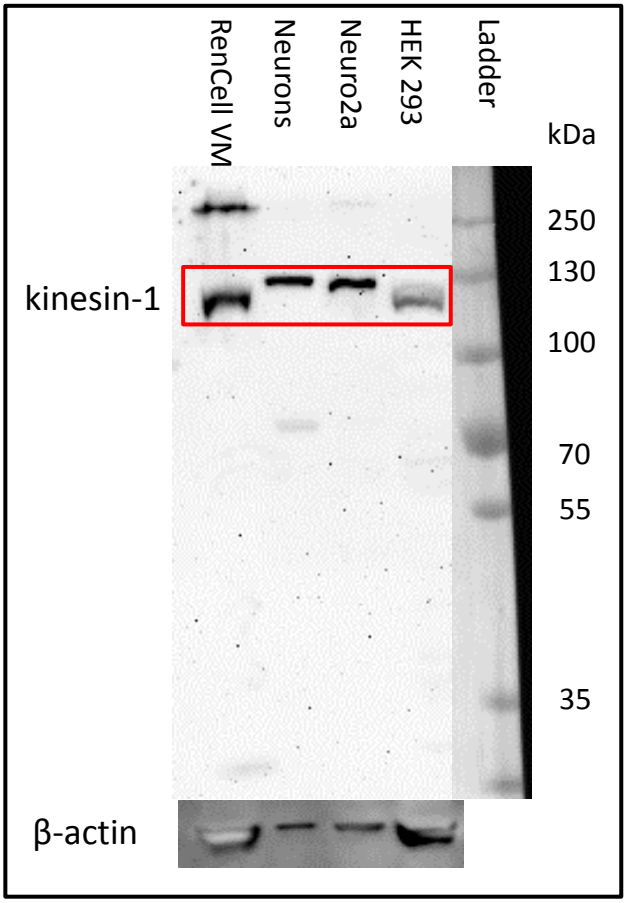

Figure 5.5 Kinesin-1 antibody (Millipore) recognised kinesin heavy chain of the kinesin-1 protein in the hippocampal neurons in culture

Cellular expression of kinesin-1 in HEK293, Neuro2a, hippocampal neuronal culture and ReNcell VM was recognised by the kinesin-1 antibody. The size of the protein detected by kinesin-1 antibody for ReNcell VM was similar to HEK293 cells suggesting that only Kif5B was detected in ReNcell VM.

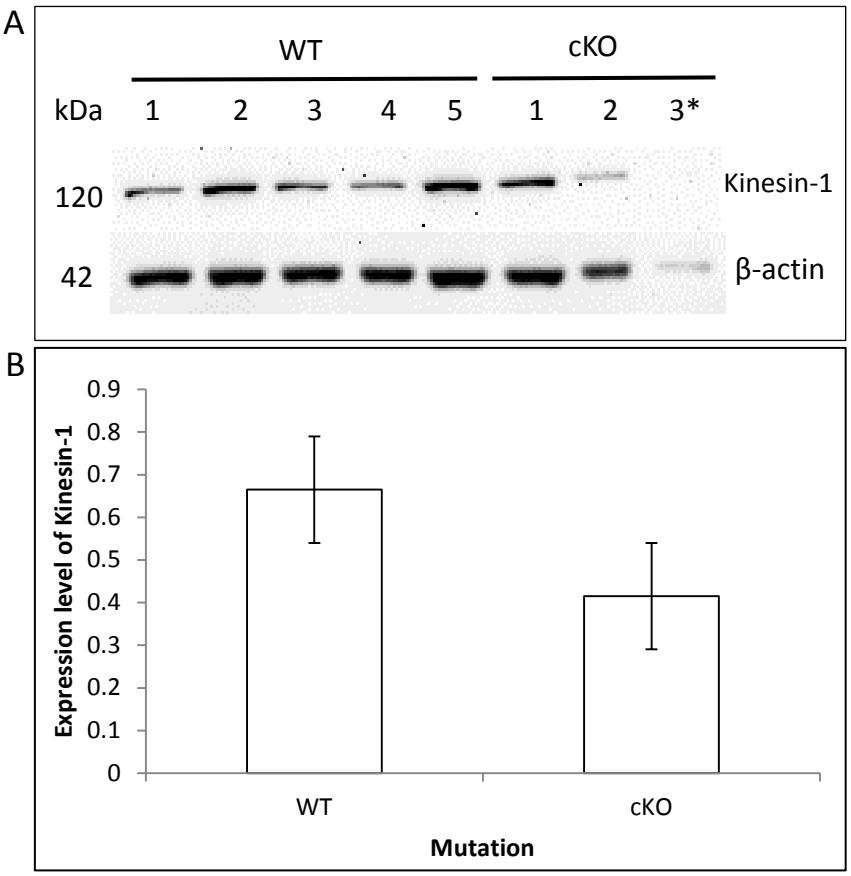

Figure 5.6 The level of kinesin-1 in three days *in vitro* wild-type and Usp9X-null hippocampal neuronal culture was similar

(A) Immunoblot analysis of kinesin-1 protein levels in hippocampal neuronal cultures from wild-type (WT) and Usp9X-null (cKO) embryos. (B) Densitometry was performed for kinesin-1 and normalised with β-actin. There was no statistically significant difference in the total level of kinesin-1 between wild-type and Usp9X null neurons. WT: wild-type; cKO: Usp9X knockout. Student's *t* test $p = 0.21$ (n=five for wild-type and 3 for Usp9X knockout embryos). Error bars represent standard error of the mean. *= the amount of the protein was under loaded and might affect the densitometry result.

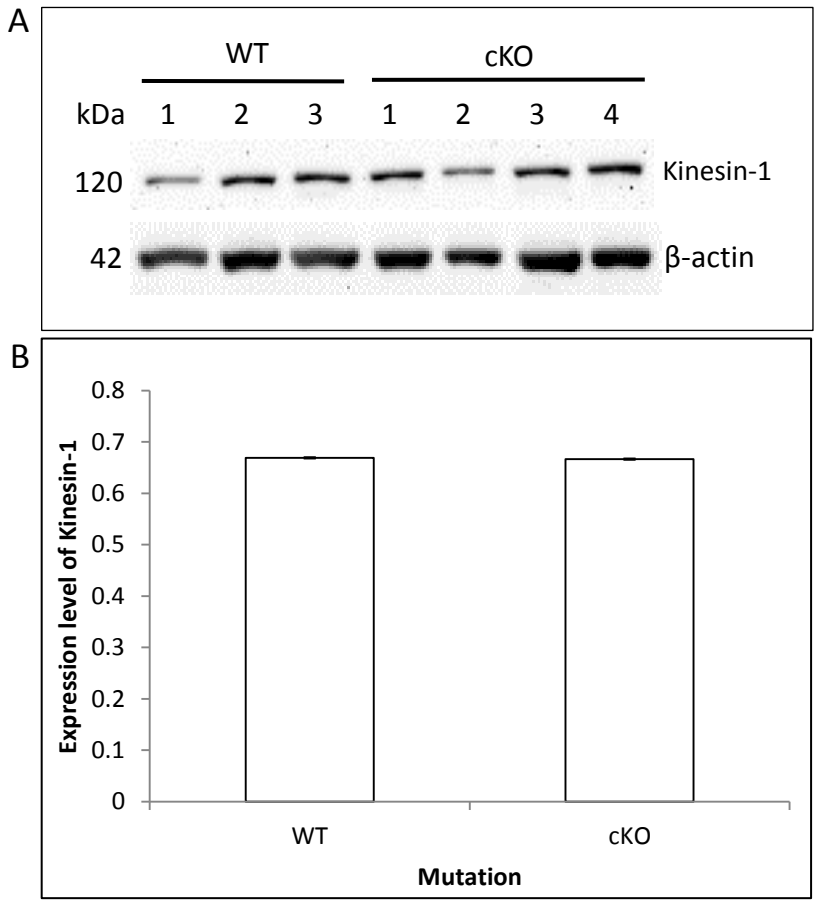

Figure 5.7 The level of kinesin-1 in five days *in vitro* wild-type and Usp9X null hippocampal neuronal culture was similar

(A) Immunoblot analysis of kinesin-1 protein levels in hippocampal neuronal cultures from wild-type (WT) and Usp9X-null (cKO) embryos. (B) Densitometry was performed for kinesin-1 and normalised with β-actin. There was no statistically significant difference in the total level of kinesin-1 between wild-type and Usp9X null neurons. WT: wild-type; cKO: Usp9X knockout. Student's *t* test $p = 0.95$ (n=three for wild-type and 4 for Usp9X knockout embryos). Error bars= standard error of the mean.

Given the ambiguity of which KIF5 isoform was detected in the hippocampal neurons, and the relative difficulty in obtaining enough cellular material, it was decided to examine if the expression of Kif5B was reduced in the absence of Usp9X in other cell lines. Usp9X protein was knocked-down using siRNA in Neuro2a and HEK293 cells, the latter expressing only Kif5B. Both Neuro2a and HEK293 cells were treated with 25nM of siRNA for Usp9X and scrambled siRNA (control) protein lysate extracted for immunoblotting analyses at 24, 48 and 72 hours. ImageJ was used to analyse the band intensity for Usp9X and normalised against β-actin and compared between cells treated with siRNA for Usp9X and scrambled. As shown in **Figure 5.8A**, the expression level for Usp9X in Neuro2a cells remained high at approximately 100%, 93% and 74% of scrambled siRNA at 24, 48 and 72 hours respectively. For HEK293 cells, the expression of Usp9X was reduced to approximately 82%, 42% and 19% at 24, 48 and 72 hours, respectively (**Figure 5.8B**).

The siRNA knock-down of Usp9X was more effective in HEK293 than Neuro2a cells (**Figure 5.8 A and B**). To confirm the maximal level of reduction for Usp9X in HEK293 cells, HEK293 cells were treated with 100nM of siRNA for Usp9X and scrambled for 96 hours. Increased concentration of siRNA treatment displayed unhealthy cell morphology and with a lot of floating cells, indicating that 100nM of siRNA might be toxic to the cells. However, the cells were collected and immunoblotting was performed. The expression level for Usp9X was approximately 82%, 46% and 52% at 48, 72 and 96 hours respectively (**Figure 5.8C**).

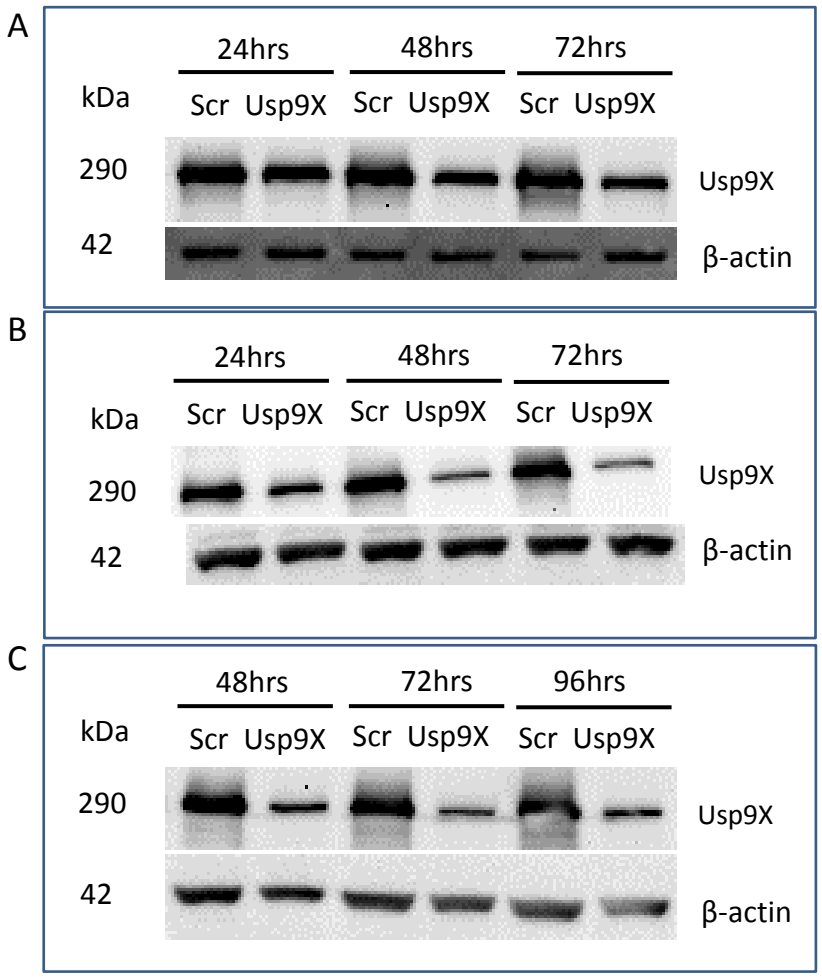

Figure 5.8 siRNA knock-down for Usp9X in HEK293 and Neuro2a cells

Analyses of Usp9X expression in Neuro2a (A), HEK293 (B) treated with 25nM siRNA and HEK293 treated with 100nM siRNA (C). For assay treated with 25nM siRNA, Usp9X expression in Neuro2a cells remained 100%, 93% and 74% respectively at 24, 48 and 72 hours; Usp9X expression was reduced to 82%, 42% and 19% at 24, 48 and 72 hours respectively. For HEK293 cells treated with 100nM of siRNA, the expression of Usp9X remained at a level of 82%, 46% and 52% at 48, 72 and 96 hours respectively. Scr: siRNA scramble.

To examine the level of Kif5B after Usp9X deletion, the membrane for HEK293 cells treated with 25nM siRNA and probed with Usp9X antibody as shown in **Figure 5.8B** was probed with Kif5B (Abcam) antibody. Again multiple bands were detected. There was no observable difference in expression level for Kif5B (109kDa) after Usp9X knock-down even at 72 hours when Usp9X expression was reduced to only 20% (**Figure 5.8B and 5.9**). The expression of Kif5B was analysed with densitometry, showing approximately 110%, 94% and 100% of Kif5B protein level at 24, 48 and 72 hours respectively, confirming there is no reduction in Kif5B expression following Usp9X knock-down in HEK293 cells (**Figure 5.8B**).

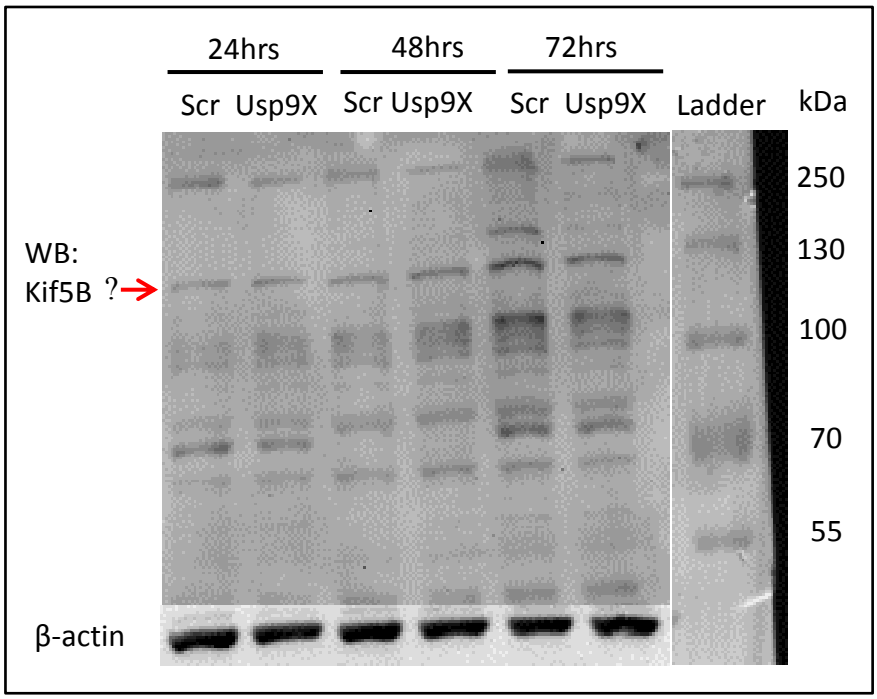

Figure 5.9 Kif5B expression was not affected in HEK293 cells following reduction of Usp9X

Protein lysate for HEK293 cells treated with 25nM siRNA was probed with Kif5B antibody. There was no reduction in the intensity of any of the bands detected by the Kif5B antibody, at any time point, in HEK293 cells after Usp9X expression was reduced. Scr: Scramble siRNA.

5.3 Co-localisation of Usp9X and Kif5B in neurons

Kif5B expression was reduced in 3DIV and 5DIV of hippocampal neuron in culture, as detected by immunofluorescence (**Figure 5.1**). To examine if Usp9X co-localised with Kif5B, double-labelling of Usp9X and Kif5B was performed for stage 3 dissociated wild-type hippocampal neurons and images were taken on a structured illumination (SIM) super resolution microscope. The correlation between the two channels (red: Usp9X; green: Kif5B) for regions of interest, including the cell body, axon and growth cone, were analysed. Pearson's coefficient analysis indicates the amount of co-localisation by measuring pixels containing both signals. Based on the fluorescence images (**Figures 5.10**) Usp9X and Kif5B co-localise in the axon (**Figure 5.10B**; mean Pearson's coefficient: 0.44) and growth cone (**Figure 5.10C**; mean Pearson's coefficient: 0.39) but not in the cell body (**Figure 5.10A**; mean Pearson's coefficient: 0.06). Due to time constraints only ten neurons from a wild-type embryo were analysed.

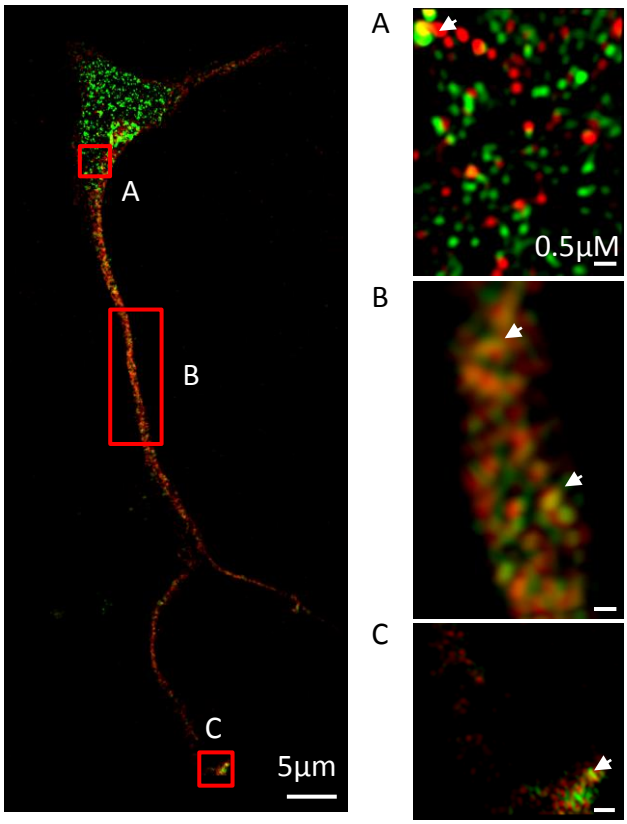

Figure 5.10 Usp9X and Kif5B co-localise in the axon and growth cone

The correlation between red (Usp9X) and green (Kif5B) channels measured in regions of interest in cell body (A), axon (B) and growth cone (C). The mean Pearson's coefficient in the cell body was 0.06; axon was 0.44 and growth cone was 0.39. Ten neurons from a wild-type embryo were analysed.

5.4 Interaction between Usp9X and Kineisn-1 or Kif5B

The yeast-two-hybrid screen of human fetal brain library identified Kif5B interacting with Usp9X. To examine if Kif5B complexes with Usp9X in mammalian cells, co-immunoprecipitation (Co-IP) was performed using Usp9X and kinesin-1 antibodies. Kif5B is one of the isotypes of kineisn-1 (Vidal et al., 2012). As noted above (**Figure 5.4**), the Kif5B antibody did not appear to recognise Kif5B protein in the hippocampal neuronal culture and mouse brain lysates (data not shown), therefore, kinesin-1 (Millipore) antibody was used for Co-IP. Firstly, E18.5 wild-type brain lysate was precipitated with Usp9X antibody and then probed with Usp9X antibody. Usp9X (~290kDa) was detected in Usp9X elution and input, suggesting that the IP worked (**Figure 5.11A**). However, when probed with kinesin-1 antibody, no band was detected for kinesin-1 (~120kDa) in the Usp9X elution (**Figure 5.11**).

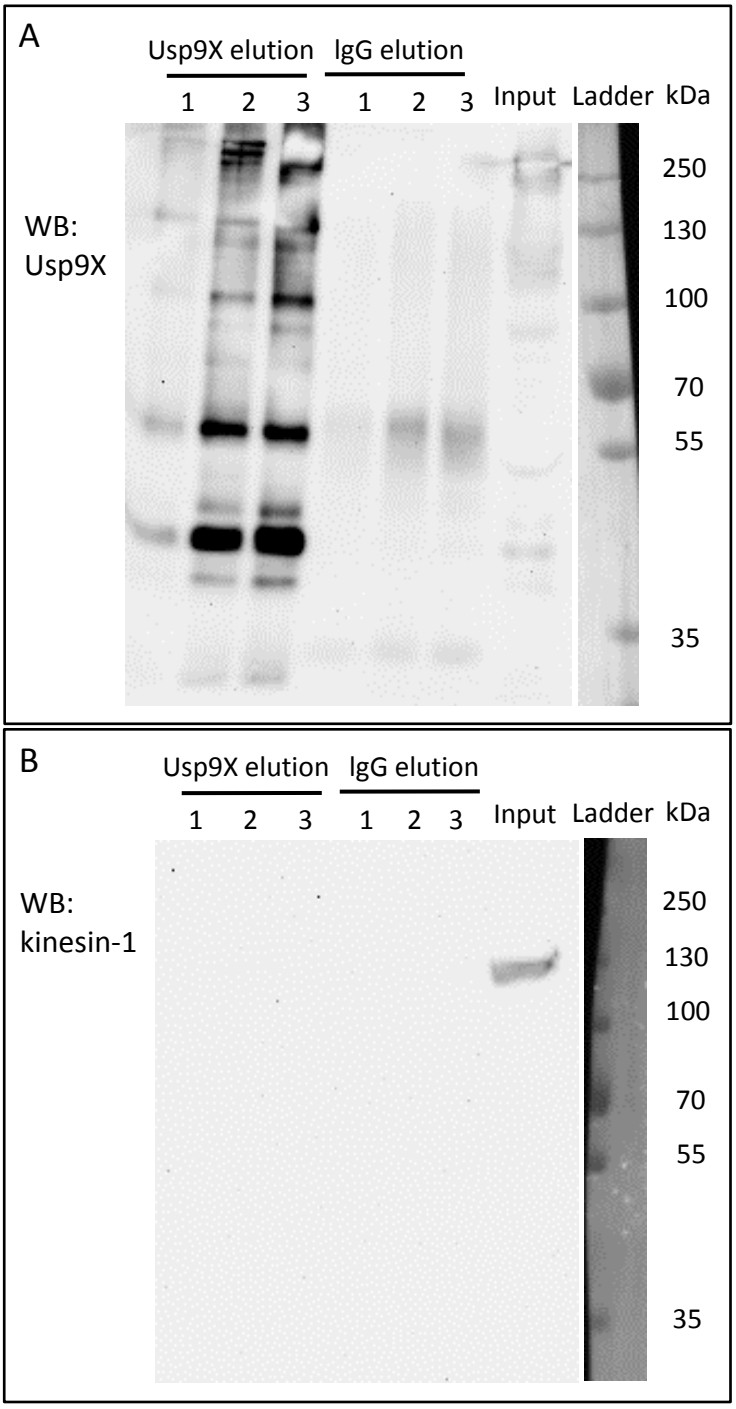

Figure 5.11 Kineisn-1 does not immunoprccipitate with Usp9X from mouse brain lysate

The brain lysate for E18.5 wild-type mouse embryo was imunoprecipitated using Usp9X (290kDa) (A) and kinesin-1 (B) antibodies before immunoblot analysis. No band was detected by the kinesin-1 antibody following Usp9X elution, suggesting that Usp9X does not interact with kinesin-1 under the conditions used.

It is possible that Usp9X only interacts with a subpopulation of Kif5B in the cells. Therefore to increase expression levels HEK293 cells were first co-transfected with V5-tagged Usp9X and HA-tagged Kif5B plasmids at three different ratios of 1:1, 3:1 and 1:3 by transient transfection using Lipofectamine 2000 reagent. After 48 hours, the cell lysates were extracted for immunoblotting. The samples were probed with V5 and HA antibodies which recognised V5-Usp9X (~290kDa) and HA-Kif5B (~110kDa) respectively, as shown in **Figure 5.12**. Co-transfection of V5-tagged Usp9X and HA-tagged Kif5B plasmids at 1:1 ratio was chosen for the Co-IP.

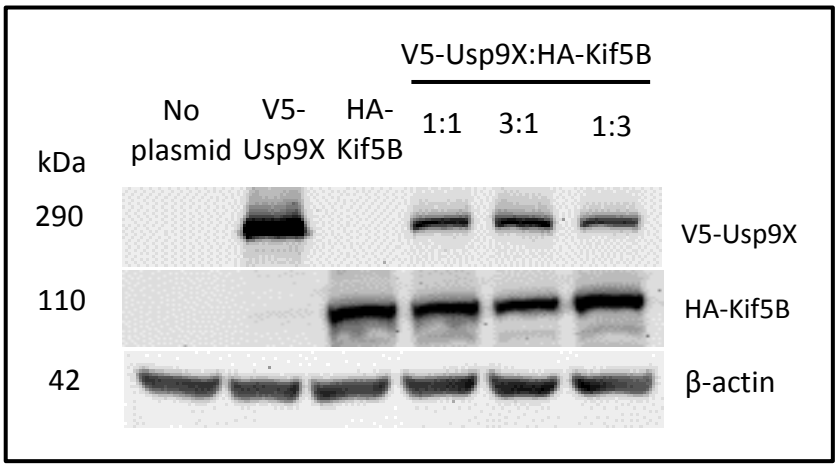

Figure 5.12 Co-transfection of V5-tagged Usp9X and HA-tagged Kif5B plasmids into HEK293 cells results in high protein levels.

HEK293 cells was co-transfected with V5-Usp9X and HA-Kif5B plasmid at 1:1, 3:1 and 1:3 ratio using Lipofectamine 2000 reagent. The cells were collected for immunoblotting and probed with V5 and HA antibodies. Co-transfection of V5-Usp9X and HA-Kif5B at 1:1 ration was used for subsequent Co-IP experiments in HEK293 cells.

For Co-IP, HEK293 cells were transfected with V5-Usp9X and HA-Kif5B at 1:1 ratio and the cells were collected after 48 hours. The protein lysate was first precipitated with V5 antibody and probed with V5 antibody. Bands at approximately 290kDa were detected in the input and V5 elution (**Figure 5.13A**). The elution samples and input were also probed with HA antibody, however, no band was detected by HA antibody at the expected size of approximately 110kDa in the V5 elution (**Figure 5.13B**).

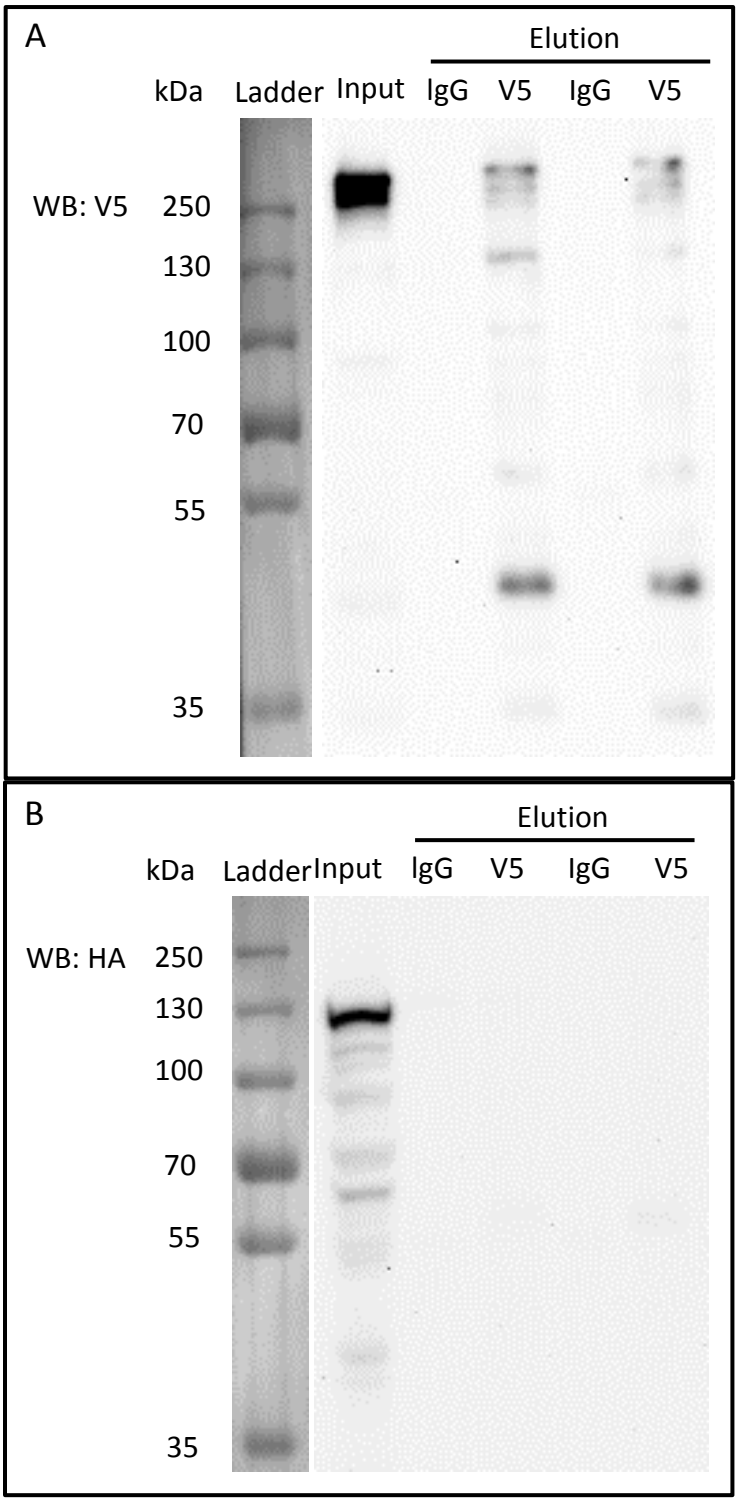

Figure 5.13 Kif5B is not in a complex with Usp9X in HEK293 cells

HEK923 cells were co-transfected with V5-Usp9X and HA-Kif5B plasmids and protein extracted after 48 hours, precipitated with V5 antibody and probed with V5 (A) an HA (B) antibodies. No band was detected by the HA antibody at the anticipated size of 110kDa in the V5 elution samples, suggesting that Usp9X does not interact with Kif5B in HEK293 cells.

5.5 Ubiquitylation of Kif5B or kineisn-1

Usp9X is a deubiquitylating enzyme that rescues some of its substrates from proteosomal degradation (Mouchantaf et al., 2006, Schwickart et al., 2009, Xu et al., 2010). To examine if Kif5B is ubiquitylated, HEK293 cells were treated for six hours with 25nM of epoxomicin, a proteasome inhibitor (Han et al., 2012, Stewart et al., 2010). Protein lysate was collected from epoxomicin treated and untreated cells and examined by immunoblotting. The protein lysates were first probed with an ubiquitin antibody. Epoxomicin treated protein lysate showed a greater amount of ubiquitin-positive high molecular weight proteins suggesting the assay was working (**Figure 5.14A**). The protein lysates were probed with kinesin-1 and Kif5B antibodies. As mentioned earlier, only Kif5B is expressed in HEK293 (Kanai et al., 2000). The levels and size of both kinesin-1 and Kif5B proteins treated and untreated with epoxomicin were similar, suggesting that Kif5B is not ubiquitylated in HEK293 cells.

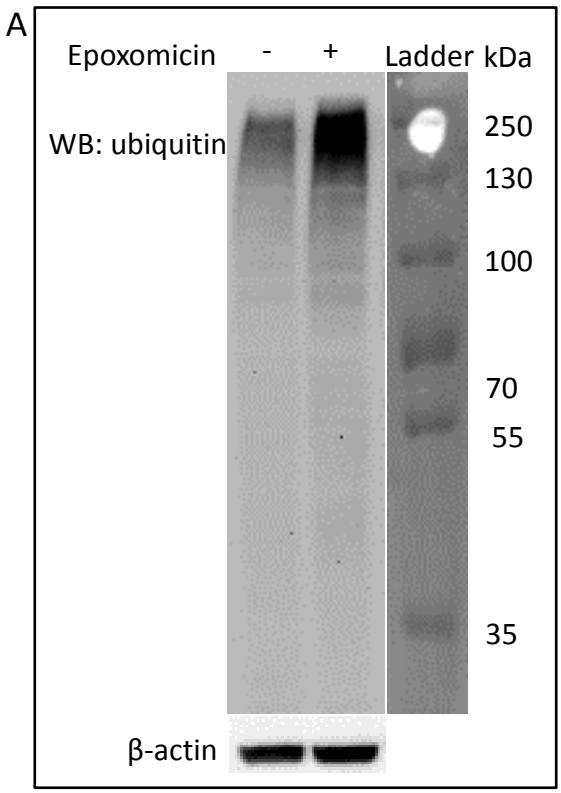

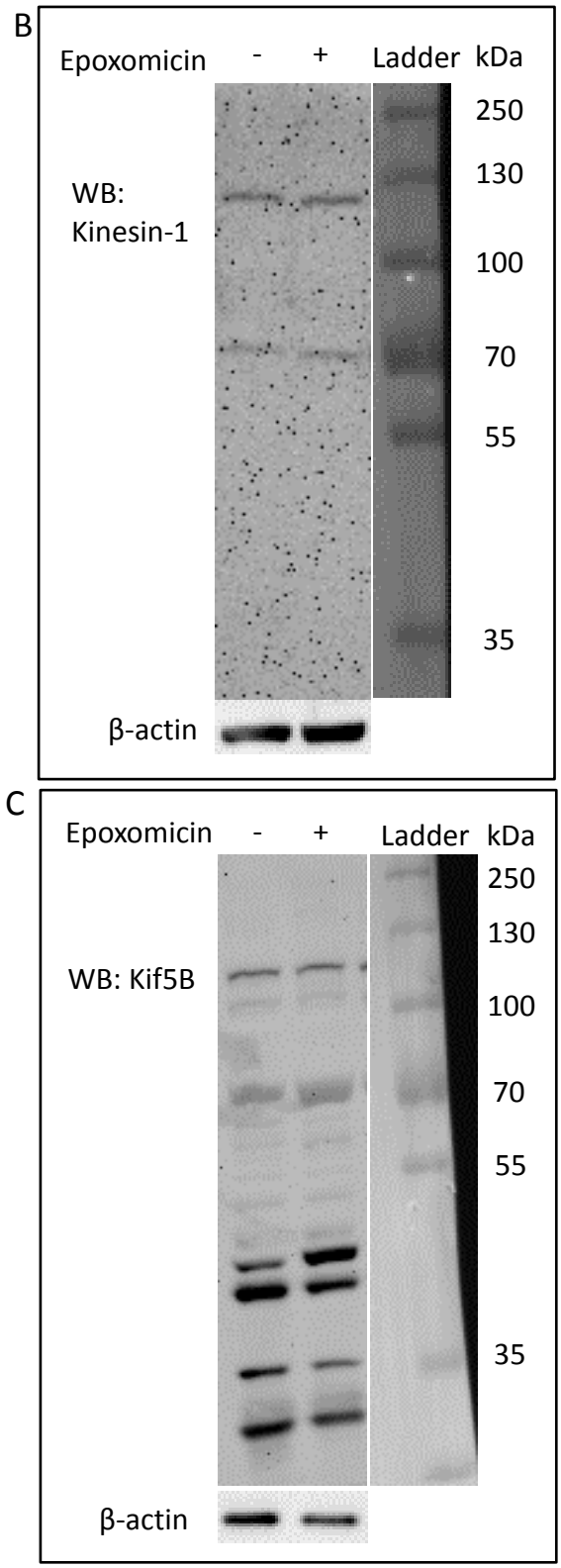

Figure 5.14 Kif5B and kinesin-1 are not ubiquitylated in HEK293 cells

Immunoblotting analyses for ubiquitin (A), kinesin-1 (B) and Kif5B (C) in HEK293 cells after treatment with 25nM of epoxomicin for six hours. - untreated; +: treated with epoxomicin.

The dramatic reduction of Kif5B immunoreactivity was observed in 3DIV hippocampal neurons (**Figure 5.1**). To examine if Kif5B is ubiquitylated in hippocampal neurons, wild-type hippocampal neurons in culture were treated with 25nM of epoxomicin three days after plating. After six hours of treatment, neurons were collected for immunoblotting analysis. Firstly, the epoxomicin treated and untreated protein lysates were probed with ubiquitin antibody. The expression level of ubiquitin increased in the epoxomicin treated sample, suggesting the assay was working (**Figure 5.15A**). However, the expression levels of kineisn-1 in both epoxomicin treated and untreated neuronal culture were similar as was the size of the band, suggesting that the kinesin-1 is not ubiquitylated in three days *in vitro* hippocampal neurons (**Figure 5.15B**).

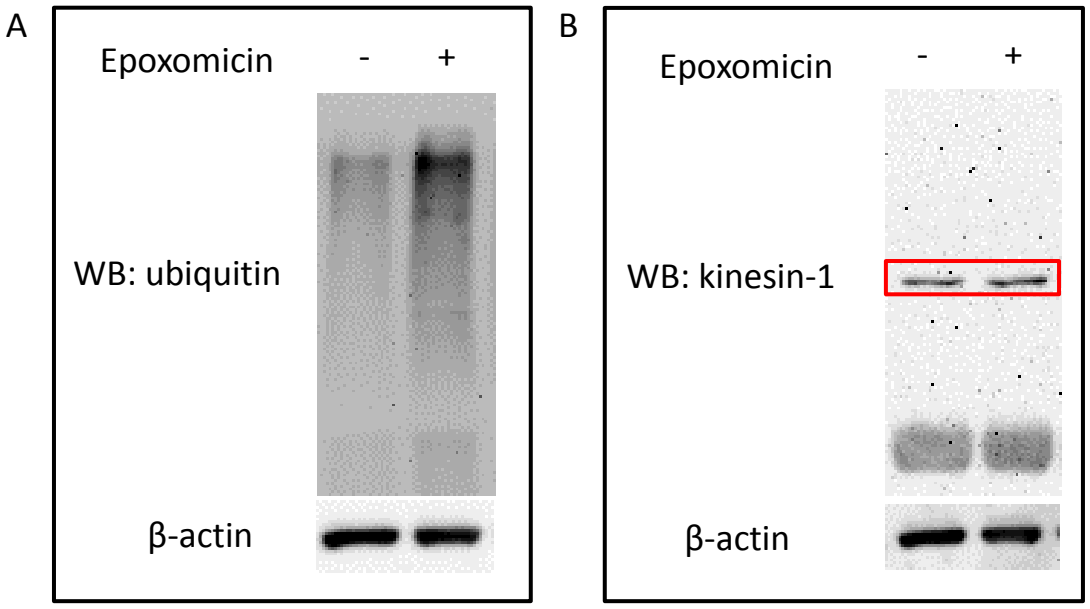

Figure 5.15 Kineisn-1 is not ubiquitylated in 3DIV hippocampal neurons Immunoblotting analyses for ubiquitin (A) and kinesin-1 (B) in 3DIV hippocampal neurons after treatment with 25nM of epoxomicin for six hours. - untreated; + treated with epoxomicin.

5.6 Transportation of syntaxin-1 and mitochondria by Kif5B

Kif5B is a microtubule-based motor protein, which transports the active zone (AZ) compartments to the nerve terminal for presynaptic plasticity in the developing neurons (Su et al., 2004, Cai et al., 2007). When the precursor AZ vesicle reaches the nerve terminal, it fuses to the plasma membrane and assemble AZs, forming a site for neurotransmitter release and new synapse. The precursor AZ transport vesicle contains membranous syntaxin-1 which acts as a receptor and is linked to Kif5B for axonal transport by syntabulin. Synatxin-1 is widely distributed in the dissociated hippocampal neurons in culture (Cai et al., 2007).

To examine the functional consequence, if any, of reduced Kif5B in Usp9X-null neurons, the subcellular distribution of syntaxin-1 was studied in 5DIV hippocampal neurons by immunofluorescence. Due to the higher structural complexity of the neurons at 5DIV, where axons from neighbouring neurons often overlap, therefore, lower cell density of the cultures was used to enable better resolution of individual neurons. Images of 20 neurons derived from three wild-type and three Usp9X knock-out culture were taken and the cellular distribution of syntaxin-1 compared. Syntaxin-1 was present throughout both wild-type and Usp9X-null neurons and there was no observable difference at this level of resolution (**Figure 5.16**).

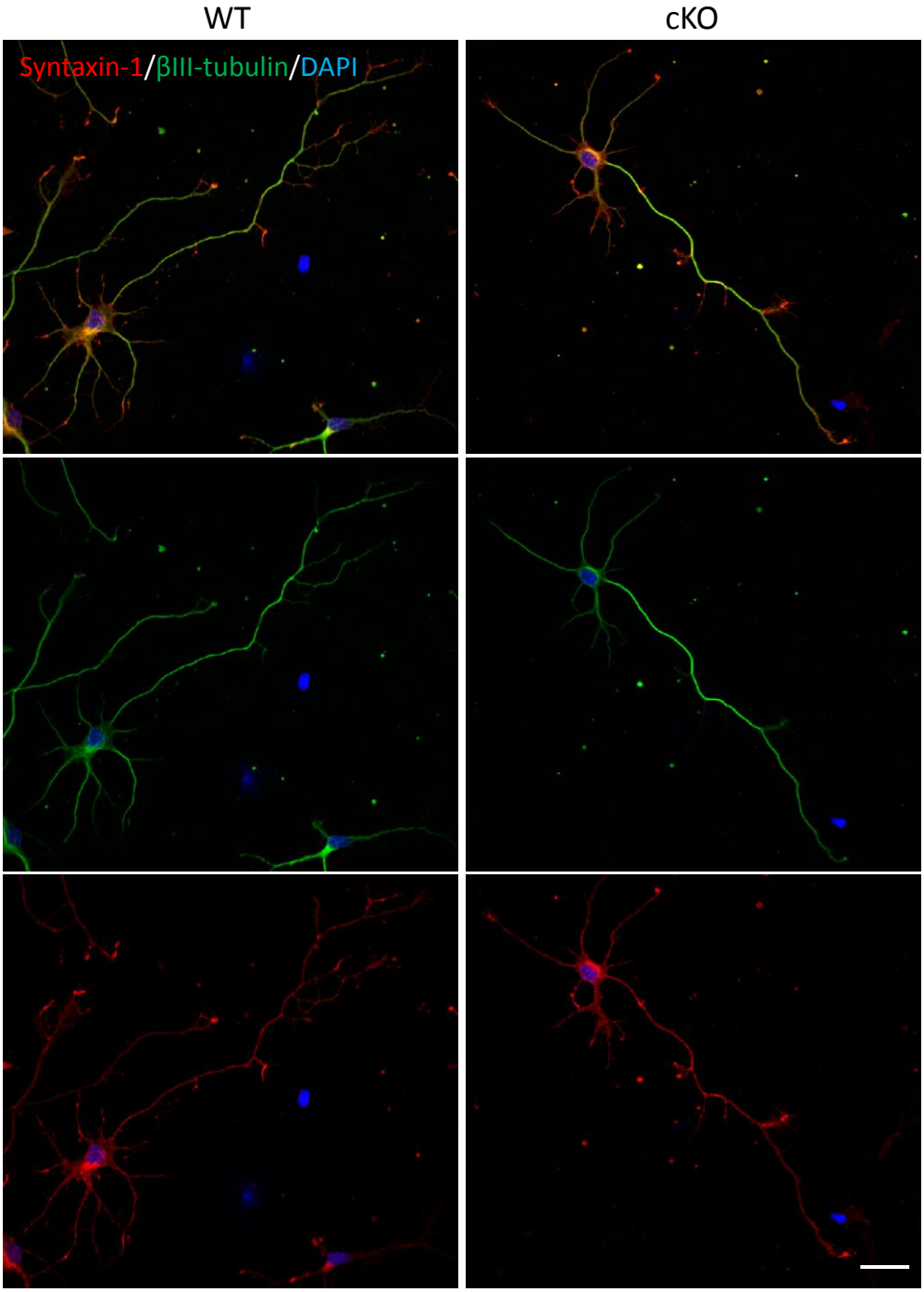

Figure 5.16 Subcellular distribution for syntaxin-1 is not affected in Usp9X-null culture with reduced Kif5B expression level

Double-staining of syntaxin-1 (red) and βIII-tubulin (green) in 5DIV hippocampal neurons. Cell nuclei were stained DAPI (blue). WT: wild-type, cKO: Usp9X knockout. Scale bar represents 20μm.

Kif5B has also been shown to transport mitochondria *in vitro* (Tanaka et al., 1998). To examine if the distribution of mitochondria in the axon was affected in the absence of Usp9X, the dissociated hippocampal neurons were incubated with 400nM mitotracker for 30 minutes at 37°C three days after plating. The cells were fixed for immunofluorescence. As shown in **Figure 5.17A&B**, mitochondria were distributed along the axon for both wild-type and Usp9X-null neurons. The number of mitochondria of 80μm for both the distal and proximal ends of the axon was counted. 10 neurons per culture (n=3 embryos per genotype) were used for analysis. The percentage of mitochondria at the proximal end for Usp9X-null neurons was significantly lower than of wild-type neurons (Student's t-test p=0.05). At the distal of the axon, percentage of mitochondria for Usp9X cKO neurons was significantly higher than of wild-type neurons (Student's t-test p=0.05), suggesting that the mitochondria tend to distribute at the distal end of the axon in the absence of Usp9X **(Figure 5.17C)**.

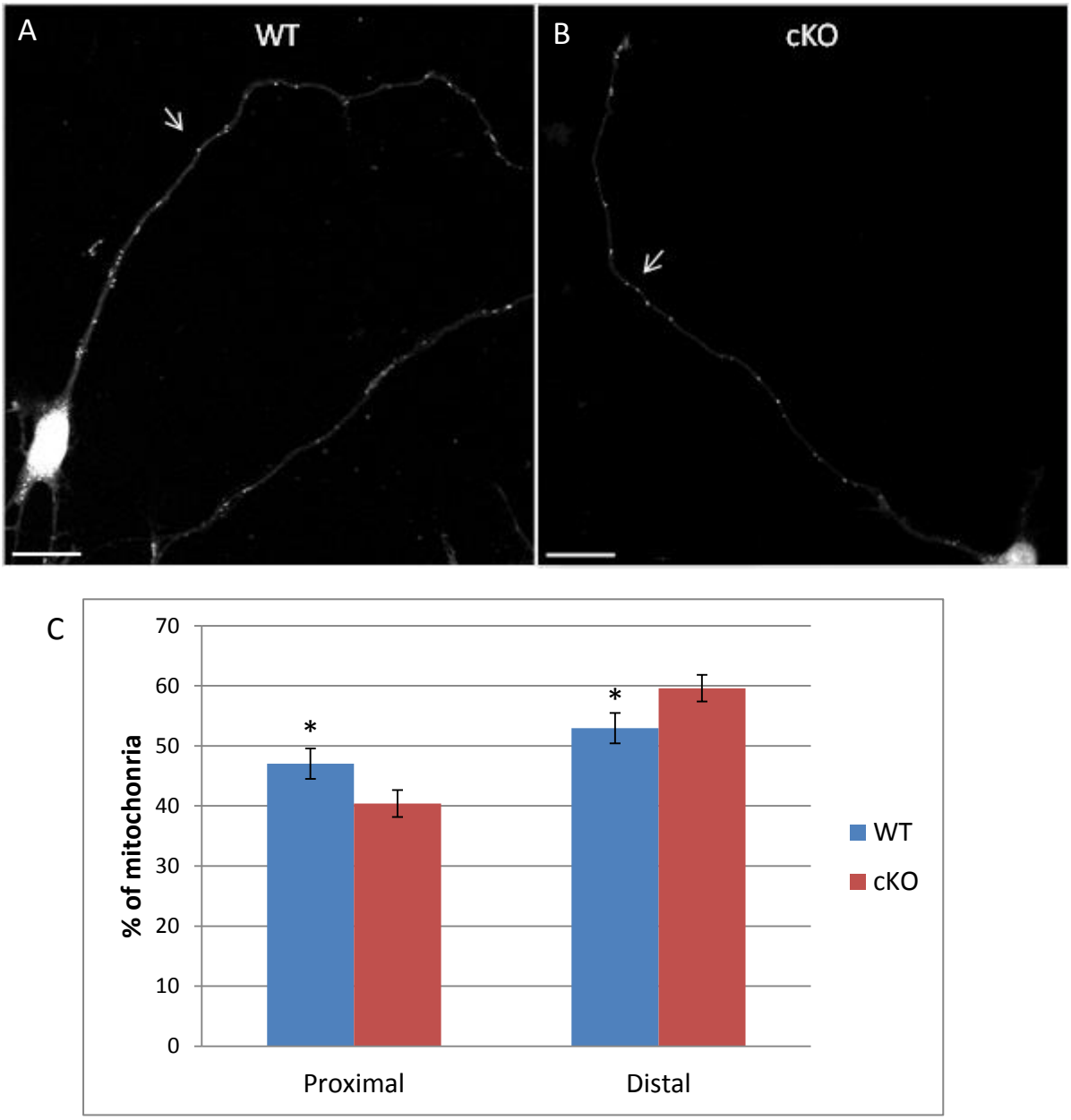

Figure 5.17 Mitochondria tend to distribute to the distal end of the axon in the absence of Usp9X

Three days after plating, the dissociated hippocampal neurons were incubated with mitotracker for 30 minutes at 37°C. The neurons were fixed for imaging. White arrows (A,B) indicated the mitochondria along the axon. (C) The percentage of mitochondria at proximal and distal ends for both WT and Usp9X cKO neurons. 10 neurons per culture (n=3 embryos per genotype) were analysed with Student's t-test p=0.0501. WT: wild-type, cKO: Usp9X knockout. Scale bar: 50μm.

5.7 Restoration of Kif5B in Usp9X-null neurons

Loss of Usp9X resulted in delayed axon specification (**Chapter 3**), shorter axonal length and reduced number of axonal termini in cultured hippocampal neurons (Stegeman et al., 2013, Homan et al., 2014). As shown in **Figure 5.1**, in the absence of Usp9X the expression level of Kif5B is dramatically reduced in 3DIV and 5DIV hippocampal neurons. To examine if the shorter axonal length in Usp9X-null neurons is due to the reduction of Kif5B expression, a rescue experiment was attempted by transfecting dissociated Usp9X-null hippocampal neurons with YFP-tagged Kif5B (Rivera et al., 2007). In a pilot study we failed to detect YFP in neurons following transfection with YFP-Kif5B using Amaxa Nucleofection Kit. Therefore we sought to determine where the problem lay. Firstly, to confirm the whether the YFP-Kif5B plasmid we received expressed YFP, both YFP-Kif5B and pMAX-GFP control plasmids were transfected into HEK293 cells using Lipofectamine® 2000 reagent. The cells were fixed at 48 hours post-transfection for imaging. YFP fluorescence was detected in approximately 50% of HEK293 cells. Interestingly, YFP was detected mainly in the nuclei of the cells suggesting YFP-Kif5B fusion protein would also be nuclear (**Figure 5.18**). The transfection of YFP-Kif5B was subsequently attempted into wild-type hippocampal neurons using the Amaxa Nucleofection Kit. The expression of YFP-Kif5B was extremely low (**Figure 5.19**) and unable to be picked up at even x63 higher magnification (data not shown) whereas GFP expressed from a control plasmid was readily detectable. The nuclear localisation of YFP and the low expression of YFP-Kif5B in neurons, suggested this plasmid was not suitable for the rescue experiment.

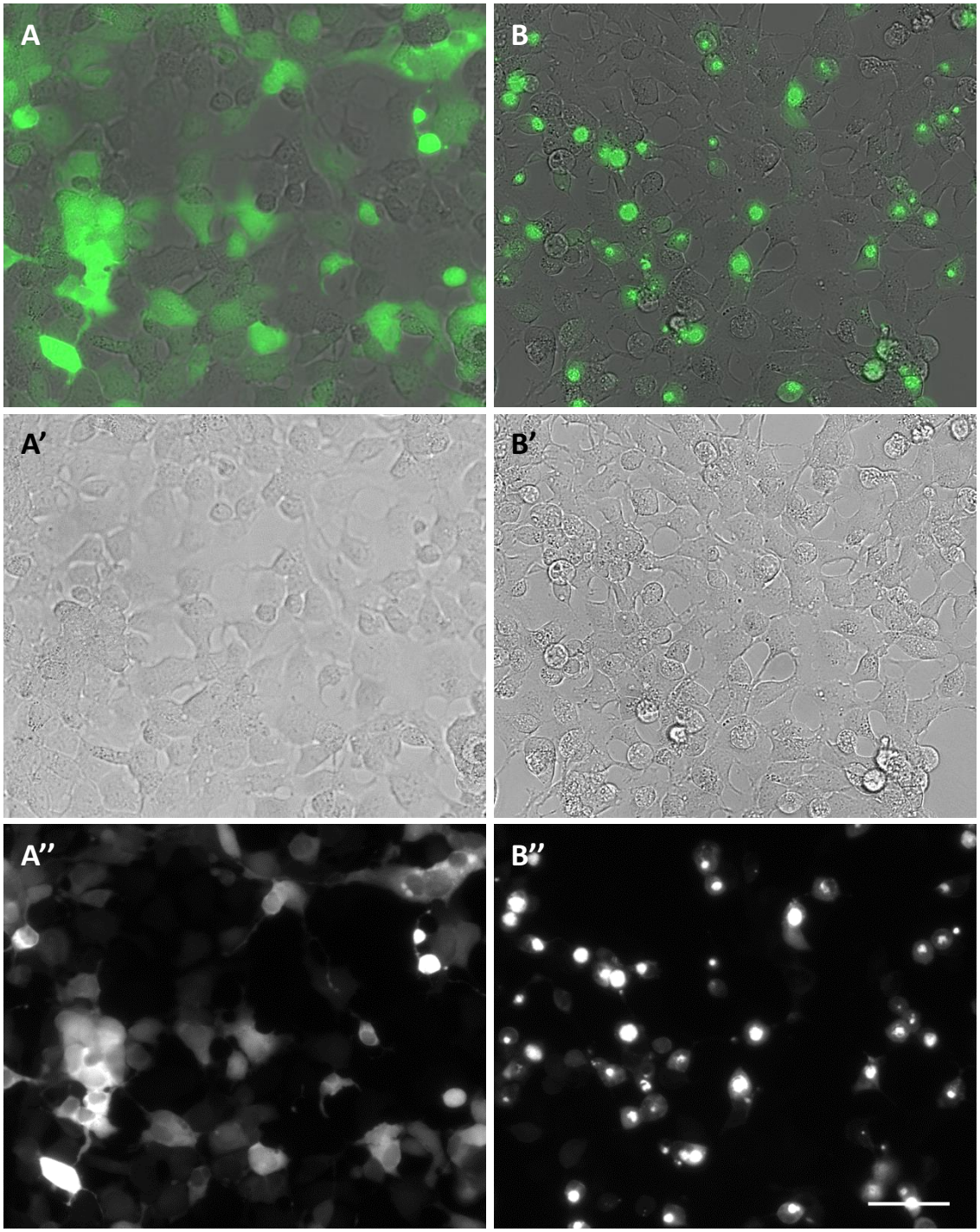

Figure 5.18 YFP-Kif5B is expressed in the nuclei of HEK293 cells

HEK293 cells were transfected with (A) pMAX-GFP and (B) YFP-Kif5B with Lipofectamine® 2000 reagent. Merged (A, B), bright field (A', B') and fluorescence (A'', B'') images were taken 48 hours after transfection. YFP-Kif5B shows nuclei expression in HEK293 cells. Scale bar represent 20μm.

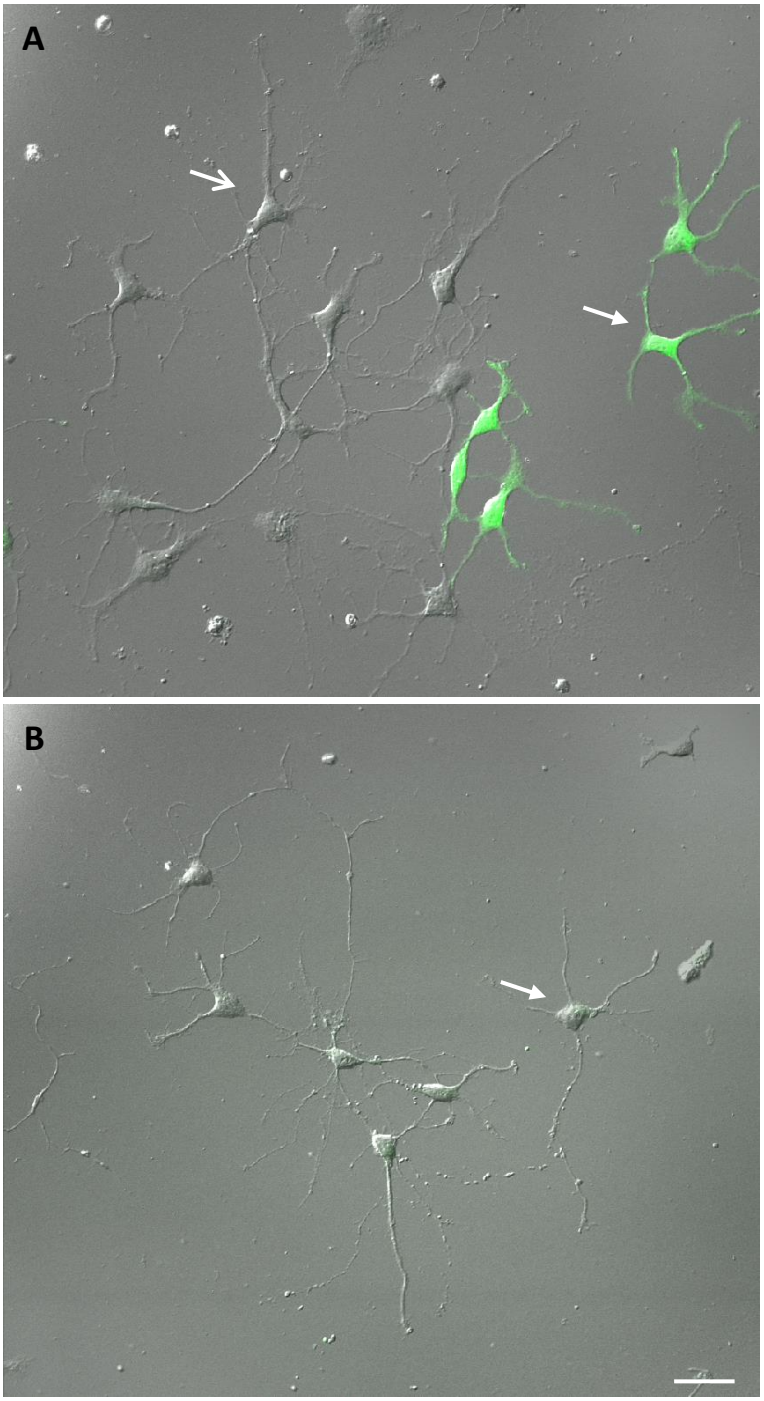

Figure 5.19 Expression level of YFP-Kif5B is negligible in the dissociated hippocampal neurons

The dissociated hippocampal neurons were transfected with (A) pMAX-GFP and (B) YFP-Kif5B. Three days after plating, merged images of bright field and fluorescence were taken. The expression of YFP-KIF5B was negligible. Closed arrowhead shows the transfected neuron while open arrowhead shows the un-transfected cells. Scale bar indicate 20μm.

5.8 Discussion

A yeast-two-hybrid screening of a human fetal brain cDNA library identified an interaction between Kif5B with Usp9X. This suggested the possible regulation of Kif5B by Usp9X which in turn might be required for axon specification (**Chapter 3**) or axon growth in dissociated hippocampal neurons (Stegeman et al., 2013, Homan et al., 2014). In this study, immunofluorescence data showed that loss of Usp9X resulted in the dramatic reduction of Kif5B expression in 3DIV and 5DIV dissociated hippocampal neurons (**Figure 5.1**). However, the reduction of Kif5B expression level was not observed in the symmetrical stage 2 neurons when Usp9X was absent (**Figure 5.3**). This indicates that Usp9X-dependent Kif5 expression is stage specific and that the regulation of Kif5B by Usp9X might only involve axonal growth but not axon specification.

An apparent lack of antibody specificity to Kif5B hampered the analysis and needs to be addressed here. Immunoblotting analysis was performed to confirm or reject the immunofluorescence data. Immunoblotting using kinesin-1 antibody for 3DIV and 5DIV of the dissociated hippocampal neurons culture was performed (**Figure 5.6** and **5.7**). Taking into account that the kinesin-1 antibody used in this study is directed against a kinesin heavy chain region that is highly conserved in all three isotypes of kinesin-1, (Kif5A, 5B and 5C) and the expression of Kif5A, Kif5B and Kif5C was reported in dissociated hippocampal neurons (Vidal et al., 2012, Kanai et al., 2000, Nakajima et al., 2012), immunoblotting analysis demonstrated that loss of Usp9X did not affect the total expression level of kinesin-1 in 3DIV and 5DIV hippocampal neurons. However they do not define the contribution of each isotype. Kif5A (~117kDa) and Kif5C (~107kDa) are reportedly expressed highly in neurons while Kif5B (~109kDa) is expressed in neuronal and non-neuronal cells (Kanai et al., 2000, Nakajima et al., 2012). Therefore, data from the imunoblotting analysis could not confirm the reduction of Kif5B in Usp9X null neurons as shown in **Figure 5.1**, but neither did it reject the hypothesis. In future, specific antibodies for all three isotypes of kinesin-1 heavy chain should be used.

An alternative explanation could be that the kinesin-1 antibody detected only Kif5A in the dissociated hippocampal neurons. This assumption was made based on the larger molecular weight band detected (**Figure 5.5**) and unpublished microarray data

for ReNcell VM showing that Kif5A is not expressed in ReNcell VM (there was no probe detecting Kif5C). As shown in **Figure 5.5**, the size of the protein detected in ReNcell VM by kinesin-1 antibody was similar to HEK293 cells, which only expresses Kif5B (109kDa), suggesting that only Kif5B is expressed in ReNcell VM. The size of the protein detected in hippocampal neuron ran higher than HEK293 and ReNcell VM, therefore, it is possible that kinesin-1 antibody only recognised Kif5A (117kDa) in the hippocampal neuronal cultures. This could indicate that Kif5A expression was not affected when Usp9X was absent on 3DIV and 5DIV (**Figure 5.6** and **5.7**) but no conclusions can be drawn about Kif5B. The specificity of kinesin-1 antibody only to Kif5A could be resolved by examining the expression of kinesin-1 after knockdown of Kif5A in HEK293 cells using siRNA.

Double-labelling of Usp9X and Kif5B in stage 3 hippocampal neurons suggest that Usp9X and Kif5B co-localise in the axon and growth cone (**Figures 5.10**). This is supported with Pearson's coefficient data which measure the correlation between red (Usp9X) and green (Kif5B) channels for regions of interest in the cell body, axon and growth cone. Pearson's coefficient indicates the amount of co-localisation by measuring pixel which contains both signals. The analyses show higher mean Pearson's coefficient in the axon and growth cone compared to cell body, suggesting that there is higher co-localisation of Usp9X and Kif5B in the axon and growth cone.

Co-IP using mouse brain lysate failed to detect an interaction between Usp9X and kinesin-1 (Kif5A, 5B and 5C) under the conditions used (**Figure 5.11**). For this project, HEK293 cells were used for biochemical assays because the high transfection efficiency in these cells is required for Co-IP and ubiquitylation assays. Co-transfection of V5-Usp9X and HA-Kif5B plasmids in HEK293 cells for Co-IP failed to detect an interaction between Usp9X and Kif5B. However, as shown in **Figure 5.13A**, low band intensity for V5-Usp9X was detected in the V5 elution. Therefore if Usp9X only interacts with a subpopulation of Kif5B in the cells, the interaction between Usp9X and Kif5B might be difficult to be detected. Usp9x only interacts with subpools of other substrates including ASG3 (Xu et al., 2010) and EFA6 (Theard et al., 2010). Therefore, given time, this experiment needs to be repeated with higher number of cells for immunoprecipitation. The over-expression of the plasmid containing the catalytically inactive form of Usp9X might be more suitable for Co-IP as it may bind its substrates longer.

Until now, there is no published data indicating that Kif5B is ubiquitylated or is targeted for proteosomal degradation. From this study, treatment of epoxomicin in HEK293 cells and dissociated hippocampal neurons suggest that Kif5B and kinesin-1 is not degraded by the proteasome (**Figure 5.14** & **5.15**). These data also suggests that the reduction of Kif5B expression in Usp9X-null hippocampal neurons may not be due to the classical role of Usp9X as a deubiquitylating enzyme (Mouchantaf et al., 2006, Schwickart et al., 2009, Xu et al., 2010). As well as protein stability, Usp9X also regulates the localisation and activation of proteins, which has been shown in Smad4 and MARK4 *in vitro* (Al-Hakim et al., 2008, Dupont et al., 2009). Our initial analysis suggests that Kif5B expression level was reduced without showing any mislocalisation in Usp9X-null neurons (**Figure 5.1**). However it is conceivable that all the cellular Kif5B may re-localise to the peri-nuclear region in Usp9X-null neurons (**Figure 5.1**). This needs to be resolved at higher microscopic resolution.

One of the roles for Kif5B is to transport mitochondria anterogradely in the cells (Tanaka et al., 1998). It is hypothesized that reduced Kif5B expression in Usp9X-null hippocampal neuron might reduce the transportation of mitochondria to the distal end of the axon. As shown in **Figure 5.17**, the distribution pattern of mitochondria for wild-type and Usp9X cKO neurons is not statistically significant, however, it has a strong trend towards significance which could be due to the inherent variability of the biological systems which may be compounding this data. Live cell imaging might be a more suitable method to study the forward transport of mitochondria along the axon in real time as transport rates rather than overall distribution may be affected.

Given that Kif5A, Kif5B and Kif5C show high similarity in their amino acid sequences, it is possible that there is functional redundancy among the three kineisn-1 motor proteins (Kanai et al., 2000). This suggests that reduced Kif5B expression in hippocampal neurons might not result in any functional defect in Usp9X-null dissociated hippocampal neurons.

The transfection of Usp9X-null neurons with YFP-Kif5B to restore the Kif5B expression level and rescue the shorter axonal length is important to show the interaction between Usp9X and Kif5B. YFP-Kif5B plasmid was a gift from Professor Don Arnold, which it has been used for the examination of localization for

Kv1 K(+) channels along the axon of the cultured cortical neurons (Rivera et al., 2007). However as shown in **Figure 5.18** and **5.19**, the transfection of YFP-Kif5B in HEK293 cells and hippocampal neurons showed the nuclei expression of Kif5B and low fluorescence expression of YFP from the plasmid respectively, suggesting that this plasmid is not suitable for the rescue experiments.

6. General discussion and future directions

6.1 Usp9X in neuronal development

Usp9X is involved in multiple stages of neuronal development. Based on the data obtained from this project, Usp9X facilitates neurite initiation as Usp9X-null neurons displayed delayed progression from filopodia and lamellipodia presenting stage 1 neurons to those with neurites (stage 2). In addition, Usp9X is required for axon specification and growth based on the dramatically delayed neuronal progression from stage 2 to 3 and significantly shorter axonal length. This is consistent with the previous *in vitro* findings, which demonstrated the importance of Usp9X for normal axonal elongation and branching in later stage neurons (Stegeman et al., 2013, Homan et al., 2014). The requirement of Usp9X for axon formation is further supported by *in vivo* data where loss of Usp9X results is a smaller corpus callosum in the adult brain and reduced neuronal projections in the embryonic brain (Stegeman et al., 2013). Usp9X also regulates neuronal migration as shown in neurospheres isolated from the dorsal cortex of the embryonic brain (Homan et al., 2014).

The analysis of Usp9X regulation of axon development and migration has been demonstrated predominantly at the cellular level in *in vitro* cultured neurons. For future studies, to visualise how a single neuron develops an axon and grows in the cortical region of the brain, in utero electroporation of a control GFP vector or a plasmid expressing Cre recombinase tagged with GFP into the lateral ventricles of E14.5 embryos carrying a conditional Usp9X-null mutant allele ($Usp9X^{floxed}$) to label the newborn neurons and collected for *ex vivo* slice culture (Yi et al., 2010). Cortical slices are then divided into ventricular zone, subventricular zone and cortical plate based on the distance from the lateral ventricle (Yi et al., 2010, Hand et al., 2005) and axon formation and migration can be analysed at different time points. Combination of the *in vivo* and *in vitro* data would provide clearer and more relevant information about Usp9X regulation of neurons.

6.2 Usp9X and cell function: polarity

Usp9X is required for the establishment and maintenance of polarity in a number of different cell types. In polarized epithelial cells, the apical membrane is separated from the basolateral membrane by the tight junctions (TJs) and adherens junctions (AJs) (Farquhar and Palade, 1963). TJs are the most apical component of the junctional complex, which serve as barriers to prevent solutes and water passing through the paracellular pathway. While AJ proteins connect to the actin cytoskeleton for further maturation of the junction (Kriegstein and Gotz, 2003). Usp9X regulates multiple substrates some of which are adhesion and polarity proteins, including AF-6 (Afadin), β-catenin and EFA6 (Taya et al., 1998, Taya et al., 1999, Theard et al., 2010).

In cultured MDCK cells, Usp9X regulates TJ biogenesis by controlling the levels of EFA6, a protein essential for TJ formation (Theard et al., 2010). Usp9X mediated deubiquitylation of EFA6 is required for the establishment of TJ during a narrow temporal window, which precedes the establishment of polarity (Theard et al., 2010). In the polarised intestinal epithelial cell line T84, Usp9X co-localises with multiple adhesion proteins including β-catenin, p120 catenin and Z0-1. Interestingly, Usp9X only interacts with β-catenin and E-cadherin in subconfluent cells where adhesion junctions are unstable and undergoing dynamic rearrangements (Murray et al., 2004). The E-cadherin-β-catenin complex plays an essential role in the establishment and maintenance of AJs and is targeted for degradation by the ubiquitin-proteasome pathway.

Usp9X is a strong candidate to play a role in neural progenitor (NP) polarity where cell polarity is central to dictating self-renewal and cell fate decisions (Jolly et al., 2009). In embryonic stem cell derived NPs, over-expression of Usp9X promotes the formation of polarized neural cell clusters which express markers of radial glial cells with adherens junction proteins and apical markers concentrated at the centre. This in turn also promotes the self-renewal capacity for NP and increases the numbers of NPs and neurons in *vitro.* These studies suggest that Usp9X is important for the formation of intercellular junctions during cell polarisation.

In vivo, Usp9X is highly expressed in the pluripotent stem cells of mouse pre-implantation embryos (Pantaleon et al., 2001). Depletion of Usp9X from two-cell mouse embryos results in failure of the embryos to develop to blastocyst. Usp9X deficiency not only results in slower blastomere cleavage rate, but inhibition of cell adhesion as well as loss of cell polarity (Pantaleon et al., 2001). In addition, Nestin-Cre mediated deletion of Usp9X from mouse brain affects adhesion and polarity proteins at embryonic stages. Deletion of Usp9X results in decreased levels of adhesion proteins (N-cadherin, AF-6) and polarity proteins (aPKCζ, CD133) at E12.5 although these returned to normal at E14.5 and E16.5 (SAW, unpublished). These data further support the hypothesis that Usp9X is essential for cell polarity and adhesion.

Usp9X is also involved in axon-dendritic polarity, as loss of Usp9X in dissociated hippocampal neurons results in delayed axon specification (**Chapter 3**), shorter axonal length and fewer axonal branches (Stegeman et al., 2013, Homan et al., 2014). Although neurons do not contain adherens junctions, other factors associated with the actin/microtubule cytoskeleton play important roles in maintaining neuronal polarity. Evidence from yeast-two-hybrid and 2D proteomic analysis (Homan et al., 2014) indicates that Usp9X regulates some of these cytoskeletal proteins. In this project, some of the cytoskeletal proteins which regulate microtubule dynamics, such as stathmin-1, Kif5B and CRMP2 were examined in Usp9X-null hippocampal neurons. Interestingly, a dramatic reduction of Kif5B was observed in neurons in the absence of Usp9X. In future studies, the regulation of Usp9X with Kif5B and its consequences for axonal growth should be examined.

6.3 Usp9X and cytoskeletal proteins

Actin filaments are structurally important for the formation of filopodia and branches, as well as growth cone motility. 2D proteomic analysis of *in vitro* hippocampal neurons suggests that Usp9X might regulate cofilin and Arp2/3 complex which are both important for actin dynamics (Ichetovkin et al., 2002, Homan et al., 2014). Cofilin is a severing protein that de-polymerizes F-actin. In wild-type hippocampal neuron, active and non-phosphorylated forms of cofilin are enriched at the growth cone and are necessary for normal axon formation (Garvalov et al., 2007). Deletion of Cdc42 in dissociated hippocampal neurons results in increased cofilin

phosphorylation at the growth cone, and thus disrupts neuronal polarization (Garvalov et al., 2007). While for Arp2/3 complex, it promotes actin polymerization. Depletion of Arp2/3 complex in dissociated hippocampal neurons and neuroblastoma cells, using small interfering RNA, showed decreases in F-actin content, inhibition of retrograde flow in the growth cone and disruption in filopodia dynamics, and also disruption in neuritogenesis and neuronal differentiation (Korobova and Svitkina, 2008). Given that Usp9X is required for normal axon development and initial neurite formation, and lamellipodia and filopodia structures are highly dependent on the actin dynamic, for future studies, the regulation of cofilin and Arpc2/3 complex by Usp9X is worthwhile pursuing.

6.4 Usp9X and neuronal trafficking

Three single point variants at the C-terminal region of human Usp9X have been identified in individuals with X-linked intellectual disability. All the Usp9X variants resulted in the depletion of Usp9X localisation specifically at the axonal growth cone, but not elsewhere in the neuron, and were associated with defects in axonal growth and neuronal migration (Homan et al., 2014). The C-terminal region Usp9X interacts with doublecortin. However, doublecortin is not a Usp9X substrate and their interaction is proposed to transport Usp9X along the axon and other neuronal processes (Friocourt et al., 2005). Mutations in doublecortin in humans cause type1-lissencephaly and subcortical laminar heterotopia (Gleeson et al., 1998). Therefore, it suggests proper Usp9X-doubelcortin interaction is required to prevent some neurological disorders (Friocourt et al., 2005). Usp9X trafficking by doublecortin may facilitate interactions between Usp9X and other substrates or component proteins essential for axonal and neurite formation.

6.5 Usp9X and TGFβ signalling pathway

The TGFβ signalling pathway regulates both axon specification and growth in cultured hippocampal neurons (Ishihara et al., 1994, Yi et al., 2010). These phenotypes parallel the findings in dissociated hippocampal neurons of Usp9X knock-out mice which display delayed axon specification and shorter axonal length. This raises the possibility of Usp9X regulating axon production via the TGF-β signaling pathway (Stegeman et al., 2013). Previous studies have shown Usp9X is

required for neurons to respond to the TGFβ ligand (Stegeman et al., 2013) as TGFβ treatment increased the length of the axon and number of axon and dendritic termini in wild-type but not Usp9X-null neurons. Hippocampal neurons transfected with TGFβ luciferase reporter constructs did not respond to increasing concentrations of TGFβ when Usp9X was absent. At the mRNA level, BDNF showed no response to TGFβ ligand as compared to the wild-type neurons.

There are several possible molecular mechanisms mediating Usp9X regulation of the TGFβ pathway during axon development. Two could be through the known Usp9X substrates, Smad4 and Smurf1 of the TGFβ pathway (Dupont et al., 2009, Xie et al., 2013). Smad4 activates TGFβ pathway while Smurf1 antogonizes TGFβ pathway and perhaps directly or indirectly through the known TGFβ pathway target gene, BDNF (Sometani et al., 2001, Stegeman et al., 2013). A further possibility is PJA1 identified in the yeast-2-hybrid (S. Wood personal communication) and mass spectrometry from Usp9X affinity purification, PJA1 (Agrawal et al., 2012). Future studies about the regulation of Usp9X in TGFβ pathway for normal neuronal development is required.

Appendix- Supplementary figures

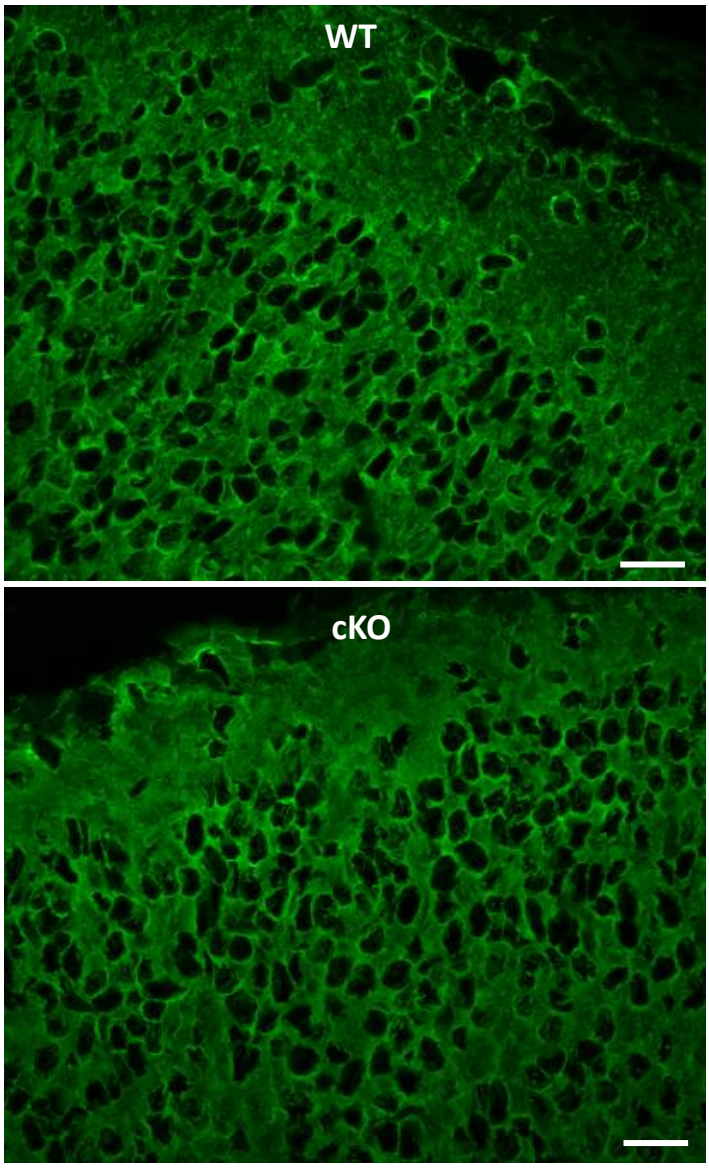

Figure 1 Expression of CRMP-2 in the cortical region of Usp9X cKO embryonic mouse brain

CRMP-2 (green) was ubiquitously expressed in the cortical region of E18.5 mouse brain for wild-type and Usp9X-null models (n=1). WT: wild-type; cKO: Usp9X knockout. Scale bar: 20μm.

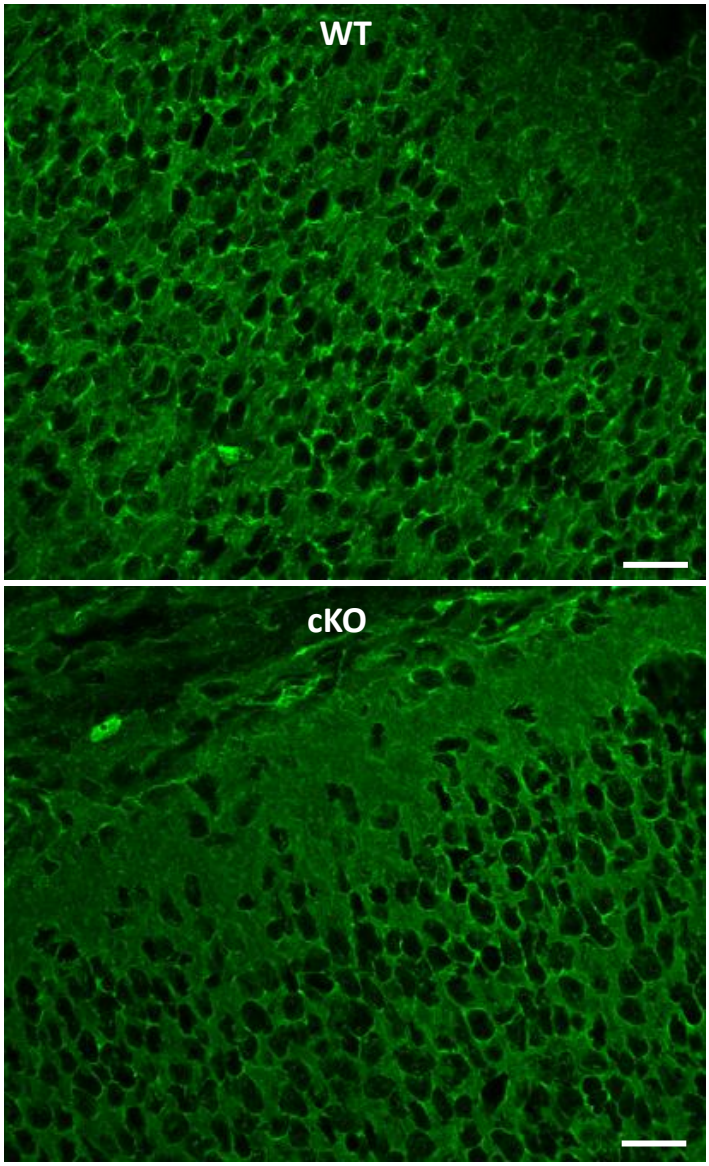

Figure 2 Expression of PJA1 in the cortical region of Usp9X cKO embryonic mouse brain

PJA1(green) was ubiquitously expressed in the cortical region of E18.5 mouse brain for wild-type and Usp9X-null models (n=1). WT: wild-type; cKO: Usp9X knockout. Scale bar: 20μm.

References

AGRAWAL, P., CHEN, Y. T., SCHILLING, B., GIBSON, B. W. & HUGHES, R. E. 2012. Ubiquitin-specific peptidase 9, X-linked (USP9X) modulates activity of mammalian target of rapamycin (mTOR). *J Biol Chem,* 287**,** 21164-75.

AL-BASSAM, J. & CHANG, F. 2011. Regulation of microtubule dynamics by TOG-domain proteins XMAP215/Dis1 and CLASP. *Trends Cell Biol,* 21**,** 604-14.

AL-HAKIM, A. K., ZAGORSKA, A., CHAPMAN, L., DEAK, M., PEGGIE, M. & ALESSI, D. R. 2008. Control of AMPK-related kinases by USP9X and atypical Lys(29)/Lys(33)-linked polyubiquitin chains. *Biochem J,* 411**,** 249-60.

ALONSO, M., MEDINA, J. H. & POZZO-MILLER, L. 2004. ERK1/2 activation is necessary for BDNF to increase dendritic spine density in hippocampal CA1 pyramidal neurons. *Learn Mem,* 11**,** 172-8.

ANDERSEN, S. S. & BI, G. Q. 2000. Axon formation: a molecular model for the generation of neuronal polarity. *Bioessays,* 22**,** 172-9.

ARBOUR, N., VANDERLUIT, J. L., LE GRAND, J. N., JAHANI-ASL, A., RUZHYNSKY, V. A., CHEUNG, E. C., KELLY, M. A., MACKENZIE, A. E., PARK, D. S., OPFERMAN, J. T. & SLACK, R. S. 2008. Mcl-1 is a key regulator of apoptosis during CNS development and after DNA damage. *J Neurosci,* 28**,** 6068-78.

ASADA, N., SANADA, K. & FUKADA, Y. 2007. LKB1 regulates neuronal migration and neuronal differentiation in the developing neocortex through centrosomal positioning. *J Neurosci,* 27**,** 11769-75.

BARNES, A. P. & POLLEUX, F. 2009. Establishment of axon-dendrite polarity in developing neurons. *Annu Rev Neurosci,* 32**,** 347-81.

BIERNAT, J., WU, Y. Z., TIMM, T., ZHENG-FISCHHOFER, Q., MANDELKOW, E., MEIJER, L. & MANDELKOW, E. M. 2002. Protein kinase MARK/PAR-1 is required for neurite outgrowth and establishment of neuronal polarity. *Mol Biol Cell,* 13**,** 4013-28.

BRADKE, F. & DOTTI, C. G. 1999. The role of local actin instability in axon formation. *Science,* 283**,** 1931-4.

CAI, Q., PAN, P. Y. & SHENG, Z. H. 2007. Syntabulin-kinesin-1 family member 5B-mediated axonal transport contributes to activity-dependent presynaptic assembly. *J Neurosci,* 27**,** 7284-96.

CHEN, H., POLO, S., DI FIORE, P. P. & DE CAMILLI, P. V. 2003. Rapid Ca2+-dependent decrease of protein ubiquitination at synapses. *Proc Natl Acad Sci U S A,* 100**,** 14908-13.

CHENG, P. L., LU, H., SHELLY, M., GAO, H. & POO, M. M. 2011a. Phosphorylation of E3 ligase Smurf1 switches its substrate preference in support of axon development. *Neuron,* 69**,** 231-43.

CHENG, P. L., SONG, A. H., WONG, Y. H., WANG, S., ZHANG, X. & POO, M. M. 2011b. Self-amplifying autocrine actions of BDNF in axon development. *Proc Natl Acad Sci U S A,* 108**,** 18430-5.

CHENN, A. & WALSH, C. A. 2002. Regulation of cerebral cortical size by control of cell cycle exit in neural precursors. *Science,* 297**,** 365-9.

CHOI, Y. J., DI NARDO, A., KRAMVIS, I., MEIKLE, L., KWIATKOWSKI, D. J., SAHIN, M. & HE, X. 2008. Tuberous sclerosis complex proteins control axon formation. *Genes Dev,* 22**,** 2485-95.

CONDE, C. & CACERES, A. 2009. Microtubule assembly, organization and dynamics in axons and dendrites. *Nat Rev Neurosci,* 10**,** 319-32.

CRAIG, A. M. & BANKER, G. 1994. Neuronal polarity. *Annu Rev Neurosci,* 17**,** 267-310.

CRUMP, J. G., ZHEN, M., JIN, Y. & BARGMANN, C. I. 2001. The SAD-1 kinase regulates presynaptic vesicle clustering and axon termination. *Neuron,* 29**,** 115-29.

CUI, Y., HE, S., XING, C., LU, K., WANG, J., XING, G., MENG, A., JIA, S., HE, F. & ZHANG, L. 2011. SCFFBXL^{15} regulates BMP signalling by directing the degradation of HECT-type ubiquitin ligase Smurf1. *EMBO J,* 30**,** 2675-2689.

DA SILVA, J. S., MEDINA, M., ZULIANI, C., DI NARDO, A., WITKE, W. & DOTTI, C. G. 2003. RhoA/ROCK regulation of neuritogenesis via profilin IIa-mediated control of actin stability. *J Cell Biol,* 162**,** 1267-79.

DAJAS-BAILADOR, F., JONES, E. V. & WHITMARSH, A. J. 2008. The JIP1 scaffold protein regulates axonal development in cortical neurons. *Curr Biol,* 18**,** 221-6.

DEHMELT, L., SMART, F. M., OZER, R. S. & HALPAIN, S. 2003. The role of microtubule-associated protein 2c in the reorganization of microtubules and lamellipodia during neurite initiation. *J Neurosci,* 23**,** 9479-90.

DENT, E. W., KWIATKOWSKI, A. V., MEBANE, L. M., PHILIPPAR, U., BARZIK, M., RUBINSON, D. A., GUPTON, S., VAN VEEN, J. E., FURMAN, C., ZHANG, J., ALBERTS, A. S., MORI, S. & GERTLER, F. B. 2007. Filopodia are required for cortical neurite initiation. *Nat Cell Biol,* 9**,** 1347-59.

DERYNCK, R. & ZHANG, Y. E. 2003. Smad-dependent and Smad-independent pathways in TGF-beta family signalling. *Nature,* 425**,** 577-84.

DEVAUX, S., POULAIN, F. E., DEVIGNOT, V., LACHKAR, S., IRINOPOULOU, T. & SOBEL, A. 2012. Specific serine-proline phosphorylation and glycogen synthase kinase 3beta-directed subcellular targeting of stathmin 3/Sclip in neurons. *J Biol Chem,* 287**,** 22341-53.

DI PAOLO, G., LUTJENS, R., OSEN-SAND, A., SOBEL, A., CATSICAS, S. & GRENNINGLOH, G. 1997. Differential distribution of stathmin and SCG10 in developing neurons in culture. *J Neurosci Res,* 50**,** 1000-1009.

DIANTONIO, A., HAGHIGHI, A., PORTMAN, S., LEE, J., AMARANTO, A. & GOODMAN, C. 2001. Ubiquitination-dependent mechanisms regulate synaptic growth and function. *Nature,* 412**,** 449-452.

DINSMORE, J. H. & SOLOMON, F. 1991. Inhibition of MAP2 expression affects both morphological and cell division phenotypes of neuronal differentiation. *Cell,* 64**,** 817-26.

DONATO, R., MILJAN, E. A., HINES, S. J., AOUABDI, S., POLLOCK, K., PATEL, S., EDWARDS, F. A. & SINDEN, J. D. 2007. Differential development of neuronal physiological responsiveness in two human neural stem cell lines. *BMC Neurosci,* 8**,** 36.

DOTTI, C. G., SULLIVAN, C. A. & BANKER, G. A. 1988. The establishment of polarity by hippocampal neurons in culture. *J Neurosci,* 8**,** 1454-68.

DREWES, G., EBNETH, A., PREUSS, U., MANDELKOW, E. M. & MANDELKOW, E. 1997. MARK, a novel family of protein kinases that

phosphorylate microtubule-associated proteins and trigger microtubule disruption. *Cell,* 89**,** 297-308.
DUNCAN, J. E., LYTLE, N. K., ZUNIGA, A. & GOLDSTEIN, L. S. 2013. The Microtubule Regulatory Protein Stathmin Is Required to Maintain the Integrity of Axonal Microtubules in Drosophila. *PloS one,* 8.
DUPONT, S., MAMIDI, A., CORDENONSI, M., MONTAGNER, M., ZACCHIGNA, L., ADORNO, M., MARTELLO, G., STINCHFIELD, M. J., SOLIGO, S., MORSUT, L., INUI, M., MORO, S., MODENA, N., ARGENTON, F., NEWFELD, S. J. & PICCOLO, S. 2009. FAM/USP9x, a deubiquitinating enzyme essential for TGFbeta signaling, controls Smad4 monoubiquitination. *Cell,* 136**,** 123-35.
DUPONT, S., ZACCHIGNA, L., CORDENONSI, M., SOLIGO, S., ADORNO, M., RUGGE, M. & PICCOLO, S. 2005. Germ-layer specification and control of cell growth by Ectodermin, a Smad4 ubiquitin ligase. *Cell,* 121**,** 87-99.
EBISAWA, T., FUKUCHI, M., MURAKAMI, G., CHIBA, T., TANAKA, K., IMAMURA, T. & MIYAZONO, K. 2001. Smurf1 interacts with transforming growth factor-beta type I receptor through Smad7 and induces receptor degradation. *J Biol Chem,* 276**,** 12477-80.
FARQUHAR, M. G. & PALADE, G. E. 1963. Junctional complexes in various epithelia. *J Cell Biol,* 17**,** 375-412.
FENG, Z., LI, K., LIU, M. & WEN, C. 2010. NRAGE is a negative regulator of nerve growth factor-stimulated neurite outgrowth in PC12 cells mediated through TrkA-ERK signaling. *J Neurosci Res,* 88**,** 1822-1828.
FERRARI, A., FARACI, P., CECCHINI, M. & BELTRAM, F. 2010. The effect of alternative neuronal differentiation pathways on PC12 cell adhesion and neurite alignment to nanogratings. *Biomaterials,* 31**,** 2565-73.
FRANCIS, F., KOULAKOFF, A., BOUCHER, D., CHAFEY, P., SCHAAR, B., VINET, M. C., FRIOCOURT, G., MCDONNELL, N., REINER, O., KAHN, A., MCCONNELL, S. K., BERWALD-NETTER, Y., DENOULET, P. & CHELLY, J. 1999. Doublecortin is a developmentally regulated, microtubule-associated protein expressed in migrating and differentiating neurons. *Neuron,* 23**,** 247-56.
FRIOCOURT, G., KAPPELER, C., SAILLOUR, Y., FAUCHEREAU, F., RODRIGUEZ, M., BAHI, N., VINET, M.-C., CHAFEY, P., POIRIER, K., TAYA, S., WOOD, S., DARGEMONT, C., FRANCIS, F. & CHELLY, J. 2005. Doublecortin interacts with the ubiquitin protease DFFRX, which associates with microtubules in neuronal processes. *Molecular and cellular neurosciences,* 28**,** 153-164.
FU, X., BROWN, K. J., YAP, C. C., WINCKLER, B., JAISWAL, J. K. & LIU, J. S. 2013. Doublecortin (Dcx) family proteins regulate filamentous actin structure in developing neurons. *J Neurosci,* 33**,** 709-21.
FUKATA, Y., ITOH, T., KIMURA, T., MÉNAGER, C., NISHIMURA, T., SHIROMIZU, T., WATANABE, H., INAGAKI, N., IWAMATSU, A., HOTANI, H. & KAIBUCHI, K. 2002. CRMP-2 binds to tubulin heterodimers to promote microtubule assembly. *Nature cell biology,* 4**,** 583-591.
FUKUHARA, A., IRIE, K., NAKANISHI, H., TAKEKUNI, K., KAWAKATSU, T., IKEDA, W., YAMADA, A., KATATA, T., HONDA, T., SATO, T., SHIMIZU, K., OZAKI, H., HORIUCHI, H., KITA, T. & TAKAI, Y. 2002. Involvement of nectin in the localization of junctional adhesion molecule at tight junctions. *Oncogene,* 21**,** 7642-55.

FUKUNAGA, E., INOUE, Y., KOMIYA, S., HORIGUCHI, K., GOTO, K., SAITOH, M., MIYAZAWA, K., KOINUMA, D., HANYU, A. & IMAMURA, T. 2008. Smurf2 induces ubiquitin-dependent degradation of Smurf1 to prevent migration of breast cancer cells. *J Biol Chem,* 283**,** 35660-35667.

GAO, L., JOBERTY, G. & MACARA, I. G. 2002. Assembly of epithelial tight junctions is negatively regulated by Par6. *Curr Biol,* 12**,** 221-5.

GARVALOV, B. K., FLYNN, K. C., NEUKIRCHEN, D., MEYN, L., TEUSCH, N., WU, X., BRAKEBUSCH, C., BAMBURG, J. R. & BRADKE, F. 2007. Cdc42 regulates cofilin during the establishment of neuronal polarity. *J Neurosci,* 27**,** 13117-29.

GAVET, O., EL MESSARI, S., OZON, S. & SOBEL, A. 2002. Regulation and subcellular localization of the microtubule-destabilizing stathmin family phosphoproteins in cortical neurons. *J Neurosci Res,* 68**,** 535-550.

GLEESON, J. G., ALLEN, K. M., FOX, J. W., LAMPERTI, E. D., BERKOVIC, S., SCHEFFER, I., COOPER, E. C., DOBYNS, W. B., MINNERATH, S. R., ROSS, M. E. & WALSH, C. A. 1998. Doublecortin, a brain-specific gene mutated in human X-linked lissencephaly and double cortex syndrome, encodes a putative signaling protein. *Cell,* 92**,** 63-72.

GLEESON, J. G., LIN, P. T., FLANAGAN, L. A. & WALSH, C. A. 1999. Doublecortin is a microtubule-associated protein and is expressed widely by migrating neurons. *Neuron,* 23**,** 257-71.

GRENNINGLOH, G., SOEHRMAN, S., BONDALLAZ, P., RUCHTI, E. & CADAS, H. 2004. Role of the microtubule destabilizing proteins SCG10 and stathmin in neuronal growth. *J Neurobiol,* 58**,** 60-9.

GU, C., ZHOU, W., PUTHENVEEDU, M. A., XU, M., JAN, Y. N. & JAN, L. Y. 2006. The microtubule plus-end tracking protein EB1 is required for Kv1 voltage-gated K+ channel axonal targeting. *Neuron,* 52**,** 803-16.

GU, G. J., LUND, H., WU, D., BLOKZIJL, A., CLASSON, C., VON EULER, G., LANDEGREN, U., SUNNEMARK, D. & KAMALI-MOGHADDAM, M. 2013. Role of individual MARK isoforms in phosphorylation of tau at Ser(2)(6)(2) in Alzheimer's disease. *Neuromolecular Med,* 15**,** 458-69.

GU, Y., HAMAJIMA, N. & IHARA, Y. 2000. Neurofibrillary tangle-associated collapsin response mediator protein-2 (CRMP-2) is highly phosphorylated on Thr-509, Ser-518, and Ser-522. *Biochemistry,* 39**,** 4267-4275.

GUPTA, K., LI, C., DUAN, A., ALBERICO, E., KIM, O., ALBER, M. & GOODSON, H. 2013. Mechanism for the catastrophe-promoting activity of the microtubule destabilizer Op18/stathmin. *Proc Natl Acad Sci U S A,* 110**,** 20449-20454.

HAMILTON, A. & ZITO, K. 2013. Breaking it down: the ubiquitin proteasome system in neuronal morphogenesis. *Neural plasticity,* 2013**,** 196848.

HAN, K. J., FOSTER, D. G., ZHANG, N. Y., KANISHA, K., DZIECIATKOWSKA, M., SCLAFANI, R. A., HANSEN, K. C., PENG, J. & LIU, C. W. 2012. Ubiquitin-specific protease 9x deubiquitinates and stabilizes the spinal muscular atrophy protein-survival motor neuron. *J Biol Chem,* 287**,** 43741-52.

HAND, R., BORTONE, D., MATTAR, P., NGUYEN, L., HENG, J. I., GUERRIER, S., BOUTT, E., PETERS, E., BARNES, A. P., PARRAS, C., SCHUURMANS, C., GUILLEMOT, F. & POLLEUX, F. 2005. Phosphorylation of Neurogenin2 specifies the migration properties and the dendritic morphology of pyramidal neurons in the neocortex. *Neuron,* 48**,** 45-62.

HARADA, A., TENG, J., TAKEI, Y., OGUCHI, K. & HIROKAWA, N. 2002. MAP2 is required for dendrite elongation, PKA anchoring in dendrites, and proper PKA signal transduction. *J Cell Biol,* 158**,** 541-9.

HAYASHI, I. & IKURA, M. 2003. Crystal structure of the amino-terminal microtubule-binding domain of end-binding protein 1 (EB1). *J Biol Chem,* 278**,** 36430-4.

HEGDE, A. 2010. The ubiquitin-proteasome pathway and synaptic plasticity. *Learning & memory (Cold Spring Harbor, N.Y.),* 17**,** 314-327.

HEGDE, A. N. & UPADHYA, S. C. 2007. The ubiquitin-proteasome pathway in health and disease of the nervous system. *Trends Neurosci,* 30**,** 587-95.

HERSHKO, A. & CIECHANOVER, A. 1998. The ubiquitin system. *Annu Rev Biochem,* 67**,** 425-79.

HIRAI, S., BANBA, Y., SATAKE, T. & OHNO, S. 2011. Axon formation in neocortical neurons depends on stage-specific regulation of microtubule stability by the dual leucine zipper kinase-c-Jun N-terminal kinase pathway. *J Neurosci,* 31**,** 6468-80.

HIROKAWA, N., FUNAKOSHI, T., SATO-HARADA, R. & KANAI, Y. 1996. Selective stabilization of tau in axons and microtubule-associated protein 2C in cell bodies and dendrites contributes to polarized localization of cytoskeletal proteins in mature neurons. *J Cell Biol,* 132**,** 667-79.

HIROKAWA, N., NIWA, S. & TANAKA, Y. 2010. Molecular motors in neurons: transport mechanisms and roles in brain function, development, and disease. *Neuron,* 68**,** 610-38.

HOMAN, C. C., KUMAR, R., NGUYEN, L. S., HAAN, E., RAYMOND, F. L., ABIDI, F., RAYNAUD, M., SCHWARTZ, C. E., WOOD, S. A., GECZ, J. & JOLLY, L. A. 2014. Mutations in USP9X Are Associated with X-Linked Intellectual Disability and Disrupt Neuronal Cell Migration and Growth. *Am J Hum Genet,* 94**,** 470-8.

HORESH, D., SAPIR, T., FRANCIS, F., WOLF, S. G., CASPI, M., ELBAUM, M., CHELLY, J. & REINER, O. 1999. Doublecortin, a stabilizer of microtubules. *Hum Mol Genet,* 8**,** 1599-610.

HUR, E. M., SAIJILAFU & ZHOU, F. Q. 2012. Growing the growth cone: remodeling the cytoskeleton to promote axon regeneration. *Trends Neurosci,* 35**,** 164-74.

ICHETOVKIN, I., GRANT, W. & CONDEELIS, J. 2002. Cofilin produces newly polymerized actin filaments that are preferred for dendritic nucleation by the Arp2/3 complex. *Curr Biol,* 12**,** 79-84.

INAGAKI, N., CHIHARA, K., ARIMURA, N., MÉNAGER, C., KAWANO, Y., MATSUO, N., NISHIMURA, T., AMANO, M. & KAIBUCHI, K. 2001. CRMP-2 induces axons in cultured hippocampal neurons. *Nature neuroscience,* 4**,** 781-782.

ISAKA, F., ISHIBASHI, M., TAKI, W., HASHIMOTO, N., NAKANISHI, S. & KAGEYAMA, R. 1999. Ectopic expression of the bHLH gene Math1 disturbs neural development. *Eur J Neurosci,* 11**,** 2582-8.

ISHIHARA, A., SAITO, H. & ABE, K. 1994. Transforming growth factor-beta 1 and -beta 2 promote neurite sprouting and elongation of cultured rat hippocampal neurons. *Brain research,* 639**,** 21-25.

IWASAWA, N., NEGISHI, M. & OINUMA, I. 2012. R-Ras controls axon branching through afadin in cortical neurons. *Mol Biol Cell,* 23**,** 2793-804.

JACINTO, E., LOEWITH, R., SCHMIDT, A., LIN, S., RÜEGG, M., HALL, A. & HALL, M. 2004. Mammalian TOR complex 2 controls the actin cytoskeleton and is rapamycin insensitive. *Nature cell biology,* 6**,** 1122-1128.

JACOBSON, C., SCHNAPP, B. & BANKER, G. A. 2006. A change in the selective translocation of the Kinesin-1 motor domain marks the initial specification of the axon. *Neuron,* 49**,** 797-804.

JOBERTY, G., PETERSEN, C., GAO, L. & MACARA, I. G. 2000. The cell-polarity protein Par6 links Par3 and atypical protein kinase C to Cdc42. *Nat Cell Biol,* 2**,** 531-9.

JOHANSSON, A., DRIESSENS, M. & ASPENSTROM, P. 2000. The mammalian homologue of the Caenorhabditis elegans polarity protein PAR-6 is a binding partner for the Rho GTPases Cdc42 and Rac1. *J Cell Sci,* 113 (Pt 18)**,** 3267-75.

JOLLY, L. A., TAYLOR, V. & WOOD, S. A. 2009. USP9X enhances the polarity and self-renewal of embryonic stem cell-derived neural progenitors. *Mol Biol Cell,* 20**,** 2015-29.

KAECH, S. & BANKER, G. 2006. Culturing hippocampal neurons. *Nat Protoc,* 1**,** 2406-15.

KANAI, Y., OKADA, Y., TANAKA, Y., HARADA, A., TERADA, S. & HIROKAWA, N. 2000. KIF5C, a novel neuronal kinesin enriched in motor neurons. *J Neurosci,* 20**,** 6374-84.

KIM, J. H., PARK, K. C., CHUNG, S. S., BANG, O. & CHUNG, C. H. 2003. Deubiquitinating enzymes as cellular regulators. *J Biochem,* 134**,** 9-18.

KIM, W. Y., ZHOU, F. Q., ZHOU, J., YOKOTA, Y., WANG, Y. M., YOSHIMURA, T., KAIBUCHI, K., WOODGETT, J. R., ANTON, E. S. & SNIDER, W. D. 2006. Essential roles for GSK-3s and GSK-3-primed substrates in neurotrophin-induced and hippocampal axon growth. *Neuron,* 52**,** 981-96.

KIMURA, T., WATANABE, H., IWAMATSU, A. & KAIBUCHI, K. 2005. Tubulin and CRMP-2 complex is transported via Kinesin-1. *J Neurochem,* 93**,** 1371-1382.

KOROBOVA, F. & SVITKINA, T. 2008. Arp2/3 complex is important for filopodia formation, growth cone motility, and neuritogenesis in neuronal cells. *Mol Biol Cell,* 19**,** 1561-74.

KRIEGSTEIN, A. R. & GOTZ, M. 2003. Radial glia diversity: a matter of cell fate. *Glia,* 43**,** 37-43.

KURIYAMA, M., HARADA, N., KURODA, S., YAMAMOTO, T., NAKAFUKU, M., IWAMATSU, A., YAMAMOTO, D., PRASAD, R., CROCE, C., CANAANI, E. & KAIBUCHI, K. 1996. Identification of AF-6 and canoe as putative targets for Ras. *J Biol Chem,* 271**,** 607-10.

LEWIS, T. L., JR., COURCHET, J. & POLLEUX, F. 2013. Cell biology in neuroscience: Cellular and molecular mechanisms underlying axon formation, growth, and branching. *J Cell Biol,* 202**,** 837-48.

LI, Y. H., WERNER, H. & PUSCHEL, A. W. 2008. Rheb and mTOR regulate neuronal polarity through Rap1B. *J Biol Chem,* 283**,** 33784-92.

LIN, D., EDWARDS, A. S., FAWCETT, J. P., MBAMALU, G., SCOTT, J. D. & PAWSON, T. 2000. A mammalian PAR-3-PAR-6 complex implicated in Cdc42/Rac1 and aPKC signalling and cell polarity. *Nat Cell Biol,* 2**,** 540-7.

MANDAI, K., NAKANISHI, H., SATOH, A., OBAISHI, H., WADA, M., NISHIOKA, H., ITOH, M., MIZOGUCHI, A., AOKI, T., FUJIMOTO, T., MATSUDA, Y., TSUKITA, S. & TAKAI, Y. 1997. Afadin: A novel actin

filament-binding protein with one PDZ domain localized at cadherin-based cell-to-cell adherens junction. *J Cell Biol,* 139**,** 517-28.
MANDELKOW, E. M., THIES, E., TRINCZEK, B., BIERNAT, J. & MANDELKOW, E. 2004. MARK/PAR1 kinase is a regulator of microtubule-dependent transport in axons. *J Cell Biol,* 167**,** 99-110.
MATENIA, D. & MANDELKOW, E. M. 2009. The tau of MARK: a polarized view of the cytoskeleton. *Trends Biochem Sci,* 34**,** 332-42.
MECHA, M., RABADAN, M. A., PENA-MELIAN, A., VALENCIA, M., MONDEJAR, T. & BLANCO, M. J. 2008. Expression of TGF-betas in the embryonic nervous system: analysis of interbalance between isoforms. *Dev Dyn,* 237**,** 1709-17.
MILLARD, S. M. & WOOD, S. A. 2006. Riding the DUBway: regulation of protein trafficking by deubiquitylating enzymes. *J Cell Biol,* 173**,** 463-8.
MISHRA, L., KATURI, V. & EVANS, S. 2005. The role of PRAJA and ELF in TGF-beta signaling and gastric cancer. *Cancer Biol Ther,* 4**,** 694-9.
MOORES, C. A., PERDERISET, M., KAPPELER, C., KAIN, S., DRUMMOND, D., PERKINS, S. J., CHELLY, J., CROSS, R., HOUDUSSE, A. & FRANCIS, F. 2006. Distinct roles of doublecortin modulating the microtubule cytoskeleton. *EMBO J,* 25**,** 4448-57.
MORITA, T. & SOBUE, K. 2009. Specification of neuronal polarity regulated by local translation of CRMP2 and Tau via the mTOR-p70S6K pathway. *J Biol Chem,* 284**,** 27734-45.
MOUCHANTAF, R., AZAKIR, B. A., MCPHERSON, P. S., MILLARD, S. M., WOOD, S. A. & ANGERS, A. 2006. The ubiquitin ligase itch is auto-ubiquitylated in vivo and in vitro but is protected from degradation by interacting with the deubiquitylating enzyme FAM/USP9X. *J Biol Chem,* 281**,** 38738-47.
MURRAY, R. Z., JOLLY, L. A. & WOOD, S. A. 2004. The FAM deubiquitylating enzyme localizes to multiple points of protein trafficking in epithelia, where it associates with E-cadherin and beta-catenin. *Mol Biol Cell,* 15**,** 1591-9.
NAIK, E., WEBSTER, J. D., DEVOSS, J., LIU, J., SURIBEN, R. & DIXIT, V. M. 2014. Regulation of proximal T cell receptor signaling and tolerance induction by deubiquitinase Usp9X. *J Exp Med,* 211**,** 1947-55.
NAKAJIMA, K., YIN, X., TAKEI, Y., SEOG, D. H., HOMMA, N. & HIROKAWA, N. 2012. Molecular motor KIF5A is essential for GABA(A) receptor transport, and KIF5A deletion causes epilepsy. *Neuron,* 76**,** 945-61.
NG, J. 2008. TGF-beta signals regulate axonal development through distinct Smad-independent mechanisms. *Development,* 135**,** 4025-35.
NIJMAN, S. M., LUNA-VARGAS, M. P., VELDS, A., BRUMMELKAMP, T. R., DIRAC, A. M., SIXMA, T. K. & BERNARDS, R. 2005. A genomic and functional inventory of deubiquitinating enzymes. *Cell,* 123**,** 773-86.
NISHIMURA, T., KATO, K., YAMAGUCHI, T., FUKATA, Y., OHNO, S. & KAIBUCHI, K. 2004. Role of the PAR-3-KIF3 complex in the establishment of neuronal polarity. *Nat Cell Biol,* 6**,** 328-34.
NISHIMURA, T., YAMAGUCHI, T., KATO, K., YOSHIZAWA, M., NABESHIMA, Y., OHNO, S., HOSHINO, M. & KAIBUCHI, K. 2005. PAR-6-PAR-3 mediates Cdc42-induced Rac activation through the Rac GEFs STEF/Tiam1. *Nat Cell Biol,* 7**,** 270-7.
O'KEEFE, D. D., EDGAR, B. A. & SAUCEDO, L. J. 2011. EndoGI modulates Notch signaling and axon guidance in Drosophila. *Mech Dev,* 128**,** 59-70.

OOMS, L. M., FEDELE, C. G., ASTLE, M. V., IVETAC, I., CHEUNG, V., PEARSON, R. B., LAYTON, M. J., FORRAI, A., NANDURKAR, H. H. & MITCHELL, C. A. 2006. The inositol polyphosphate 5-phosphatase, PIPP, Is a novel regulator of phosphoinositide 3-kinase-dependent neurite elongation. *Mol Biol Cell,* 17**,** 607-22.

OVERLY, C. C., RIEFF, H. I. & HOLLENBECK, P. J. 1996. Organelle motility and metabolism in axons vs dendrites of cultured hippocampal neurons. *J Cell Sci,* 109 (Pt 5)**,** 971-80.

PANTALEON, M., KANAI-AZUMA, M., MATTICK, J. S., KAIBUCHI, K., KAYE, P. L. & WOOD, S. A. 2001. FAM deubiquitylating enzyme is essential for preimplantation mouse embryo development. *Mech Dev,* 109**,** 151-60.

PARK, D., XIANG, A. P., MAO, F. F., ZHANG, L., DI, C. G., LIU, X. M., SHAO, Y., MA, B. F., LEE, J. H., HA, K. S., WALTON, N. & LAHN, B. T. 2010. Nestin is required for the proper self-renewal of neural stem cells. *Stem Cells,* 28**,** 2162-71.

PEREZ-MANCERA, P. A., RUST, A. G., VAN DER WEYDEN, L., KRISTIANSEN, G., LI, A., SARVER, A. L., SILVERSTEIN, K. A., GRUTZMANN, R., AUST, D., RUMMELE, P., KNOSEL, T., HERD, C., STEMPLE, D. L., KETTLEBOROUGH, R., BROSNAN, J. A., MORGAN, R., KNIGHT, S., YU, J., STEGEMAN, S., COLLIER, L. S., TEN HOEVE, J. J., DE RIDDER, J., KLEIN, A. P., GOGGINS, M., HRUBAN, R. H., CHANG, D. K., BIANKIN, A. V., GRIMMOND, S. M., WESSELS, L. F., WOOD, S. A., IACOBUZIO-DONAHUE, C. A., PILARSKY, C., LARGAESPADA, D. A., ADAMS, D. J. & TUVESON, D. A. 2012. The deubiquitinase USP9X suppresses pancreatic ductal adenocarcinoma. *Nature,* 486**,** 266-70.

POLLEUX, F. & SNIDER, W. 2010. Initiating and growing an axon. *Cold Spring Harbor perspectives in biology,* 2.

POPE, B. & KENT, H. M. 1996. High efficiency 5 min transformation of Escherichia coli. *Nucleic Acids Res,* 24**,** 536-7.

RIVERA, J., CHU, P. J., LEWIS, T. L., JR. & ARNOLD, D. B. 2007. The role of Kif5B in axonal localization of Kv1 K(+) channels. *Eur J Neurosci,* 25**,** 136-46.

ROTT, R., SZARGEL, R., HASKIN, J., BANDOPADHYAY, R., LEES, A. J., SHANI, V. & ENGELENDER, S. 2011. alpha-Synuclein fate is determined by USP9X-regulated monoubiquitination. *Proc Natl Acad Sci U S A,* 108**,** 18666-71.

RYAN, K. & PIMPLIKAR, S. 2005. Activation of GSK-3 and phosphorylation of CRMP2 in transgenic mice expressing APP intracellular domain. *J Cell Biol,* 171**,** 327-335.

SAHA, T., VARDHINI, D., TANG, Y., KATURI, V., JOGUNOORI, W., VOLPE, E. A., HAINES, D., SIDAWY, A., ZHOU, X., GALLICANO, I., SCHLEGEL, R., MISHRA, B. & MISHRA, L. 2006. RING finger-dependent ubiquitination by PRAJA is dependent on TGF-beta and potentially defines the functional status of the tumor suppressor ELF. *Oncogene,* 25**,** 693-705.

SAPIR, T., HORESH, D., CASPI, M., ATLAS, R., BURGESS, H. A., WOLF, S. G., FRANCIS, F., CHELLY, J., ELBAUM, M., PIETROKOVSKI, S. & REINER, O. 2000. Doublecortin mutations cluster in evolutionarily conserved functional domains. *Hum Mol Genet,* 9**,** 703-12.

SAVITT, J. M., JANG, S. S., MU, W., DAWSON, V. L. & DAWSON, T. M. 2005. Bcl-x is required for proper development of the mouse substantia nigra. *J Neurosci,* 25**,** 6721-8.
SAXTON, W. M. & HOLLENBECK, P. J. 2012. The axonal transport of mitochondria. *J Cell Sci,* 125**,** 2095-104.
SCHWICKART, M., HUANG, X., LILL, J. R., LIU, J., FERRANDO, R., FRENCH, D. M., MAECKER, H., O'ROURKE, K., BAZAN, F., EASTHAM-ANDERSON, J., YUE, P., DORNAN, D., HUANG, D. C. & DIXIT, V. M. 2009. Deubiquitinase USP9X stabilizes MCL1 and promotes tumour cell survival. *Nature,* 463**,** 103-7.
SHAO, C. Y., ZHU, J., XIE, Y. J., WANG, Z., WANG, Y. N., WANG, Y., SU, L. D., ZHOU, L., ZHOU, T. H. & SHEN, Y. 2013. Distinct functions of nuclear distribution proteins LIS1, Ndel1 and NudCL in regulating axonal mitochondrial transport. *Traffic,* 14**,** 785-97.
SHELLY, M., CANCEDDA, L., HEILSHORN, S., SUMBRE, G. & POO, M. M. 2007. LKB1/STRAD promotes axon initiation during neuronal polarization. *Cell,* 129**,** 565-77.
SHI, S. H., JAN, L. Y. & JAN, Y. N. 2003. Hippocampal neuronal polarity specified by spatially localized mPar3/mPar6 and PI 3-kinase activity. *Cell,* 112**,** 63-75.
SHI, Y. & MASSAGUE, J. 2003. Mechanisms of TGF-beta signaling from cell membrane to the nucleus. *Cell,* 113**,** 685-700.
SHU, L. & HOUGHTON, P. 2009. The mTORC2 complex regulates terminal differentiation of C2C12 myoblasts. *Molecular and cellular biology,* 29**,** 4691-4700.
SLACK, S. E., GRIST, J., MAC, Q., MCMAHON, S. B. & PEZET, S. 2005. TrkB expression and phospho-ERK activation by brain-derived neurotrophic factor in rat spinothalamic tract neurons. *J Comp Neurol,* 489**,** 59-68.
SOMETANI, A., KATAOKA, H., NITTA, A., FUKUMITSU, H., NOMOTO, H. & FURUKAWA, S. 2001. Transforming growth factor-beta1 enhances expression of brain-derived neurotrophic factor and its receptor, TrkB, in neurons cultured from rat cerebral cortex. *J Neurosci Res,* 66**,** 369-376.
STAGI, M., GORLOVOY, P., LARIONOV, S., TAKAHASHI, K. & NEUMANN, H. 2006. Unloading kinesin transported cargoes from the tubulin track via the inflammatory c-Jun N-terminal kinase pathway. *FASEB J,* 20**,** 2573-5.
STEGEMAN, S., JOLLY, L., PREMARATHNE, S., GECZ, J., RICHARDS, L., MACKAY-SIM, A. & WOOD, S. 2013. Loss of Usp9x disrupts cortical architecture, hippocampal development and TGFβ-mediated axonogenesis. *PloS one,* 8.
STEWART, D. P., KOSS, B., BATHINA, M., PERCIAVALLE, R. M., BISANZ, K. & OPFERMAN, J. T. 2010. Ubiquitin-independent degradation of antiapoptotic MCL-1. *Mol Cell Biol,* 30**,** 3099-110.
SU, Q., CAI, Q., GERWIN, C., SMITH, C. L. & SHENG, Z. H. 2004. Syntabulin is a microtubule-associated protein implicated in syntaxin transport in neurons. *Nat Cell Biol,* 6**,** 941-53.
SU, Y. Y., YE, M., LI, L., LIU, C., PAN, J., LIU, W. W., JIANG, Y., JIANG, X. Y., ZHANG, X., SHU, Y. & BAO, L. 2013. KIF5B promotes the forward transport and axonal function of the voltage-gated sodium channel Nav1.8. *J Neurosci,* 33**,** 17884-96.
SUN, T., YU, N., ZHAI, L. K., LI, N., ZHANG, C., ZHOU, L., HUANG, Z., JIANG, X. Y., SHEN, Y. & CHEN, Z. Y. 2013. c-Jun NH2-terminal kinase (JNK)-

interacting protein-3 (JIP3) regulates neuronal axon elongation in a kinesin- and JNK-dependent manner. *J Biol Chem,* 288**,** 14531-43.
SUTER, D. M. & MILLER, K. E. 2011. The emerging role of forces in axonal elongation. *Prog Neurobiol,* 94**,** 91-101.
TAKEFUJI, M., MORI, K., MORITA, Y., ARIMURA, N., NISHIMURA, T., NAKAYAMA, M., HOSHINO, M., IWAMATSU, A., MUROHARA, T., KAIBUCHI, K. & AMANO, M. 2007. Rho-kinase modulates the function of STEF, a Rac GEF, through its phosphorylation. *Biochem Biophys Res Commun,* 355**,** 788-94.
TAN, M., MA, S., HUANG, Q., HU, K., SONG, B. & LI, M. 2013. GSK-3α/β-mediated phosphorylation of CRMP-2 regulates activity-dependent dendritic growth. *J Neurochem,* 125**,** 685-697.
TANAKA, Y., KANAI, Y., OKADA, Y., NONAKA, S., TAKEDA, S., HARADA, A. & HIROKAWA, N. 1998. Targeted disruption of mouse conventional kinesin heavy chain, kif5B, results in abnormal perinuclear clustering of mitochondria. *Cell,* 93**,** 1147-58.
TAYA, S., YAMAMOTO, T., KANAI-AZUMA, M., WOOD, S. A. & KAIBUCHI, K. 1999. The deubiquitinating enzyme Fam interacts with and stabilizes beta-catenin. *Genes Cells,* 4**,** 757-67.
TAYA, S., YAMAMOTO, T., KANO, K., KAWANO, Y., IWAMATSU, A., TSUCHIYA, T., TANAKA, K., KANAI-AZUMA, M., WOOD, S. A., MATTICK, J. S. & KAIBUCHI, K. 1998. The Ras target AF-6 is a substrate of the fam deubiquitinating enzyme. *J Cell Biol,* 142**,** 1053-62.
TAYLOR, K. R., HOLZER, A. K., BAZAN, J. F., WALSH, C. A. & GLEESON, J. G. 2000. Patient mutations in doublecortin define a repeated tubulin-binding domain. *J Biol Chem,* 275**,** 34442-50.
TEUBER, J., MUELLER, B., FUKABORI, R., LANG, D., ALBRECHT, A. & STORK, O. 2013. The ubiquitin ligase Praja1 reduces NRAGE expression and inhibits neuronal differentiation of PC12 cells. *PloS one,* 8.
THEARD, D., LABARRADE, F., PARTISANI, M., MILANINI, J., SAKAGAMI, H., FON, E. A., WOOD, S. A., FRANCO, M. & LUTON, F. 2010. USP9x-mediated deubiquitination of EFA6 regulates de novo tight junction assembly. *EMBO J,* 29**,** 1499-509.
TIMM, T., MATENIA, D., LI, X. Y., GRIESSHABER, B. & MANDELKOW, E. M. 2006. Signaling from MARK to tau: regulation, cytoskeletal crosstalk, and pathological phosphorylation. *Neurodegener Dis,* 3**,** 207-17.
TINT, I., JEAN, D., BAAS, P. W. & BLACK, M. M. 2009. Doublecortin associates with microtubules preferentially in regions of the axon displaying actin-rich protrusive structures. *J Neurosci,* 29**,** 10995-1010.
TORIYAMA, M., SAKUMURA, Y., SHIMADA, T., ISHII, S. & INAGAKI, N. 2010. A diffusion-based neurite length-sensing mechanism involved in neuronal symmetry breaking. *Molecular systems biology,* 6**,** 394.
TORIYAMA, M., SHIMADA, T., KIM, K., MITSUBA, M., NOMURA, E., KATSUTA, K., SAKUMURA, Y., ROEPSTORFF, P. & INAGAKI, N. 2006. Shootin1: A protein involved in the organization of an asymmetric signal for neuronal polarization. *J Cell Biol,* 175**,** 147-157.
TRINCZEK, B., BRAJENOVIC, M., EBNETH, A. & DREWES, G. 2004. MARK4 is a novel microtubule-associated proteins/microtubule affinity-regulating kinase that binds to the cellular microtubule network and to centrosomes. *J Biol Chem,* 279**,** 5915-23.

TRONCHE, F., KELLENDONK, C., KRETZ, O., GASS, P., ANLAG, K., ORBAN, P. C., BOCK, R., KLEIN, R. & SCHUTZ, G. 1999. Disruption of the glucocorticoid receptor gene in the nervous system results in reduced anxiety. *Nat Genet,* 23**,** 99-103.

VIDAL, R. L., FUENTES, P., VALENZUELA, J. I., ALVARADO-DIAZ, C. P., RAMÍREZ, O. A., KUKULJAN, M. & COUVE, A. 2012. RNA interference of Marlin-1/Jakmip1 results in abnormal morphogenesis and migration of cortical pyramidal neurons. *Molecular and cellular neurosciences,* 51**,** 1-11.

VOGEL, T., AHRENS, S., BUTTNER, N. & KRIEGLSTEIN, K. 2010. Transforming growth factor beta promotes neuronal cell fate of mouse cortical and hippocampal progenitors in vitro and in vivo: identification of Nedd9 as an essential signaling component. *Cereb Cortex,* 20**,** 661-71.

WATABE-UCHIDA, M., JOHN, K. A., JANAS, J. A., NEWEY, S. E. & VAN AELST, L. 2006. The Rac activator DOCK7 regulates neuronal polarity through local phosphorylation of stathmin/Op18. *Neuron,* 51**,** 727-39.

WEN, H.-L., LIN, Y.-T., TING, C.-H., LIN-CHAO, S., LI, H. & HSIEH-LI, H. 2010. Stathmin, a microtubule-destabilizing protein, is dysregulated in spinal muscular atrophy. *Hum Mol Genet,* 19**,** 1766-1778.

WITTE, H., NEUKIRCHEN, D. & BRADKE, F. 2008. Microtubule stabilization specifies initial neuronal polarization. *J Cell Biol,* 180**,** 619-32.

WULLSCHLEGER, S., LOEWITH, R. & HALL, M. N. 2006. TOR signaling in growth and metabolism. *Cell,* 124**,** 471-84.

XIE, Y., AVELLO, M., SCHIRLE, M., MCWHINNIE, E., FENG, Y., BRIC-FURLONG, E., WILSON, C., NATHANS, R., ZHANG, J., KIRSCHNER, M., HUANG, S.-M. A. & CONG, F. 2013. Deubiquitinase FAM/USP9X interacts with the E3 ubiquitin ligase SMURF1 protein and protects it from ligase activity-dependent self-degradation. *J Biol Chem,* 288**,** 2976-2985.

XU, Z., XIA, B., GONG, Q., BAILEY, J., GROVES, B., RADEKE, M., WOOD, S. A., SZUMLINSKI, K. K. & MA, D. 2010. Identification of a deubiquitinating enzyme as a novel AGS3-interacting protein. *PloS one,* 5**,** e9725.

YAN, D., GUO, L. & WANG, Y. 2006. Requirement of dendritic Akt degradation by the ubiquitin-proteasome system for neuronal polarity. *J Cell Biol,* 174**,** 415-24.

YANG, Q., ZHANG, X. F., POLLARD, T. D. & FORSCHER, P. 2012. Arp2/3 complex-dependent actin networks constrain myosin II function in driving retrograde actin flow. *J Cell Biol,* 197**,** 939-56.

YI, J. J., BARNES, A. P., HAND, R., POLLEUX, F. & EHLERS, M. D. 2010. TGF-beta signaling specifies axons during brain development. *Cell,* 142**,** 144-57.

YOSHIDA, H., WATANABE, A. & IHARA, Y. 1998. Collapsin response mediator protein-2 is associated with neurofibrillary tangles in Alzheimer's disease. *J Biol Chem,* 273**,** 9761-9768.

YOSHIMURA, T., KAWANO, Y., ARIMURA, N., KAWABATA, S., KIKUCHI, A. & KAIBUCHI, K. 2005. GSK-3beta regulates phosphorylation of CRMP-2 and neuronal polarity. *Cell,* 120**,** 137-149.

ZHADANOV, A. B., PROVANCE, D. W., JR., SPEER, C. A., COFFIN, J. D., GOSS, D., BLIXT, J. A., REICHERT, C. M. & MERCER, J. A. 1999. Absence of the tight junctional protein AF-6 disrupts epithelial cell-cell junctions and cell polarity during mouse development. *Curr Biol,* 9**,** 880-8.

ZHOU, F. Q., ZHOU, J., DEDHAR, S., WU, Y. H. & SNIDER, W. D. 2004. NGF-induced axon growth is mediated by localized inactivation of GSK-3beta and

functions of the microtubule plus end binding protein APC. *Neuron,* 42**,** 897-912.
ZHU, H., KAVSAK, P., ABDOLLAH, S., WRANA, J. & THOMSEN, G. 1999. A SMAD ubiquitin ligase targets the BMP pathway and affects embryonic pattern formation. *Nature,* 400**,** 687-693.